

IntechOpen

Becoming Human with Humanoid

From Physical Interaction to Social Intelligence

*Edited by Ahmad Hoirul Basori,
Ali Leylavi Shoushtari and Andon Venelinov Topalov*



Becoming Human with Humanoid - From Physical Interaction to Social Intelligence

*Edited by Ahmad Hoirul Basori,
Ali Leylavi Shoushtari
and Andon Venelinov Topalov*

Published in London, United Kingdom



IntechOpen





Supporting open minds since 2005



Becoming Human with Humanoid – From Physical Interaction to Social Intelligence

<http://dx.doi.org/10.5772/intechopen.73377>

Edited by Ahmad Hoirul Basori, Ali Leylavi Shoushtari and Andon Venelinov Topalov

Contributors

Joel Perez, Senthil Kumar J, Sivasankar G, Yuji Yamakawa, Shouren Huang, Akio Namiki, Masatoshi Ishikawa, Carlos Toshinori Ishi, Guillermo Santamaria-Bonfil, Orlando Grabiél Toledano López, Valerie Stehling, Daniela Janssen, Christoph Henke, Yusie Rizal, Hacene Ameddah

© The Editor(s) and the Author(s) 2020

The rights of the editor(s) and the author(s) have been asserted in accordance with the Copyright, Designs and Patents Act 1988. All rights to the book as a whole are reserved by INTECHOPEN LIMITED. The book as a whole (compilation) cannot be reproduced, distributed or used for commercial or non-commercial purposes without INTECHOPEN LIMITED's written permission. Enquiries concerning the use of the book should be directed to INTECHOPEN LIMITED rights and permissions department (permissions@intechopen.com).

Violations are liable to prosecution under the governing Copyright Law.



Individual chapters of this publication are distributed under the terms of the Creative Commons Attribution 3.0 Unported License which permits commercial use, distribution and reproduction of the individual chapters, provided the original author(s) and source publication are appropriately acknowledged. If so indicated, certain images may not be included under the Creative Commons license. In such cases users will need to obtain permission from the license holder to reproduce the material. More details and guidelines concerning content reuse and adaptation can be found at <http://www.intechopen.com/copyright-policy.html>.

Notice

Statements and opinions expressed in the chapters are these of the individual contributors and not necessarily those of the editors or publisher. No responsibility is accepted for the accuracy of information contained in the published chapters. The publisher assumes no responsibility for any damage or injury to persons or property arising out of the use of any materials, instructions, methods or ideas contained in the book.

First published in London, United Kingdom, 2020 by IntechOpen

IntechOpen is the global imprint of INTECHOPEN LIMITED, registered in England and Wales, registration number: 11086078, 7th floor, 10 Lower Thames Street, London, EC3R 6AF, United Kingdom

Printed in Croatia

British Library Cataloguing-in-Publication Data

A catalogue record for this book is available from the British Library

Additional hard and PDF copies can be obtained from orders@intechopen.com

Becoming Human with Humanoid – From Physical Interaction to Social Intelligence

Edited by Ahmad Hoirul Basori, Ali Leylavi Shoushtari and Andon Venelinov Topalov

p. cm.

Print ISBN 978-1-78985-483-1

Online ISBN 978-1-78985-484-8

eBook (PDF) ISBN 978-1-78985-726-9

We are IntechOpen, the world's leading publisher of Open Access books Built by scientists, for scientists

4,700+

Open access books available

121,000+

International authors and editors

135M+

Downloads

151

Countries delivered to

Our authors are among the
Top 1%

most cited scientists

12.2%

Contributors from top 500 universities



WEB OF SCIENCE™

Selection of our books indexed in the Book Citation Index
in Web of Science™ Core Collection (BKCI)

Interested in publishing with us?
Contact book.department@intechopen.com

Numbers displayed above are based on latest data collected.
For more information visit www.intechopen.com



Meet the editors



Ahmad Hoirul Basori, received his BSc (Software Engineering) degree from Institut Teknologi Sepuluh Nopember Surabaya in 2004 and his PhD (Computer Graphics) from Universiti Teknologi Malaysia, Johor Bahru, Johor, in 2011. In 2011, he was appointed as Assistant Professor in the Department of Computer Graphics and Multimedia, Universiti Teknologi Malaysia. In 2016, he was promoted to Associate Professor in the Faculty of Computing and Information Technology Rabigh, King Abdulaziz University. He is a member of editorial boards of several international journals and has published more than 80 articles. He is also a member of IEEE, ACM SIGGRAPH, IAENG, and a senior member of IACSIT. His research interests include computer graphics, facial animation, cloth simulation, medical visualization, haptic interaction, man machine interaction and robotics.



Ali Leylavi received his PhD in Biorobotics from Scuola Superiore Sant'Anna, Pisa and his MSc in Mechatronics from South Tehran Branch, Azad University. During his PhD he designed and developed a bio-inspired inverse kinematic algorithm for anthropomorphic robotic manipulators, and designed and developed a unified motion planning and compliance control framework for upper-arm neuro-rehabilitation robotic task. He has also undertaken research on design, fabrication, and modeling on soft origami actuators at the Center for Micro-BioRobotics (CMBR), IIT as a postdoctoral researcher. In 2019 he joined the Computer Vision and Robotics Division, Farm Tech Group at Wageningen University & Research and is currently working on soft adhesive grippers for delicate crop handling. His research interests include: robotics, self-learning, self-modelling, control, human-robot interaction, soft robotics, and soft actuators.



Dr. Andon V. Topalov received his MSc degree in Control Engineering from the Faculty of Information Systems, Technologies, and Automation at Moscow State University of Civil Engineering (MGGU) in 1979. He then received his PhD degree in Control Engineering from the Department of Automation and Remote Control at Moscow State Mining University (MGU), Moscow, in 1984. From 1985 to 1986, he was a Research Fellow in the Research Institute for Electronic Equipment, ZZU AD, Plovdiv, Bulgaria. In 1986, he joined the Department of Control Systems, Technical University of Sofia at the Plovdiv campus, where he is presently a Full Professor. He has been elected to the grade of IEEE senior member, awarded the gold badge of the Federation of Scientific and Technical Unions of Bulgaria, and has held long-term visiting professor/scholar positions at various institutions in South Korea, Turkey, Mexico, Greece, Belgium, UK, and Germany. Prof. Topalov has co-authored three books, edited three books, and authored or co-authored more than 100 research papers in conference proceedings and journals. His current research interests are in the fields of intelligent control, and smart and collaborative robots.

Contents

Preface	XIII
Section 1	
Robotics and Emotional Intelligence	1
Chapter 1	3
Motion Generation during Vocalized Emotional Expressions and Evaluation in Android Robots <i>by Carlos T. Ishi</i>	
Chapter 2	23
Computer Simulation of Human-Robot Collaboration in the Context of Industry Revolution 4.0 <i>by Yusie Rizal</i>	
Chapter 3	45
Emoji as a Proxy of Emotional Communication <i>by Guillermo Santamaría-Bonfil and Orlando Grabiel Toledano López</i>	
Chapter 4	65
Living and Interacting with Robots: Engaging Users in the Development of a Mobile Robot <i>by Valerie Varney, Christoph Henke and Daniela Janssen</i>	
Section 2	
Robotics Control	75
Chapter 5	77
Electromechanical Analysis (MEMS) of a Capacitive Pressure Sensor of a Neuromate Robot Probe <i>by Hacene Ameddah</i>	
Chapter 6	89
Physical Interaction and Control of Robotic Systems Using Hardware-in-the-Loop Simulation <i>by Senthil Kumar Jagatheesa Perumal and Sivasankar Ganesan</i>	
Chapter 7	105
Toward Dynamic Manipulation of Flexible Objects by High-Speed Robot System: From Static to Dynamic <i>by Yuji Yamakawa, Shouren Huang, Akio Namiki and Masatoshi Ishikawa</i>	

Trajectory Tracking Using Adaptive Fractional PID Control of
Biped Robots with Time-Delay Feedback

by Joel Perez Padron, Jose P. Perez, C.F. Mendez-Barrios and V. Ramírez-Rivera

Preface

Robotics research has increased significantly in the past decades and continued to strengthen when the industry revolution 4.0 was recently announced. The robot has changed significantly from a simple machine to become a reliable assistant. It has various shapes to enable it to do a variety of tasks, from a simple form to complicated forms such as humanoid form or animal form. Currently, the researchers are focused on making the robot more intelligent and to behave like a human. The evolution of sensors has made the robot more flexible and advanced. The sensor has evolved enough to cover the five human senses (visual, auditory, touch, taste, and smell).

The goal of this book is to give a clear vision toward the growth of robotics research, especially on the area of humanoid robots and emotional intelligence. *Humanoid* is related to the shape of a robot that resembles a human, not only in appearance but how they move, talk, or respond to the command. The humanoid form is very complicated and involves various sensors and controls such as a gyroscope to manage the walk and constant balancing, sonar sensor to detect and avoid an obstacle, etc. Emotional intelligence is responsible for making the robot smart and it controls their behavior, such as giving the robot the feeling of taste like a human being. Adding emotional intelligence to a humanoid robot will enrich the interaction rates. An individual user, such as a child, needs a robot that can understand their feeling and behave like their friend, so there will be intense interaction between them. Children do not have strong affection when the robot behaves like a machine and acts motionless. Therefore, to allow for robot co-existence with human, a robot must do complicated analysis, such as face scans, gait analysis mimics, and voice or gesture recognition.

This book can be used as a reference for researchers, students, or even practitioners in various fields such as medical, engineering, education, etc. The book consists of eight chapters that are divided into two main sections. The first section focuses on the emotional intelligence application and the second section concentrates on robotics control. The chapters in this book are sorted alphabetically based on the first name of the authors. The chapters should give the reader a general perspective on the direction of robotics research and emotional intelligence. Chapter 1 describes the motion generation during vocalized emotional expression to enrich human-robot interaction. Chapter 2 reports the general overview related to computer simulation of human-robot collaboration. In Chapter 3, emoji is presented as a proxy for emotional communication, and Chapter 4 focuses on how humans can live and interact with a robot.

As mentioned previously, the second section describes the control of the robotics in general. Chapter 5 presents an electromechanical analysis for giving capacitive touch sensation in a robot. Chapter 6 provides a discussion about physical

interaction and control of the robot. Chapter 7 reports on how a robot can manipulate flexible objects and Chapter 8 presents trajectory tracking based on adaptive PID control.

Ahmad Hoirul Basori

Faculty of Computing and Information Technology Rabigh,
Department of Information Technology Rabigh,
King Abdulaziz University,
Makkah, Saudi Arabia

Ali Leylavi Shoushtari, PhD

Postdoctoral Research Associate,
Computer Vision and Robotics Division,
Farm Technology Group,
Plant Sciences Department,
Wageningen University & Research,
Wageningen, The Netherlands

Andon Venelinov Topalov

Department of Control Systems,
Technical University of Sofia,
Branch in Plovdiv,
Plovdiv, Bulgaria

Section 1

Robotics and Emotional Intelligence

Motion Generation during Vocalized Emotional Expressions and Evaluation in Android Robots

Carlos T. Ishi

Abstract

Vocalized emotional expressions such as laughter and surprise often occur in natural dialogue interactions and are important factors to be considered in order to achieve smooth robot-mediated communication. Miscommunication may be caused if there is a mismatch between audio and visual modalities, especially in android robots, which have a highly humanlike appearance. In this chapter, motion generation methods are introduced for laughter and vocalized surprise events, based on analysis results of human behaviors during dialogue interactions. The effectiveness of controlling different modalities of the face, head, and upper body (eyebrow raising, eyelid widening/narrowing, lip corner/cheek raising, eye blinking, head motion, and torso motion control) and different motion control levels are evaluated using an android robot. Subjective experiments indicate the importance of each modality in the perception of motion naturalness (humanlikeness) and the degree of emotional expression.

Keywords: emotion expression, laughter, surprise, motion generation, human-robot interaction, nonverbal information

1. Introduction

Vocalized emotional expressions such as laughter and surprise (usually accompanied by verbal interjectional utterances) often occur in daily dialogue interactions, having important social functions in human-human communication. Laughter and surprise utterances are not only simply related to funny or emotional reactions but also can express an attitude (like friendliness or interest) [1, 2].

Therefore, it is important to account for such vocalized emotional/attitudinal expressions in robot-mediated communication as well. Since android robots have a highly humanlike appearance, natural communication with humans can be achieved through several types of nonverbal information, such as facial expressions and head/body gestures. There are numerous studies regarding facial expression generation in robots [3–11]. Most of these are related to symbolic (static) facial expression of the six traditional emotions (happy, sad, anger, disgust, fear, and surprise). However, in real daily interactions, humans can express several types of emotions and attitudes by making subtle changes in facial expression and head/body motion.

When expressing an emotion, humans not only use facial expressions but also synchronize other modalities, such as head and body movements as well as vocalic expressions. Due to a high humanlike appearance in androids, the lack of a modality or of a suitable synchronization among different modalities can cause a strongly negative impression (the “uncanny valley”), when an unnatural facial expression or motion is produced. Therefore, it is important to clarify methodologies to generate motions that look natural, through appropriate timing control.

The author’s research group has been working on improving human-robot communication, by implementing humanlike motions in several types of humanoid robots. So far, several methods for automatically generating lip and head motions of a humanoid robot in synchrony with the speech signal have been proposed and evaluated [12–15]. Throughout the evaluation experiments, it has been observed that more natural (humanlike) behaviors by a robot are expected, as the appearance of the robot approaches the one of a human, such as in android robots. Furthermore, it has been observed that unnaturalness occurs when there is a mismatch between voice and motion, especially during short-term emotional expressions, like in laughter and surprise. To achieve a smooth human-robot interaction, it is essential that natural (humanlike) behaviors are expressed by the robot.

In this chapter, motion generation for two vocalized emotional expressions, laughter and surprise, is being focused on. These are usually shorter in duration in comparison to other emotion expressions like happiness, sadness, anger, and fear, and thus it is important to account for a suitable timing control between voice and movements of facial parts, head, and body. The control of different modalities is investigated for achieving natural motion generation during laughter and surprise events of humanoid robots (i.e., when the robot produces a laughter or a vocalized surprise reaction).

In Section 2, related works on motion analysis and generation during emotion expression are presented. In Section 3, the motion generation methods for laughter and surprise expressions are described, along with the motion control methods of an android robot. The motion generation methods are based on analysis results of human behaviors during dialogue interactions [16, 17]. Sections 4 and 5 present evaluation results on the effectiveness of controlling different modalities of the face, head, and upper body (eyebrow raising, eyelid widening/narrowing, lip corner/cheek raising, eye blinking, head motion and torso motion control) and different motion control levels for laughter and surprise expressions. The effects of each modality are investigated through subjective experiments using an android robot as test bed. Section 6 concludes the chapter and presents future work topics. The contents of this chapter are partially included in the author’s previously published studies [18, 19]. Readers are invited to refer to those studies, for more details on the motion analysis results.

2. Related work

As stated in the introduction, it is important to synchronize a variety of modalities, including facial movements, speech, and head/body movements, in order to suitably express an emotion.

It has been reported in the emotion-recognition field that the use of both audio and visual modalities provides higher recognition rates than using a single modality [20, 21]. It is also reported that using face and head modalities in combination to the speech modality improves the expression of an emotion in CG (computer graphics) animation, in comparison to using only the face modality [22].

The synchronization of speech and facial expression has also been investigated.

It has been reported that the emotion perceived from the facial expression is altered, when there is a mismatch between the emotions conveyed by the voice and by facial expressions [23]. It has also been reported that when both voice and facial expressions are presented, the judgment of the perceived emotion is strongly influenced by one of the modalities, if the emotion expression of the other modality is ambiguous [24]. It has also been reported that there is a systematic link between eyebrow movements and the fundamental frequency of the voice [25].

Various methods have been proposed for generating several types of facial expressions in android robots [5–11]. However, most of these methods are based on FACS (facial action coding system [26]) for positioning and controlling the actuators to reproduce humanlike facial expressions or for modeling skin deformation based on mechanical deformation models. Furthermore, there has been no evaluation of the synchronization of speech and facial expression and the face-body-head coordination, in all of these works. It is important to evaluate the effects of multimodal expression, for expressing differences of nuance in emotion rather than merely evaluating symbolic facial expressions. Previous studies indicate that the facial parts should also be moved in synchrony with the changes in speech features, in order to achieve natural motion generation. From the same perspective, head and body modalities should also be controlled in synchrony with speech.

However, no previous studies have tackled the challenge of developing suitable multimodal expression control in android robots.

Regarding laughter motion generation particularly, several studies have been reported in the CG animation field. Most of them are related to the ILHAIRE project [27]. For example, a model which generates facial motion position only from laughter intensity is proposed, based on the relation between laughter intensity and facial motion [28]. In [29], the laughter synthesis model above is extended by adding laughter duration as input and selecting recorded facial motion sequences from human motion data. A multimodal laughter animation synthesis method is proposed in [30], by generating lip and jaw motions from speech and pseudo-phoneme features, head and eyebrow motions from pseudo-phoneme and duration features, and torso and shoulder motions from head pitch rotation. In [31], methods to generate rhythmic body movements (torso leaning and shoulder vibration) during laughter are proposed. The torso leaning and shoulder vibrations are reconstructed from human-captured data through synthesis of two harmonics.

Another issue regarding robotics application is that android robots have limitations in the motion DOF (degrees of freedom) and motion range, different from CG agents. Those studies on CG agents have assumed rich 3D models for facial motions, which cannot be directly applied to the android robot control. Therefore, it is important to clarify the effectiveness of different motion generation strategies for providing natural impressions during emotional expressions, under limited DOFs. Some studies have implemented facial expression of smiling or laughing in robots for human-robot interaction [3, 4]. However, these dealt with symbolic facial expressions, so that dynamic features and other modalities during laughter are not taken into account.

In this study, the motion coordination and the effects of several modalities are taken into account for the motion generation in laughter and vocalized surprise expressions.

3. Motion generation in laughter and surprise expressions

The motion generation methods during laughter and surprise utterances are based on analysis results on human-human dialogue interaction data [16–19]. The motion generation methods account for dynamic properties of a motion in synchrony with speech (i.e., when a motion starts and ends relative to the laughter/

surprise expression). The main results of motion timing analyses are summarized in Section 3.1. The motion generation approaches for laughter and surprise expressions and the motion control methods in an android robot are described in Section 3.2.

3.1 Motion timing analysis results

Analysis on laughter motion data indicates that the start time of the smiling facial expression (eye narrowing and lip corner raising) usually matches with the start time of the laughing speech, while the end time of the smiling face (i.e., the instant the face turns back to the normal face) is usually delayed relatively to the end time of the laughing speech by 1.2 ± 0.5 s. An eye blinking is usually accompanied at the instant the face turns back from the smiling face to the normal face. This was observed in 70% of the laughter events. Regarding lip corner raising, it was observed that the lip corners are clearly raised at the laughter segments by expressing a smiling face, while they are slightly raised over a longer period in non-laughing intervals by expressing a slightly smiling face. The percentage in time of smiling faces was 20%, while by including slight smiling faces the percentage in time was 81% on average, ranging from 65 to 100% (i.e., one of the speakers showed slight smiling facial expressions over the whole dialogue). Obviously, these percentages are dependent on the person and the dialogue context. In the analyzed data, most of the conversations were in joyful context. Regarding the upper-body motion, both forward and backward motions are observed. The pitch angle rotation velocities for upper-body motion were $10 \pm 5^\circ/\text{s}$ for forward and $-10 \pm 4^\circ/\text{s}$ for backward directions.

The main findings for the analysis on surprise motion are as follows. First, the occurrence rate of a motion during surprise utterances varies depending on whether the surprise expression is emotional/spontaneous, intentional/social, or quoted, and this rate is highly correlated to the degree of expression in emotional/spontaneous surprise. Second, different motion types have different occurrence rates according to the surprise expression degree. In particular, body backward motion appears with higher frequency when expressing high surprise degrees. Regarding motion time issues, the onset instants of face, head, and body motion are most of the time synchronized with the start time of the surprise utterances, while offset instants are usually later than the end time of the utterances, similarly to the observations in laughter motion analysis. However, the offset times were different. For eyebrow raise, the onset duration was faster than the offset duration, with averages around 200–300 ms for onset and 400–500 ms for offset. For the upper body, onset and offset durations were both around 0.8 s for small movements, and around 1.2 and 1.5 s for large movements.

More details on the motion analysis results can be found in [16–19], including different types and functionalities of laughter and surprise in natural dialogue interactions.

3.2 Description of motion generation in laughter and surprise expressions and control methods in an android robot

Based on the motion timing analysis results presented in Section 3.1, motion generation methods during laughter and surprise utterances are proposed, by accounting for the following modalities: facial expression control (eyelid narrowing and lip corner raising for laughter, eyelid widening and eyebrow raising for surprise), head motion control (head pitch direction), eye blinking control at the transition between smiling/surprising face to the neutral face, and body motion control (torso pitch direction).

Figure 1 shows a block diagram of the motion generation method for laughter and surprise utterances in an android robot. The method requires the speech signal and the laughing/surprise intervals as input. In autonomous robots, the laughing speech intervals

and surprise utterance intervals are given a priori, while in tele-operated robots, these have to be automatically detected from the speech signal of the tele-operator.

A female-type android robot, called ERICA, was used to evaluate the effects of different modalities for motion generation. However, the methodology can be applied to any robot having equivalent degrees of freedom (DOFs). **Figure 2** shows the external appearance and the actuators of the android robot.

As shown in **Figure 2**, the android ERICA has 13 degrees of freedom for the face, 3 degrees of freedom for the head motion, and 2 degrees of freedom for the upper-body motion. Among these, the following ones were controlled for laughter and surprise expressions: upper eyelid control (actuator 1), lower eyelid control (actuator 5), eyebrow raise control (actuator 6), lip corner raise control (actuator 8, cheek is also raised), lip corner stretch control (actuator 10), jaw lowering (mouth opening) control (actuator 13), head pitch control (actuator 15), and upper-body pitch control (actuator 18). All actuator commands range from 0 to 255. The numbers in red in **Figure 2** indicate default actuator values for the neutral position.

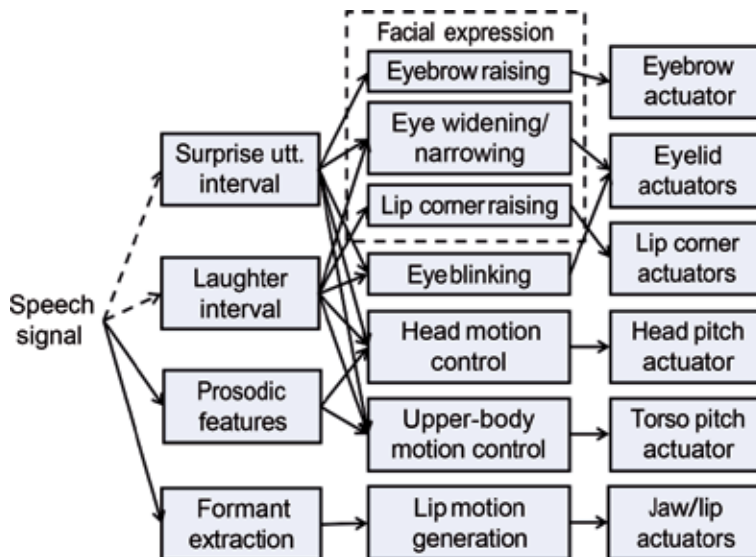


Figure 1.
 Block diagram of the motion generation during laughing speech and surprise utterances.

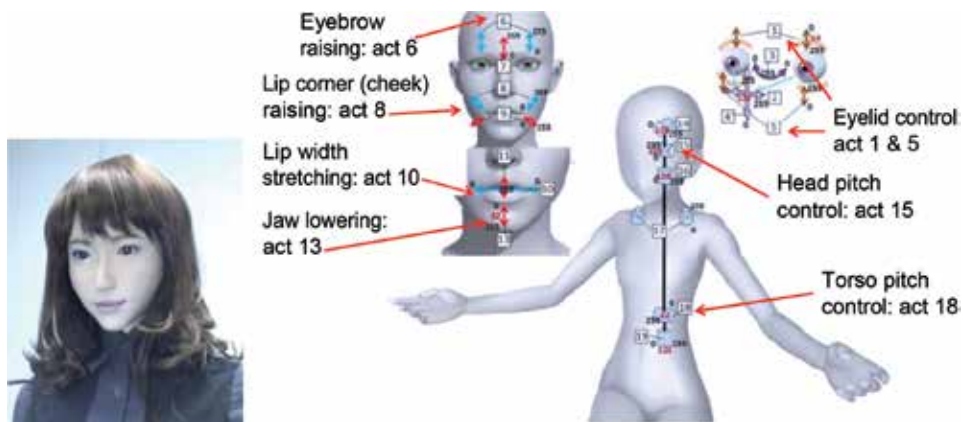


Figure 2.
 External appearance of the female-type android robot ERICA and corresponding actuators.

3.2.1 Facial motion control

Before explaining how the facial motion is controlled for different facial expressions, it is worth to clarify that the actuator values presented in this section were manually adjusted for the android ERICA, in order to achieve a desired facial expression. Thus, the actuator values are included for reference, but for other robots having different actuation ranges, these values have to be adjusted by looking at the resulting facial expressions.

For the facial expression during laughter, the lip corner is raised ($\text{act}[8] = 200$), and the eyelids are narrowed ($\text{act}[1] = 128$, $\text{act}[5] = 128$). These values were set so that a smiling face can be clearly identified, as shown in the right panel of **Figure 3** (compare the generated smiling face in the right panel with the neutral face in the left panel). The mouth aperture depends on the vocalic contents of the laughing voice, as will be explained later. The timing of the facial motion control is based on the analysis results, so that the eyelid and lip corner actuator commands are sent at the instant the laughing speech interval starts, and the actuator commands are set back to the neutral position 1–1.5 s after the end of the laughing speech interval.

During preliminary analysis on motion generation, it has been observed that the facial expression of the neutral face (i.e., in non-laughter intervals) looked scary for the context of a joyful conversation. In fact, the lip corners were slightly or clearly raised in 80% of the dialogue intervals. A slight smile face was kept during non-laughter intervals, by controlling the eyelids and lip corner actuators to have intermediate values between the laughter smiling face and the neutral (non-expression) face. For the facial expression during the idle slight smile face, the lip corner is partially raised ($\text{act}[8] = 100$), and the eyelids are partially narrowed ($\text{act}[1] = 90$, $\text{act}[5] = 80$), to obtain the impression of a slight smiling face, as shown in the middle panel of **Figure 3**.

For the facial expression in surprise utterances, the eyebrow raise and eyelid widening are coordinated and controlled at two levels of expression. The target actuator values are set by looking at the facial expressions of the android robot, in order to provide an appearance of a slight surprise face for level 1 and a clear surprise face for level 2. For the android ERICA, the target eyebrow actuators are set to $\text{act}[6] = 127$ for level 1 and $\text{act}[6] = 255$ for level 2, and the upper and lower eyelid actuators are set to $\{\text{act}[1] = 80; \text{act}[5] = 60\}$ for level 1 and $\{\text{act}[1] = 40; \text{act}[5] = 30\}$ for level 2. For the neutral idle face (corresponding to level 0), these actuators are set to $\{\text{act}[6] = 0; \text{act}[1] = 90; \text{act}[5] = 80\}$. As stated before, these values have to be manually adjusted for different robots, in a way to obtain the desired



Figure 3. Examples of generated facial expressions by eyelid and lip corner control: neutral face (left), idle slight smile face in non-laughter intervals (middle), and smile face during laughter intervals (right).

facial expression. **Figure 4** shows examples of the produced facial expressions for each of these levels. The facial expression at level 1 may not appear to be a surprised facial expression by only looking at the static picture. However, when looking at the facial movements from the neutral face, it is possible to perceive a change in the facial expression.

Regarding the timing of motion control, the eyelid and eyebrow actuator commands are sent at the instant the surprise utterance interval starts, and the actuator commands are set to move back to the neutral position within 0.5 s after the end of the utterance.

For both laughter and surprise expressions, an eye blinking motion is added, considering that an eye blinking is usually accompanied when the facial expression turns back to the neutral face. An eye blink is implemented in the android, by closing the eyes (act[1] = 255 and act[5] = 255) during a brief period of 100 ms and opening the eyes back to the neutral face (act[1] = 64, act[5] = 0) or to an idle smiling face (act[1] = 90; act[5] = 80), as shown in the left and middle panels of **Figure 3**.

3.2.2 Upper-body motion control

For laughing speech, the upper body is moved to the forward and backward directions. In order to achieve smooth movements, the upper-body actuator is controlled according to half cosine functions, as defined in the following expressions:

$$torsopitch[t] = upbody_{target} \times \frac{1 - \cos\left(\frac{\pi t}{T_{max}}\right)}{2} \quad (1)$$

The upper body is moved from the start point of a laughing speech interval, in order to achieve a maximum target angle corresponding to the actuation value $upbody_{target}$, in a time interval of T_{max} .

From the end point of the laughing speech interval, the upper body is moved back to the neutral position according to an inverse cosine function as shown in the following expression.

$$torsopitch[t] = (upbody_{end} - upbody_{neutral}) \times \frac{1 - \cos\left(\pi + \pi \frac{t - t_{end}}{T_{max}}\right)}{2} \quad (2)$$

$upbody_{end}$ and t_{end} are the actuator value and the time at the end point of the laughter speech interval, and $upbody_{neutral}$ corresponds to the actuator value for the



Figure 4. Examples of generated facial expressions for eyebrow and eyelid control at level 0 (neutral idle face, left), level 1 (slight surprise face, middle), and level 2 (clear surprise face, right).

android's neutral pose. Thus, if the laughter interval is shorter than T_{max} , the upper body does not achieve the maximum angle.

The $upbody_{target}$ was adjusted to -10 degrees (which is the mean body pitch angle range in human data), and the time interval T_{max} to achieve the maximum angle was adjusted to 1.5 s (a bit longer than the human average time, to avoid jerky motion in the android).

For surprise utterances, the upper body is moved in the backward direction at the start point of the surprise utterance and then moved back to the neutral position. Two levels are controlled corresponding to about 2 degrees for level 1 and 4 degrees for level 2 (which was the maximum angle achieved by the android).

Regarding the timing control, the upper body is moved back to the neutral position from 0.3 s after the end point of the surprise utterance interval. The onset duration to achieve the maximum angle is set to 0.8 s, while the offset duration to move back to the neutral idle position is set to 1.5 s. Half cosine functions are used to smooth motion velocity changes in the current and target positions, as in the expressions (1) and (2) for laughter motion control.

The torso pitch actuator in the android (actuator 18) is then controlled around the neutral pose actuator value ($upbody_{neutral}$), according to the following expression:

$$act[18] = upbody_{neutral} + torsopitch[t] \quad (3)$$

3.2.3 Head motion control

For the head motion control, a method for controlling the head pitch (vertical movements) from the voice pitch (fundamental frequencies, $F0$) is employed. This is based on the fact that there is some correlation between head motion and voice pitch [15, 32]. Although this correlation is not very high (i.e., this control strategy is not exactly what humans do during speech), natural head motions are expected to be generated during laughing and surprise expressions, since humans usually tend to raise the head for high $F0$ s especially in inhaling laughter intervals, and high-pitched surprise utterances. The following expression is used to convert $F0$ values to the head pitch actuator:

$$headpitch_F0[t] = (F0[t] - center_F0) \times F0_scale \quad (4)$$

where $center_F0$ is the speaker's average $F0$ value (around 120 Hz for male and around 240 Hz for female speakers) converted to semitone units and $F0$ is the current.

$F0$ value (in semitones) and $F0_scale$ is a scale factor for mapping the $F0$ (voice pitch) changes to head pitch movements. For the experiments, $F0_scale$ is set in a way that a 1-semitone change in voice pitch corresponds to ~ 1 -degree change in head pitch rotation.

Preliminary evaluation has shown that the robot motion looked unnatural during a surprise expression, when the head was facing the upward direction, while the body moved in the backward direction. In fact, it has been observed from the human motion data that the speaker is usually looking at the dialogue partner during a surprise expression. The following additional control in the head pitch actuator deals with this issue, by moving the head in the inverse direction to the body pitch movement:

$$headpitch[t] = headpitch_F0[t] - torsopitch[t] \quad (5)$$

The head pitch actuator in the android (actuator 15) is then controlled around the neutral pose actuator value ($headpitch_{neutral}$), according to the following expression:

$$act[15] = headpitch_{neutral} + headpitch[t] \quad (6)$$

3.2.4 Lip motion control

The lip motion is controlled based on a formant-based lip motion control method [12]. The method is based on the fact the first and second formants (resonance frequencies in the vocal tract) can be associated to the lip height and lip width, respectively, after some speaker normalization procedure. The jaw actuator (actuator 13) is controlled using the estimated lip heights, and the lip stretch actuator (actuator 10) is controlled using the estimated lip widths.

In this way, appropriate lip shapes can be generated in laughter segments with different vowel qualities (such as in “hahaha” and “huhuhu”) as well as in vocalized surprise segments with different vowel qualities (such as in “eh!” and “ah!”), since the method is based on the vowel formants.

4. Evaluation of the laughter motion generation

This section presents evaluation results on the laughter motion generation method, by controlling different modalities of the face, head, and body. The experimental setup is described in Section 4.1; the evaluation results and the interpretation of the results are presented in Section 4.2.

4.1 Experimental setup

Two conversation passages of about 30 s including multiple laughter events were extracted from a dialogue database, and the corresponding motion data was generated in the android ERICA, based on the method described in the Section 3.2. The speech signal and the laughter speech interval information are provided as input. The two conversation passages were extracted from different speakers and will be named “voice 1” and “voice 2.” “voice 1” includes social and embarrassed laughter, while “voice 2” includes emotional and funny laughter.

Table 1 shows the five motion types (named “A”–“E”) generated in the android, taking the effects of different modalities into account.

“Eyelids” and “lip corners” are controlled to express a smiling facial expression (corresponding to Duchenne smile faces [33]) during laughter. These are present in all conditions. “Lip corners” corresponds to a lip corner raising motion, which is also accompanied by a cheek raising motion in the android, while “eyelids” corresponds to an eye narrowing motion.

“Eye blink” corresponds to an eye blinking motion, when the face expression is turned back to the neutral (idle) face, from a smiling face. “Head” corresponds to the motion control of the head pitch (vertical head movements) from the voice pitch. “Idle smile face” corresponds to a slight smiling face during non-laughter intervals. “Upper body” corresponds to the motion control of the torso pitch (front-back upper-body movements) in long laughter events.

Video clips are recorded for each motion type and used in the subjective evaluation experiments. Video-based evaluation is conducted instead of face-to-face evaluation since the participants do not interact with the robot. Pairwise comparisons are conducted in order to investigate the effects of the different motion controls. The evaluated motion pairs are described in **Table 2**.

Motion	Controlled modalities
A	Face (eyelids + lip corners) + eye blink + head
B	Face (eyelids + lip corners) + head
C	Face (eyelids + lip corners) + eye blink
D	Face (eyelids + lip corners) + eye blink + head + idle smiling face
E	Face (eyelids + lip corners) + eye blink + head + idle smiling face + upper body

Table 1.
The controlled modalities for generating five motion types during laughter events.

Motion pair	Differences in the controlled modalities
A vs. B	Presence/absence of “eye blink” control (“eyelids,” “lip corners,” and “head” are in common)
A vs. C	Presence/absence of “head” control (“eyelids,” “lip corners,” and “eye blink” are in common)
A vs. D	Absence/presence of “idle smiling face” control (“eyelids,” “lip corners,” “eye blink” and “head” are in common)
D vs. E	Absence/presence of “upper-body” control (“eyelids,” “lip corners,” “eye blink,” “head,” and “slightly smiling face” are in common)

Table 2.
Motion pairs for comparison of the effects of different modalities in laughter.

In the evaluation experiments, pairs of videos are presented for the participants. The order of the videos for each pair is randomized. The videos are allowed to be replayed at most two times each.

After watching each pair of videos, participants are asked to grade the preference scores for pairwise comparison, and the overall naturalness scores for the individual motions, in 7-point scales, according to the questionnaire below. The numbers within parenthesis are used to quantify the perceptual scores.

Q1. Which motion looked more natural (humanlike)? Motion A is clearly more natural (−3), Motion A is more natural (−2), Motion A is slightly more natural (−1), Difficult to decide (0), Motion B is slightly more natural (1), Motion B is more natural (2), Motion B is clearly more natural (3).

Q2. Is the motion natural (humanlike)? very unnatural (−3), unnatural (−2), slightly unnatural (−1), difficult to decide (0), slightly natural (1), natural (2), very natural (3).

The first question was answered for each video pair, while the second question was answered for each of the individual videos. For the motion types A and D, which appear multiple times, individual scores are graded only once, at the first time the videos are seen. Besides the perceptual scores, participants are also asked to write the reason of their judgments, if a motion is perceived as unnatural.

The sequence of motion pairs above was evaluated for each of the conversation passages (“voice 1” and “voice 2”). Twelve remunerated subjects (male and female, aged from 20 to 40 s) participated in the evaluation experiments.

4.2 Evaluation results

Figure 5 shows the evaluation results for pairwise comparisons. Statistical analyses are conducted by t-tests (* for $p < 0.05$ and ** for $p < 0.01$ confidences). For the preference scores in the pairwise comparison, significance tests are conducted in comparison to 0 scores, which correspond to unperceivable differences.

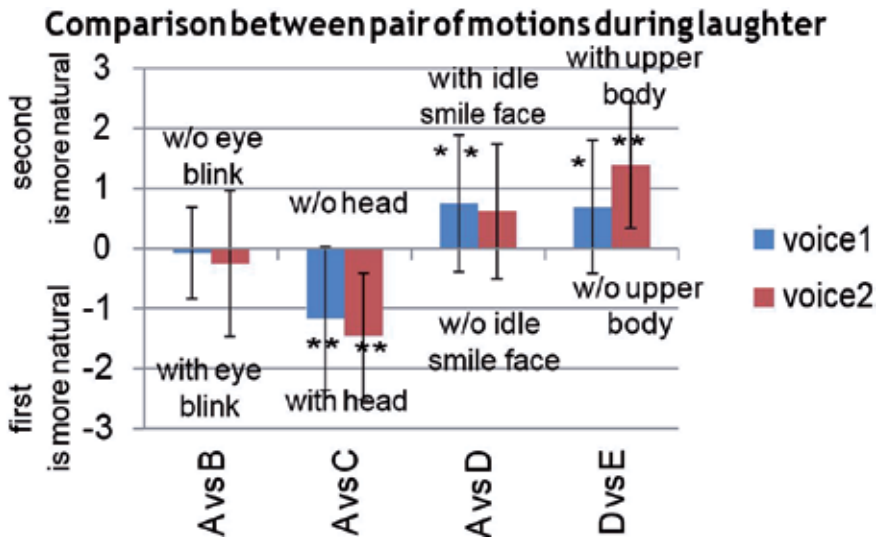


Figure 5. Subjective preference scores between motion pairs in laughter motion generation (average scores and standard deviations). (Negative average scores indicate the first condition was preferred, while positive average scores indicate that the second condition was preferred).

The differences between the motion types A and B (with and without eye blinking control) are subtle, so that most of the participants could not perceive differences. However, subjective scores showed that the inclusion of eye blinking control was evaluated to look more natural for both conversation passages (“voice 1” and “voice 2”).

The comparison between the motion types A and C (with and without head motion control) indicates that the inclusion of head motion control clearly increases the motion naturalness ($p < 0.01$) for both “voice 1” and “voice 2.” The participants’ judgments were remarkable (the differences in the motion videos were clear).

The comparison between the motion types A and D (without or with idle smile face) indicates that keeping a slight smiling face in the intervals other than laughing speech was also effective to increase motion naturalness ($p < 0.01$).

Finally, the comparison between the motion types D and E (with and without upper-body motion) indicates that the inclusion of upper-body motion also increases motion naturalness ($p < 0.05$ for “voice 1,” $p < 0.01$ for “voice 2”). The differences are more evident in “voice 2” (in comparison to “voice 1”) since “voice 2” contained longer duration for the laughter events within the conversation passage, and consequently the upper-body movements were more clear.

Figure 6 shows the results for perceived naturalness graded for each motion type. The results of subjective scores shown in **Figure 6** indicate that, overall, slightly natural to natural motions could be achieved by the laughter motion generation method including all motion control types.

The motion type C is the only one that received negative average scores, meaning that if the head does not move, the laughter motions will look unnatural. This indicates that the F_0 -based method for head pitch control is effective for increasing motion naturalness during laughter. However, some of the participants pointed out that the motions would look more natural, if other axes of the head also move. This is a topic for future work.

Regarding the insertion of eye blinking, at the instant the facial expression turns back to the neutral face (motion type B), although the comparisons between motion types A and B were not statistically significant (since the visual difference

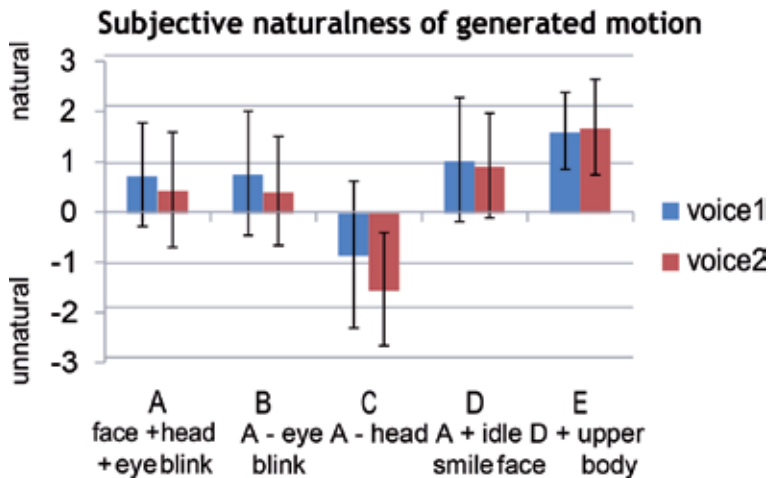


Figure 6. Subjective naturalness scores for each motion type in laughter motion generation (average scores and standard deviations).

is subtle). However, the participants who perceived the difference judged the presence of eye blinking to be more natural. The eye blinking control is thought to work as a cushion to alleviate the unnaturalness caused by sudden changes in facial expression. The insertion of such a small motion could possibly be used as a general method for other facial expressions.

The control of idle slight smile face in non-laughter intervals (motion type D) was shown to be effective to improve the naturalness, since the conversation context was in joyful situations. However, for a more appropriate control of slight smile face, detection of the situation might be important.

The reason why motion type E (with upper-body motion) was clearly judged as more natural than motion type D (without upper-body motion) for “voice 2” is that it looks unnatural if the upper body does not move during long and strong emotional laughter. The proposed upper-body motion control was effective to relieve such unnaturalness. Regarding intensity of the laughter, although it was implicitly accounted in the present work, by assuming high correlation between pitch and duration with intensity, it could also be explicitly modeled on the generated motions.

5. Evaluation of the surprise motion generation

This section presents evaluation results on the surprise motion generation method, by controlling different modalities and different control levels of the face, head, and body. The experimental setup is described in Section 5.1, and the evaluation results are presented and discussed in Section 5.2.

5.1 Experimental setup

The surprise motion generation method was evaluated for the interjectional utterances “e” and “a,” which are the ones that most frequently occurred in dialogue interactions for expressing surprise. Sixteen dialogue passages of about 10 s including interjectional utterances “e” or “a” expressing different degrees of surprise were extracted from the dialogue database. Then motion was generated in the android,

based on the method described in Section 3.2. The speech signal and the surprise utterance interval information are provided as input for motion generation.

Table 3 lists the six motion types generated in the android, for evaluating the effects of different modalities and different degrees of motion control, during surprise expressions. The motion types in **Table 3** are named according to the modality and control levels: “e” stands for eyebrow and eyelids, “h” for head, and “b” for body. The numbers following these letters indicate the control levels. Level “0” indicates no control, level “1” indicates small movements, and level “2” indicates large movements. The facial expressions of levels “1” and “2” for “eyebrows + eyelids” are shown in the middle and right panels in **Figure 4**. The levels “1” and “2” for body motion indicate maximum range of 2 and 4 degrees, respectively, as explained in Section 3.2. The head movements are controlled from the voice, so that 1-semitone change in voice pitch corresponds to ~1 degree for head pitch (Section 3.2). The six motion types were chosen in order to reduce the efforts of the annotators while allowing the comparison of pairs between presence/absence and degree of a motion.

Video clips were recorded, for each motion type and each dialogue passage, to be used in the subjective experiments.

Considering that the range and amount of body movements will be small in short interjectional utterances (around 200 ms), only the three motion types without body control (e2 + h0 + b0, e1 + h1 + b0, and e2 + h1 + b0) were evaluated for short interjectional utterances. For the long interjectional utterances, all six motion types were evaluated. From the eight “a” utterances, seven were short, while from the eight “e” utterances, four were short. Thus, a total of 63 videos ((7 + 4) × 3 short utterances + (1 + 4) × 6 long utterances) were used for evaluation.

In the experiments, the participants are asked to watch all 63 videos and to grade each video with perceptual subjective scores, according to the questionnaire below. The numbers within the parentheses were used to quantify the perceptual scores. The order of the videos is randomized, and the participants are allowed to watch at most two times each.

Q1. What is the perceived degree of surprise expression (regardless of whether an expression is emotional/spontaneous or social/intentional)? No expression (0), slight expression (1), clear expression (2), strong expression (3).

Q2. Is the motion natural (humanlike)? Very unnatural (-3), unnatural (-2), slightly unnatural (-1), difficult to decide (0), slightly natural (1), natural (2), very natural (3).

Q3. Do you feel that the surprise expression is emotional/spontaneous or social/intentional? Intentional (-2), slightly intentional (-1), difficult to decide (0), slightly emotional (1), emotional (2).

Motion type	Controlled modalities
e2 + h0 + b0	Eyebrows + eyelids (level 2)
e2 + h0 + b2	Eyebrows + eyelids (level 2) + body (level 2)
e1 + h1 + b0	Eyebrows + eyelids (level 1) + head
e2 + h1 + b0	Eyebrows + eyelids (level 2) + head
e2 + h1 + b1	Eyebrows + eyelids (level 2) + head + body (level 1)
e2 + h1 + b2	Eyebrows + eyelids (level 2) + head + body (level 2)

Table 3.
Modalities controlled for generating six motion types in surprise utterances.

Eighteen remunerated subjects (male and female, aged from 20s to 40s) participated in the evaluation experiments.

5.2 Evaluation results

We consider that the degree of surprise expression is affected by both audio and visual modalities. In order to account for the effects of the voice modality, the utterances used in the experiment were categorized into three levels, according to their perceptual degrees of surprise graded only from the voice. The resulting number of utterances was 8 for voice group 1 (all short interjections), 7 for voice group 2 (3 short and 4 long interjections), and 1 for voice group 3 (long interjection).

Figure 7 shows the average subjective scores (vertical axes) for surprise expression degree, motion naturalness, and emotional/intentional impression, according to the voice groups (horizontal axes: surprise expression degrees by voice only), for each of the six motion types. Note that the different levels in the horizontal axis are based on voice only, while the subjective scores in the vertical axes are based on voice plus motion modalities.

Pairwise comparisons are conducted to investigate the effects of presence/absence or degree of motion control, and statistical significance tests are conducted through t-tests. Firstly, the effects of controlling the motion degrees of eyebrow and eyelids are analyzed by comparing motion types $e1 + h1 + b0$ and $e2 + h1 + b0$. It can be observed in the upper panel of **Figure 7** that the average perceptual scores for surprise expression degree increase by about 0.7 points (on a 0–3-point scale) for voice group 1 ($p < 0.01$) and by about 0.5 points in voice group 3 ($p < 0.01$). This indicates that a slight change in the eyebrow/eyelid control is effective for changing the perceived degree of surprise.

Next, the effects of controlling the head motion modality are analyzed by comparing the results for the motion types $e2 + h0 + b0$ and $e2 + h1 + b0$. The differences in surprise expression degree between these two motion types are about 0.2 points for voice group 1 ($p < 0.01$) and about 0.4 points for voice group 3 (n.s., $p = 0.09$), which are slightly smaller than the effects of eyebrow/eyelid control.

The effects of controlling the body motion modality are analyzed by comparing the results between the motion types $e2 + h0 + b0$ and $e2 + h0 + b2$ (when head motion is not controlled) or between the motion types $e2 + h1 + b0$ and $e2 + h1 + b2$ (when head motion is controlled). It is observed that, when head motion is not controlled ($h0$), the effects of controlling or not the body motion ($b0$ vs. $b2$) increase the surprise degrees by about 0.4–0.5 points for voice groups 2 and 3 ($p < 0.01$). When head motion is controlled ($h1$), the increase in the perceptual surprise degree is smaller by about 0.3 points ($h1 + b0$ vs. $h1 + b2$; $p < 0.05$), probably because the contribution of head motion is superimposed. Although the differences were not statistically significant, a gradual increase can be observed for the gradual control of body motion ($b0$ vs. $b1$ vs. $b2$, for the motion type $e2 + h1$).

Regarding the naturalness scores, the results in the middle panel of **Figure 7** indicate slightly natural to natural scores in almost all motion types. By comparing the motion types $e2 + h0 + b0$ and $e2 + h1 + b0$, it can be inferred that head motion has important effects on the naturalness (humanlike) perception when the body does not move ($b0$). The naturalness scores are increased by about 0.5 points on average ($p < 0.01$), by inclusion of head motion.

Regarding the subjective spontaneity degree, the results in the bottom panel of **Figure 7** show that the average scores in motion types $e1 + h1 + b0$ and $e2 + h0 + b0$ are negative in voice group 3, indicating that if the amount of motion decreases,

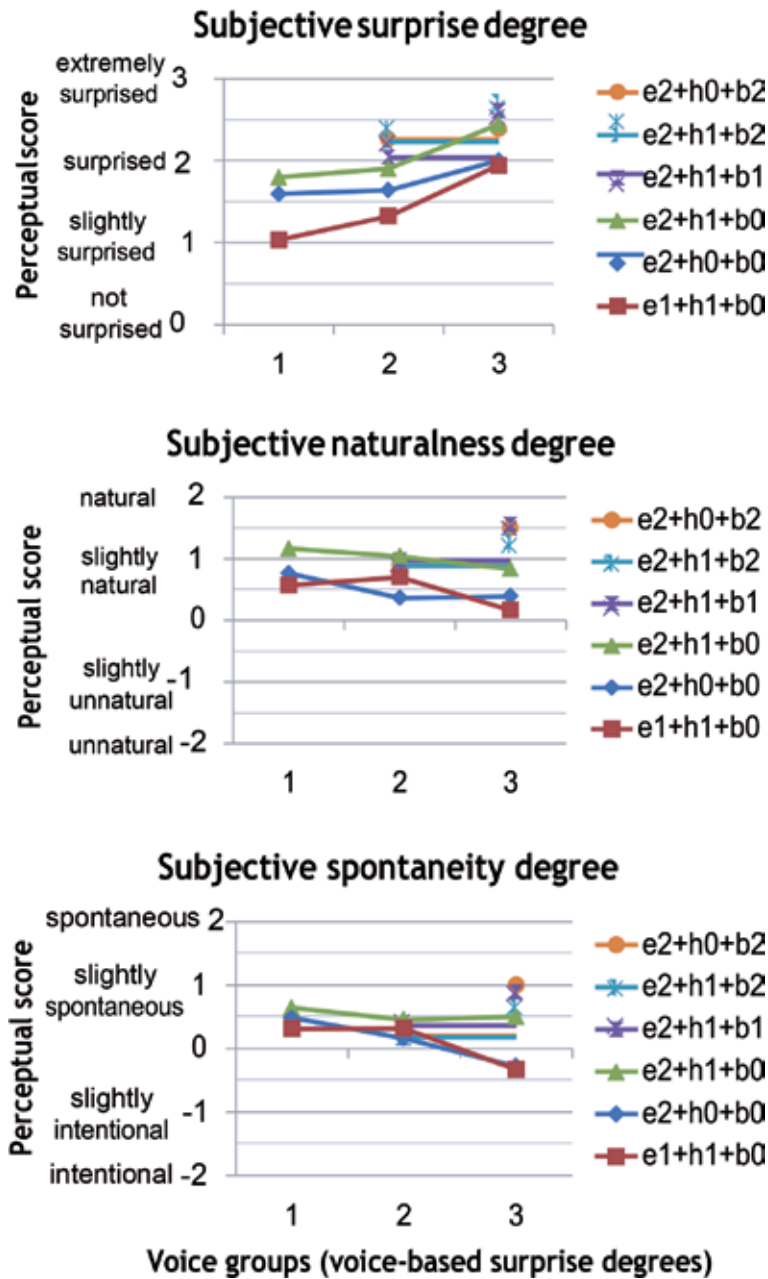


Figure 7. Subjective perceptual scores of surprise expression degree (top), naturalness degree (mid), and emotional/intentional impression degree (bottom) for each motion type, according to the voice groups (horizontal axis: voice-based surprise expression degrees).

the surprise utterances might be perceived as intentional rather than emotional ($p < 0.01$). On the other hand, the naturalness scores decrease in motion types with fewer motion (e1 + h1 + b0 and e2 + h0 + b0) in voice group 3 (high surprise expression degree by voice only), as shown in the middle panel of **Figure 7**. This is thought to be due to the mismatch between surprise expressions by voice and motion modalities. Another interpretation is that these motion types are perceived as being unnatural, because from the dialogue context, an emotional/spontaneous expression was expected.

Finally, regarding the effects of the voice modality, the results in the upper panel of **Figure 7** for the subjective surprise degrees clearly show that within a motion type, the subjective surprise degrees increase according to the voice groups (voice-based surprise degrees). This means that the perception of surprise degree is dependent on the surprise expression from the voice and, moreover, that by controlling the motion degrees of different modalities, the degree of surprise expression transmitted from the combination of voice and motion can be biased by a certain amount. For example, for the utterances in voice group 1, the subjective surprise degree can be raised to 1.8 on average by controlling the head and eye-brows ($e2 + h1 + b0$), while the utterances in voice group 3 can have their subjective surprise degree reduced to around 2 if the head and body are not controlled ($e2 + h0 + b0$).

6. Conclusion and final remarks

Methods for motion generation synchronized with laughter speech and vocalized surprise expressions were described, based on analysis results of human behaviors on facial, head, and body motions during dialogue interactions.

The effectiveness of controlling different modalities of the face, head, and upper body (eyebrow raising, eyelid widening/narrowing, lip corner/cheek raising, eye blinking, head pitch, and torso pitch motion control) and different motion control levels were evaluated using an android robot. The evaluation was conducted through subjective experiments, by comparing motions generated with different modalities and different motion control levels.

Evaluation results for laughter motion generation indicated that motion is perceived as unnatural, if only the facial expression (lip corner raising and eyelid narrowing) is controlled (without head and body motion control). The motion naturalness scores increased when head pitch, eye blinking (at the instant the facial expression turns back to neutral face), idle smile face (during non-laughter intervals), and upper-body motion are also controlled. The best naturalness scores are achieved when all modalities are controlled.

Evaluation results for surprise motion generation indicated that (1) eyebrow/eyelid motion control is effective in changing the perceptual degrees of surprise expression, (2) upper-body motion control is effective for increasing the degrees of surprise expression and naturalness, (3) head motion is more effective for increasing naturalness (rather than surprise degree), (4) the degrees of surprise expression for different motion types are biased by the surprise degrees expressed by the voice-only modality, and (5) utterances with high surprise degrees may be interpreted as intentional (rather than emotional or spontaneous) if they are not accompanied by upper-body motion.

In the present study, it was shown that with a limited number of DOFs (lip corner, eyelids, eyebrows, head pitch, torso pitch), natural motion could be generated for laughter and surprise expressions. Although the android robot ERICA is used as a test bed for evaluation, the described motion generation approach can be generalized for any robot having equivalent DOFs.

Remaining topics for future work include automatic detection of laughing speech intervals and surprise utterance intervals from acoustic features, in order to automate the motion generation process from the input speech signal. Prediction of surprise expression degrees from acoustic features and explicit modeling of laughter intensity are also remaining tasks for motion generation automation. The control strategy of head tilt and shake axes, the investigation of eye blinking insertion for alleviating unnaturalness caused by sudden changes in other facial expressions,

and the detection of situation for slight smile face control are remaining topics for improving motion naturalness.

Acknowledgements


This research was supported by JST/ERATO, Grant Number JPMJER1401. Special thanks go to Takashi Minato for the contributions in the android motion control and discussions on motion generation. The author also thanks Mika Morita, Megumi Taniguchi, Kyoko Nakanishi, and Tomo Funayama for their contributions in the data analysis and experimental setup.

Author details

Carlos T. Ishi
ATR Hiroshi Ishiguro Labs., Kyoto, Japan

*Address all correspondence to: carlos@atr.jp

IntechOpen

© 2019 The Author(s). Licensee IntechOpen. This chapter is distributed under the terms of the Creative Commons Attribution License (<http://creativecommons.org/licenses/by/3.0/>), which permits unrestricted use, distribution, and reproduction in any medium, provided the original work is properly cited. 

References

- [1] Devillers L, Vidrascu L. Positive and negative emotional states behind the laughs in spontaneous spoken dialogs. In: Proc. of Interdisciplinary Workshop on the Phonetics of Laughter; 2007. pp. 37-40
- [2] Campbell N. Whom we laugh with affects how we laugh. In: Proc. of Interdisciplinary Workshop on The Phonetics of Laughter; 2007. pp. 61-65
- [3] Breazeal C. Emotion and sociable humanoid robots. *International Journal of Human-Computer Studies*. 2003;59:119-155
- [4] Zecca M, Endo N, Momoki S, Itoh K, Takanishi A. Design of the humanoid robot KOBIAN-preliminary analysis of facial and whole body emotion expression capabilities. In: Proc. of the 8th IEEE-RAS International Conference on Humanoid Robots (Humanoids 2008); 2008. pp. 487-492
- [5] Wu Y, Thalmann NM, Thalmann D, Dynamic Wrinkle A. Model in facial animation and skin aging. *Journal of Visualization and Computer Animation*. 1995;6(4):195-205
- [6] Hashimoto T, Hiramatsu S, Tsuji T, Kobayashi H. Development of the face robot {SAYA} for rich facial expressions. In: Proceedings of the SICE-ICASE International Joint Conference; 2006. pp. 5423-5428
- [7] Lee D, Lee T, So B, Choi M, Shin E, Yang K, et al. Development of an android for emotional expression and human interaction. In: Proceedings of the 17th World Congress the International Federation of Automatic Control; 2008. pp. 4336-4337
- [8] Mazzei D, Lazzeri N, Hanson D, de Rossi D. HEFES an hybrid engine for facial expressions synthesis to control human-like androids and avatars. In: Proc. the 4th IEEE RAS/EMBS International Conference on Biomedical Robotics and Biomechatronics; 2012. pp. 95-200
- [9] Tadesse Y, Priya S. Graphical facial expression analysis and design method an approach to determine humanoid skin deformation. *Journal of Mechanisms and Robotics*. 2012;4(2):021010
- [10] Ahn H, Lee D, Choi D, Lee D, Hur M, Lee H, et al. Designing of android head system by applying facial muscle mechanism of humans. In: Proceedings of IEEE-RAS International Conference on Humanoid Robots; 2012. pp. 799-804
- [11] Loza D, Marcos S, Zalama E, Garcia-Bermejo JG, Gonzalez JL. Application of the FACS in the design and construction of a mechatronic head with realistic appearance. *Journal of Physicla Agents*. 2013;7(1):31-38
- [12] Ishi C, Liu C, Ishiguro H, Hagita N. Evaluation of formant-based lip motion generation in tele-operated humanoid robots. In: Proc. IEEE/RSJ International Conference on Intelligent Robots and Systems (IROS 2012); 2012. pp. 2377-2382
- [13] Ishi CT, Liu C, Ishiguro H, Hagita N. Head motion during dialogue speech and nod timing control in humanoid robots. In: Proc. of 5th ACM/IEEE International Conference on Human-Robot Interaction (HRI 2010); 2010. pp. 293-300
- [14] Liu C, Ishi C, Ishiguro H, Hagita N. Generation of nodding, head tilting and gazing for human-robot speech interaction. *International Journal of Humanoid Robotics (IJHR)*. 2013;10(1):1-19
- [15] Sakai K, Minato T, Ishi CT, Ishiguro H. Novel speech motion

generation by modelling dynamics of human speech production. *Frontiers in Robotics and AI*. 2017;4(49):14

[16] Ishi C, Hatano H, Ishiguro H. Audiovisual analysis of relations between laughter types and laughter motions. In: *Proc. of the 8th International Conference on Speech Prosody (Speech Prosody 2016)*; 2016. pp. 806-810

[17] Ishi C, Minato T, Ishiguro H. Motion analysis in vocalized surprise expressions. In: *Proc. Interspeech 2017*; 2017. pp. 874-878

[18] Ishi CT, Minato T, Ishiguro H. Motion analysis in vocalized surprise expressions and motion generation in android robots. *IEEE Robotics and Automation Letters*. 2017;2(3):1748-1754

[19] Ishi CT, Minato T, Ishiguro H. Analysis and generation of laughter motions, and evaluation in an android robot. *APSIPA Transactions on Signal and Information Processing*. 2019;8(e6):1-10

[20] Busso C, Deng Z, Yildirim S, Bulut M, Min Lee C, Kazemzadeh A, et al. Analysis of emotion recognition using facial expressions, speech and multimodal information. In: *Proceedings of the 6th International Conference on Multimodal Interfaces*; 2004. pp. 205-211

[21] Alonso-Mart F, Malfaz M, Sequeira J, Gorostiza JF, Salichs MA. A multimodal emotion detection system during human-robot interaction. *Sensors*. 2013;13(11):15549-15581

[22] Uz B, Gudukbay U, Ozguc B. Realistic speech animation of synthetic faces. In: *Proceedings of the Computer Animation*; 1998. pp. 111-118

[23] Adams A, Mahmoud M, Baltrusaitis T, Robinso P. Decoupling facial expressions and head motions in

complex emotions. In: *Proceedings of the 2015 International Conference on Affective Computing and Intelligent Interaction*; 2015. pp. 274-280

[24] Massaro DW, Egan PB. Perceiving affect from the voice and the face. *Psychonomic Bulletin & Review*. 1996;3(2):215-221

[25] Cave C, Guaitella I, Bertrand R, Santi S, Harlay F, Espesser R. About the relationship between eyebrow movements and *F0* variations. In: *Proceedings of the 4th International Conference on Spoken Language Processing*; 1996. pp. 2175-2179

[26] Ekman P, Friesen WV. Head and body cues in the judgment of emotion: A reformulation. *Perceptual and Motor Skills*. 1967;24(3):711-724

[27] The ILHAIRE project (Incorporating laughter into human avatar interactions: Research and experiments). Available from: <http://www.ilhaire.eu/>

[28] Niewiadomski R, Pelachaud C. Towards multimodal expression of laughter. In: *IVA*; 2012. pp. 231-244

[29] Niewiadomski R, Hofmann J, Urbain J, Platt T, Wagner J, Piot B, et al. Laugh-aware virtual agent and its impact on user amusement. In: *AAMAS*; 2013. pp. 619-626

[30] Ding Y, Prepin K, Huang J, Pelachaud C, Artieres T. Laughter animation synthesis. In: *Proceedings of the 2014 international conference on Autonomous agents and multi-agent systems*; 2014. pp. 773-780

[31] Niewiadomski R, Mancini M, Ding Y, Pelachaud C, Volpe G. Rhythmic body movements of laughter. In: *Proc. of 16th International Conference on Multimodal Interaction*; 2014. pp. 299-306

[32] Yehia HC, Kuratate T, Vatikiotis-Bateson E. Linking facial animation, head motion and speech acoustics. *Journal of Phonetics*. 2002;**30**:555-568

[33] Ekman P, Davidson RJ, Friesen WV. The Duchenne smile: Emotional expression and brain physiology II. *Journal of Personality and Social Psychology*. 1990;**58**(2):342-353

Computer Simulation of Human-Robot Collaboration in the Context of Industry Revolution 4.0

Yusie Rizal

Abstract

The essential role of robot simulation for industrial robots, in particular the collaborative robots is presented in this chapter. We begin by discussing the robot utilization in the industry which includes mobile robots, arm robots, and humanoid robots. The author emphasizes the application of collaborative robots in regard to industry revolution 4.0. Then, we present how the collaborative robot utilization in the industry can be achieved through computer simulation by means of virtual robots in simulated environments. The robot simulation presented here is based on open dynamic engine (ODE) using anyKode Marilou. The author surveys on the use of dynamic simulations in application of collaborative robots toward industry 4.0. Due to the challenging problems which related to humanoid robots for collaborative robots and behavior in human-robot collaboration, the use of robot simulation may open the opportunities in collaborative robotic research in the context of industry 4.0. As developing a real collaborative robot is still expensive and time-consuming, while accessing commercial collaborative robots is relatively limited; thus, the development of robot simulation can be an option for collaborative robotic research and education purposes.

Keywords: collaborative robot, human-robot collaboration, human-robot interaction, industry 4.0, humanoid robots, robot simulation, anyKode Marilou simulation

1. Introduction

Computer simulation has become an important tool in robotic research and development [1]. It provides a modeling and evaluation tool for complex systems that are analytically difficult to deal with. Frequently, a robot is consisted of links, joints, sensors, actuators, controller, and other structural elements which are integrated to form a whole system [2]. Indeed, developing a real robot is very expensive and time-consuming and requires multidiscipline skills. Nevertheless, a rapid prototyping environment for modeling, programming, and simulating robot is provided in robotics simulation software [3]. In computer simulation, developers are able design a robot model and evaluate the model such that it fulfills the designation requirements. This includes to identify the unexpected problems that may rise before the physical robot is realized. To some extent, computer simulation can be used to perform experiment and verify the trajectory planning or the efficacy of implemented control algorithm. On the other hand,

for example, in robot painting, computer simulation can be effectively utilized to solve robot programming complexity in design path trajectory by programming off-line instead of performing a lead teach principle [4]. Despite these advantages, computer simulation may have drawbacks, for instance, in computational overhead [5] and loss of flexibility because the simulation is developed for a specific field of application only [6].

In the past, computer simulation in robotics was conducted numerically with complex computation. The simulation is heavily relying on mathematical model where the system model is usually assumed to be in ideal case or in predefined conditions. The results obtained from simulation (i.e., usually represented in numbers or computer graphic display) require further interpretation or analysis. Some of these outdated simulation examples can be found in [7–9]. However, with advanced existing technologies, computer simulation has been evolved and tends to become more realistic and attractive with 3D visualization. The comparison study between several robot simulators in different fields of robotics from kinematics and dynamics to industrial applications is discussed in [1]. These simulations can be visually observed, and they have features which arouse interest for novice people, engineers, and scientists. Most of the robotic simulations are equipped with physics engines (ODE, Bullet, Havok, or PhysX) for real-time collision and dynamics of rigid bodies. One of the examples is the iCub humanoid robot where ODE physics engine is employed [10]. Nevertheless, different simulation platforms using MATLAB/Simulink can also be used to simulate robots [1]. In addition, there is a robotic simulation software named COSIMIR Robotics that used to simulate Mitsubishi industrial robots. It provides virtual simulation environment for robotics and automation, and it is very useful for education in mechatronics as given in [11]. In COSIMIR Robotics software, users do not need to develop a robot model from scratch—as opposed to other typical robotic simulation studios—because the industrial robot models are already provided in the list.

Digitization of manufacturing sector is the next phase of industrialization with the so-called industry revolution 4.0. It was first introduced publicly at Hannover Fair in 2011. It is the convergence of industrial production and information and communication technologies [12]. The paradigm of “I4.0”—for short—is to increase productivity and efficiency with the help of new technologies. However, this term is broader, and so it is difficult to grasp by academia and practitioners because the scope covers the entirety of industrial manufacturing [13]. At present, industry 4.0 is still on the conceptual formation stage, and several countries have set up industry 4.0 standards with different names, as it is called “i40,” “IoT,” or “Made in China 2025,” that is, well known in Germany, the USA, and China, respectively [14].

Industry 4.0 as the new phase of industrial revolution has developed gradually from embedded system to the cyber-physical system (CPS) [14]. CPS is one of the key components of industry 4.0 [15, 16], and it is basically an embedded system that exchanges data in an intelligent network which facilitate smart production [17]. The CPS term was coined around 2006 before the term “industry 4.0” was publicly introduced in 2011. This new industrial paradigm embraces the emerging technologies in robotics where the new approach is required to have some kind of self-organization and to be reconfigurable, adaptable, and flexible. For example, flexible interaction in robotics can be reflected by the development of augment reality (AR) application that augments an industrial robot to perform several tasks in maintenance or cooperative work with humans and robots [18]. Another example is the work toward multi-robot systems with improved energy efficiency, high real-time performance, and lower cost which can be achieved by integrating multi-robot

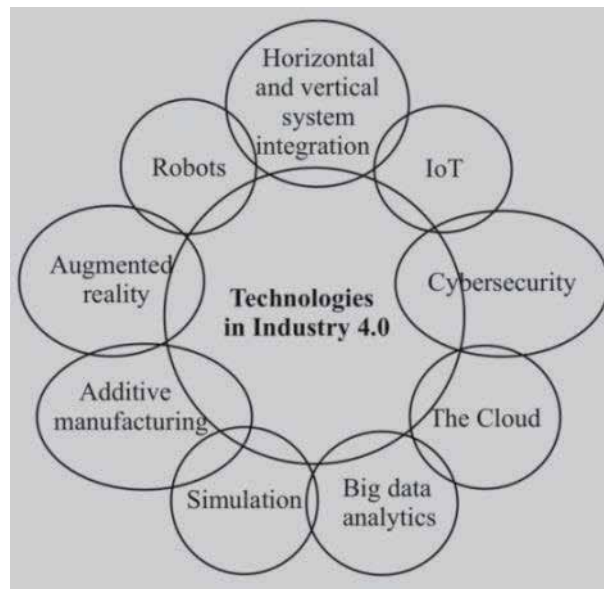


Figure 1.
Technologies associated with industry 4.0 [22].

systems with cloud computing and any other emerging technologies [19] (e.g., 5G wireless technology). Thus, the robotics technology is one of the essential drivers for industry 4.0. This technology and several other relevant technologies that associated with industry 4.0 are given in **Figure 1**.

In the last few decades, industrial robots could support human workers with complex and high-precision, repetitive, and dangerous tasks. Some of these repetitive tasks, for example, are paint and sealant applications, welding, assembly, material handling, inspection, and so on. However, this robot was not safe for humans to work side by side. Thus, the robots are usually placed in a cage or in an area where humans must stay away from them. In the era of industry 4.0, the popular robots are intelligent, able to collaborate, flexible, mobile, and connected. Several examples of such robots are Bosch APAS assistant, KUKA LBR iiwa, ABB YuMi, FANUC CR-35iA, MRK Systeme KR 5 SI, and Universal Robots UR5. The importance of collaborative robots is to increase the productivity and efficiency (as demanded in new industrial paradigm) when they work side by side with humans [20]. The deployment of these collaborative robots in the new industrialization era raises the potential for complex human-robot interaction (HRI) to create highly flexible processes by mean of symbiotic human-robot collaborative process [21].

The emerging technologies in robotics have enormous effect on education of people. However, only qualified and highly educated employee will be able to control such technologies, so collaboration between the industry and university should be more intense [23]. For example, a study on the usability and acceptance of an industrial prototype in relation to collaborative robots with humans in [24] has suggested the urgency of adaptation of assistive robot systems. It is well known that the collaborative robots (cobots) are very expensive and they are not easily accessible by common students and researchers, except for those who work in leading research institution or industry. To tackle this problem, developing a robot simulation and using it as a testbed is one of the solutions. With this regard, robot simulation is required to have some similar sensors and actuators as those of existing robots. In current robot simulation studio, those features are embedded in many robotic simulations, that is, utilizing open dynamic engine (ODE). In addition, they

are quite popular because of their reliability and performance in collision detection system [25]. Some examples of these robot simulations that are quite popular are, namely, Marilou [26], Gazebo [27], and Webots [28, 29].

This chapter discusses the utilization of robots in the industry which comply with industry 4.0 paradigm. More specifically, we elaborate the new emerging industrial robotics that is so-called collaborative robots. The collaborative robots have made humans and robots work side by side without a safety cage. The application of collaborative robots, for example, in automobile industries, has contributed to smart and intelligent manufacturing which is aligned with industry 4.0 concept. This new industrial revolution's paradigm is still in progress with some challenges. However, there are several issues with regard collaborative robots as well as its implementation in industry. In a case study, we elaborate a collaborative robot named Baxter robot as a role model of robot application that evolves toward industry 4.0. With the advanced computer technologies, computer simulation has become an essential tool in robot development. Research in the fields of robotics and its control system can be validated and analyzed using robot simulation. Thus, the computer of robotic simulations has given new opportunities with regard the new trends of collaborative robots.

2. New era of industrial robots

Robotics has played an essential role in manufacturing industries for so many years. They are tough, fast, and very accurate to perform specific tasks. In terms of speed and accuracy, robot performance is way much better than human workers. However, those robots have left significant gap because it takes hundreds of hours to program [30]. They are employed mainly for specific tasks that involve dangerous tasks and monotonous operation with great precision. Some of these applications are paint and sealant applications, welding, assembly, material handling, inspection, and so on [31]. In old-fashioned and traditional robot in industries as depicted in **Figure 2**, the working space of robots are isolated from human workers because it may harm humans if they work near robots or within the working area of robots. At present, with advanced robotics technologies, humans and robots can work side by side collaboratively. The collaboration between humans and robots is still in primitive way, in the sense that the robot is able to detect collision or foreign object and then a corresponding response is executed, for example, by reducing its speed or stopping immediately. Another collaborative robot such as Baxter robot which



Figure 2. Conventional automation factory using KUKA robotics [33].

is designed as an industrial robot can work very closely with people. However, the precision of this robot is still limited [32], and for now it cannot compete with other popular industrial robots, for example, KUKA, ABB, FANUC, Universal Robots, etc., in terms of repetitive tasks. Nevertheless, the usability of this robot is its suitable application as a robot assistant in which the precision can be tolerated.

Collaborative robots are also known as cooperative robots, cobots, or robot assistants [30]. They are mechanical devices that provide guidance through the use of servomotors, while a human operator provides motive power [34]. Generally speaking, it can be denoted as a robot that works side by side in a safe way either with another robot or with human workers to complete specific tasks. Thus, safety and productivity are the two important issues and become the main factors for design of robotic collaborative behaviors [35]. In human-robot collaboration, this behavior is related to how robots react when human physical contact occurs during execution. On the other hand, human-robot interaction in the general sense is a study of robotic systems for use by or with humans which concern with understanding, designing, and evaluating robots [36]. In physical human-robot interaction, human safety is the main concern and must be considered when evaluating robot setups in a workspace [37]. This interaction is related to a form of communication whether the robots and humans are positioned near to each other or not. Obviously, this interaction term does not necessarily mean collaborating, but merely how the two parties are communicating or interacting with each other in a certain way, while the other term means working together to achieve shared goals. Although these two terms are different in meaning, the human-robot interaction in fact can be used for collaborating. Thus, human and robot collaboration stands between the lines of manual manufacturing (where humans work manually) and full automation (where robots work independently) [30]. By collaborating between humans and robots (or machine), it is widely known that they become more productive than if each party work individually.

Collaborative robots at least have several elements, namely, the ability to detect any object within its work space and then react in order to prevent any collision [30], flexibility and situational task sharing [34], and cooperation on a mutual workplace [34]. These three elements differentiate collaborative robots from traditional robots even though the appearance between those industrial robots is the same. Their structural forms of multi-degree of freedom (multi-DOF) are intended to have the capability of reaching every specific coordinate of their workspace. In the case of task complexity or challenge situation, the collaborative robot tends to have more joints, for example, as given in **Figures 3** and **4**, that is, ABB YuMi IRB 14000 has 14 joints in total or 7 joints for each arm, while KUKA LBR iiwa has 7 joints, respectively. The structural models are reasonable because collaborative robots are designed to be ergonomic. For robotic system with many joints, the complexity of such control system becomes more difficult. Thus, research in control system for such robot is challenging problem.

The competition to bring up the elements of industry 4.0 is still under way between companies in Asia, Europe, and America [38]. There are two successful robotic implementation in industries that link to industry 4.0, namely, robotic application in automobile factories of BMW and Tesla [14]. In BMW group factory, the autonomous mobile robots are used for smart transport systems in supply logistics, while KUKA collaborative robots are utilized to work side by side with humans, for example, for lifting and positioning heavy components and welding operations [39]. On the other hand, Tesla's factory also has utilized robots with other technologies in their production lines to support smart and intelligent products [14]. One example is the use of industrial robots for repetitive tasks such as applying an even layer of paint for automobiles. For several types of repetitive tasks, fully automated production with robots is chosen instead of human workers, but for other specific



Figure 3.
ABB YuMi IRB 14000 [40].



Figure 4.
KUKA LBR iiwa [41].

tasks, human workers can not be replaced by robots because humans have skills, knowledge, and intuition. Which tasks that should performed by robots or human workers must be analyzed, otherwise the robot utilization in the industry can lead to production delays [39]. Indeed, robotic technologies must be incorporated with

any other emerging technologies to improve efficiency and productivity, but this utilization must be well prepared, properly designed, and carefully implemented for end-to-end production lines.

The collaboration between humans and robots is a new shift in industrial and service robotics as an element of strategy for industry 4.0 [30]. This strategy has a goal to set up a secure environment for human-robot collaboration. The framework for safety in industrial robot collaborative environments can be found in [20] where CPS is currently included as part of recent development in intelligent manufacturing. The use of CPS helps to bring the sharing of workspace for human-robot collaboration. The shared workspace of robots and human workers can be illustrated in **Figure 5** in which there are three possible configurations: (a) Isolated workspace where robots must be put in a cage in order to prevent any harm to human workers. (b) Some part of the area is shared among humans and robots. (c) Fully shared workspace where humans and robots work side by side to perform several tasks. In the first scenario, there is no interaction or whatsoever between humans and robots when the robot is in operation, while in the last scenario, the human worker may have contact or interaction with the robot in a safe way. Due to safety issue, the robot in the first scenario can be programmed faster than the robot in the last scenario. Thus, these three different scenarios must be designed and evaluated when they are utilized in industry so that the utilization can yield higher efficiency and productivity. This safety issue was also the subject of investigation for the critical requirements of fenceless implementation in human-robot collaboration, specifically in automotive application where the robotic system can be divided into three levels of complexity [42]. However, the new technology capabilities as suggested in [42] are already realized in collaborative robots that are built today.

The humans and robots in **Figure 5(a)** and **(b)** are not interacting with each other. On the other hand, in **Figure 5(c)**, the interaction at least is limited with physical interaction [43]. Human-robot interaction is related to communication between humans and robots whether it is remote interaction or proximity interaction [36]. The elements of human-robot interaction which consist of task structure and user attribute as discussed in [44] probably can also be investigated for future technology in human-robot collaboration. Although this research discussed in [44] is applied in ASIMO (humanoid robot), the research probably can also be implemented for collaborative robots, for example, Baxter robot and ABB YuMi. Some

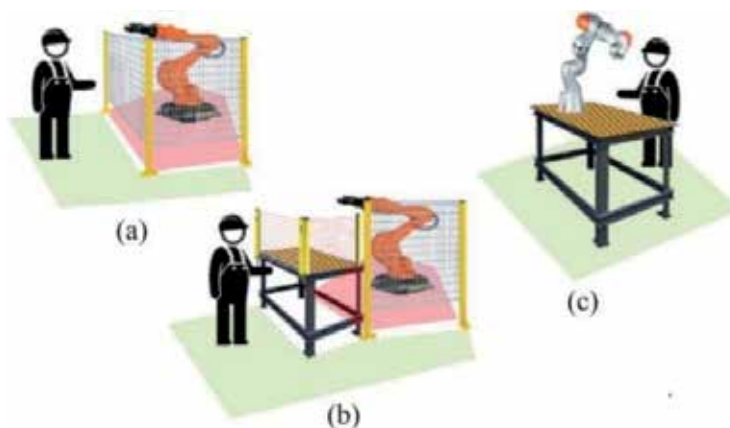


Figure 5. Illustration of shared human and robot workspace [30]. (a) human worker is totally separated with robot workspace, (b) human worker is partly shared with robot workspace, and (c) human worker is fully shared with robot workspace.



Figure 6.
OTTO 1500 self-driving vehicle [46].

research have been conducted to incorporate the human-robot interaction with human-robot collaboration to increase the productivity in completion of tasks.

On the other hand, mobile robots have become more compliant with human workers in factory. They work autonomously with self-driving and are able to detect obstacle and be aware of human existence. Some of the examples are KUKA youBot [45], mobile industrial robot (MiR), and OTTO self-driving vehicle (SDV) [46]. **Figure 6** shows OTTO 1500 SDV in which the robot is designed to move pellets, racks, and other large payloads through dynamic production environments with the ability to carry maximum load of 1500 kg. The combination between manipulator and mobile robots for one system can also be found in mobile robot KMR iiwa and mobile manipulator robot CHIMERA. Another form of collaboration between humans and robots in industry application for different tasks such as lift assist or hands on payload can be found in iTrolley module system [47].

In traditional industrial robots, there are several different modes in programming robots, namely, physical setup, lead through or teach mode, continuous walk-through mode, and software modes [2]. In software mode, there are two different approaches, namely, offline programming and online programming. In offline programming, robot simulation is used and set up in advance, while in online teaching, real robot is employed to generate robot program [48]. On the other hand, in collaborative robots, the user may program collaborative robot using task-level programming software tool which is developed based on robot skill concept [48]. The robot simulation as mentioned in programming real robots is totally different from programming robot in robotic simulation studio such as Marilou. In Marilou, the robot model is developed from scratch, and each joint with actuators and sensors is defined, and then, the controller system is designed and implemented using specified language programming. Thus, the robot programming in robotic simulation studio like Marilou is more flexible for different robot models and applications.

Figure 7 shows a robot that is the so-called Baxter by Rethink Robotics. It is a semi-humanoid robot with limbs of 7 DOF joints to form a dual-armed robot. This robot is a type of industrial robot with several unique features which include the safety for collaboration with human, user-friendliness, ability to train manually with no programming required, and ability to respond to a dynamic environment [49]. The advantage of collaborative robot such as Baxter is the ability to adapt to circumstances because the robot can be adjusted and applied to different applications by reprogramming the robot quickly. Another latest similar version from Rethink Robotics with only one arm is Sawyer. Baxter and Sawyer are both collaborative robots where they can work side by side with human workers and adapt to real-world variability in semi-structured environments.



Figure 7.
A collaborative robot: Baxter robot [52].

Some research have been conducted which involved Baxter robot for various applications and problems. For example, manipulation-based assistive robotics [50], performance assessment for point-to-point motion problem [32], and collaborative manipulation of a deformable sheet between humans and Baxter robots [51]. It is suggested that Baxter robot has a good potential for future robotic applications for home services or industrial applications.

3. Robot simulations

At present, there are many robotic simulation studios in the market for commercial use or noncommercial use license. Marilou Robotics Studio [26] is a commercial program of dynamic simulation that has different license types where the end user can choose according to their needs. It is based on Microsoft Robotics Developer Studio for modeling, programming, and simulating an environment [53]. There are various types of license, namely, home, education, project, and professional license. Similar to other robotic simulations, Marilou Robotics Studio employs open dynamic engine for physics engine. This engine is used for simulating rigid bodies and collision detection algorithm of physical interaction. ODE is basically consisted of collection of C library that encapsulates the physical laws, for example, for handling body contacts, frictions, force, collision, etc.

The phrase “simulation” is associated with computational devices used to obtain knowledge of physical system. “Robotic simulation,” on other hand, has a goal to acquire knowledge on performances of robotic systems [54]. Comparison among the three popular robotic simulations which related to product license and programming languages are given in **Table 1**. Indeed, Marilou Robotics Studio is considered as one of the leading simulator packages available today [55]. Furthermore, according to Marilou’s website [26], many research institutes (e.g., KIST, TECNALIA, INTEMPORA, etc.), and industries (e.g., KITECH, EasyRobotics, and WIFIBOT), have used this package for research and development.

A robot simulation package like Webots from Cyberbotics has a feature where the code can be implemented directly to a real robot by transferring the code after the simulation is completed, while different robot simulations do not have such

Product name	Programming language	Developer	License type
Gazebo	C++	Open Source Robotic Foundation	Free/open source
Webots	C/C++, Java, Python, URBI	Cyberbotics Inc.	Paid/commercial
Marilou	C/C++, C++, CLI, C#, J#, C mex function (MATLAB)	anyKode Marilou	Paid/commercial
OpenRAVE	C++, Python	OpenRAVE community	Free/open source
OpenHRP3	C++	AIST	Free/open source
V-REP	LUA	Coppelia Robotics	Paid/commercial

Table 1.
Comparison of different robotic simulation software.

Joint type	Actuator type	Sensor/device type
Ball	Servomotor	Force and torque sensor
Hinge for 1 axis	DC motor	Accelerometer/gyrometer/gyroscope
Hinge for 2 axes	Actuating cylinder	Infrared
Slider	Air pressure force	Ultrasonic
Slider and hinge		Emitter receiver
Piston		Absolute compass
Fixed		Touch area
Universal		GPS
		Odometer
		Laser range finder
		LIDAR
		Camera
		Panoramic spherical camera
		Bumper (force on contact)

Table 2.
Joints and embedded devices provided in Marilou robotics studio.

feature, for example, Gazebo and Marilou. However, both simulations have similar features where actuators and sensors are already provided and must be defined when the construction of robot body is developed. Unlike Webots or COSIMIR simulation packages where the robots are already provided, Marilou is a more general robot type that can be used for multipurpose robot applications, from mobile robot [56] to humanoid robot [57]. In Marilou, a robot must be designed and constructed in a CAD-like interface that is the so-called Marilou Physical Editor (MPE). All physical dimensions in MPE such as shape or geometry of body, its mass, links (between each body), and location of sensors and actuators that will be attached must be properly designed according to the dimension of proposed robot realization. Once the development of model robot is finished, the user can choose which programming language will be used. In **Table 1**, there are several robotic simulations that use open dynamic engine as their physics engine.

The features of Marilou simulation package are shown in **Table 2**. Sensors and actuators are embedded in a body of geometry or link. Based on these features, any robot's structure can be built even for the most complex and difficult robots such as humanoid robot [58] or multi-legged robot [59]. Furthermore, the virtual of real-world environments can also be developed in robotic simulation studio. However, to some extent, different license types may give the user different numbers of geometries,

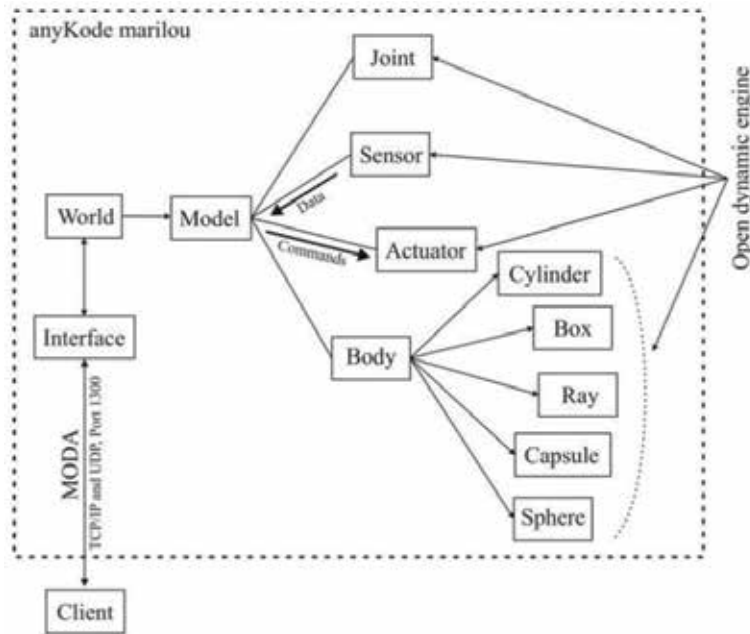


Figure 8.
General structure of anyKode Marilou.

maximal devices, and number of robot instances per computer. The maximum number of instances is 12 robots that can run in one computer simulation. This number of robots can be used, for example, in the case of two teams of robot play soccer.

The general structure of robot simulation such as Marilou simulation studio can be depicted in **Figure 8**. It consists of world, robot model, bodies, joints, interface, and client. In Marilou, the interface program, Marilou Open Device Access (MODA), is used to communicate with the client. The client sends data or commands to the robot model to the joint through actuators since the actuator is attached directly to a joint robot. Likewise, the client may receive data from sensors in which the robot is interacting with its environments. Based on this structure, the user may develop a collaborative robot, such as mobile robot, for example, in safety scenario when robots are near to humans. The human can be modeled as a dynamic obstacle. Whether the obstacles are static or dynamic, for example, wall, human, or any objects, the robot must be able to detect those obstacles, predict the movement, and perform the necessary response to prevent any collision.

Marilou simulation is able to simulate multiple robots in one computer by using MODA (Marilou Open Device Access). MODA is a default Marilou SDK and used to reach every robot at the same computer. It can be used for centralized or distributed architecture. In centralized architecture, all robots are accessed from one application program, while in the distributed architectures, each robot is accessed by different application programs separately. Those robots are considered as a single entity that has its own brain and controller whether they are different robot types or similar ones. To develop such multi-robots, usually a robot model is developed in the physics environment in Marilou. Once the robot model that consists of actuators and sensors is completed, the user may choose centralized controller by connecting all robots to one application program or distributed controller by connecting each robot to different application programs for multi-robot application.

However, there is limitation for how many robots in distributed architecture can be simulated at the same time in one computer. Marilou has different features for

multi-robot simulation depending on the type of license. For example, for professional license, the maximum number of instances that can be running per computer is 12 robots, while for education and project license is 8 robots and 2 robots, respectively. In the context of collaborative robots, human workers can be modeled as a single machine that moves independently and assumed as dynamic obstacle. The development of control algorithm and collaborative robot model can be tested and verified through computer simulation by observing how the robot behaves in dynamic environments or near human workers. This feature may serve to simulate robot-robot collaborations and human-robot collaborations in different scenarios.

The main safety system for human-robot collaboration and the essential sensors as discussed in [20] are feasible if constructed using Marilou simulation, because it has similar devices (actuators and sensors) as given in **Table 2** that can be incorporated in developed collaborative robots. These sensors include force and torque sensors, touch area, laser range finder, LIDAR, and bumper where these components can be used for safety in collaborative robots. In a practical example, the feasibility of solving a problem of 3D collision avoidance for safe human and robot coexistence as discussed in [60] can also be possibly implemented in Marilou. This dynamic simulation would be visually more attractive than computer simulation presented in [60].

An empirical application example of Marilou simulation is for developing a simulated wheelchair on a virtual environment in which brain-computer interface is used to command the wheelchair in host computer [61]. Indeed, this work is for research only and has not been applied and implemented for industrial application. Here, the author argues that Marilou simulation is, in fact, reliable enough to be used for research and development. The system developed in [61] is illustrated in **Figure 9** where brain-computer interface (BCI2000) [62] is connected to a host computer using UDP data communication protocol to control a simulated wheelchair on virtual environments. In host computer, a C++ program is developed to receive command from BCI2000 operator, and then, through MODA interface, the simulated wheelchair on virtual environment can be controlled.

In another practical problem, for example, in human-robot interaction research like in urban search and rescue (USAR) robotics as given in [63], computer simulation can be used as a simulator-based research since the system is relatively simple to model, has high fidelity dynamics for approximating robot's interaction with its environment using current physics engine, and capability of modern graphic

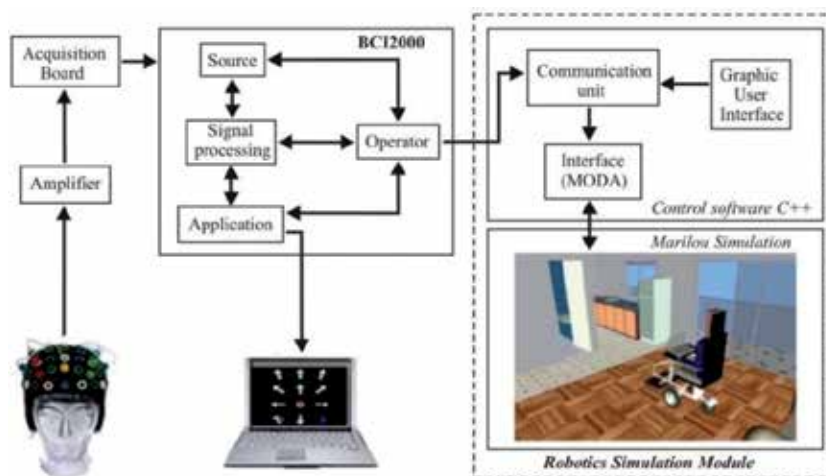


Figure 9. Brain-computer interface and Marilou simulation [61].

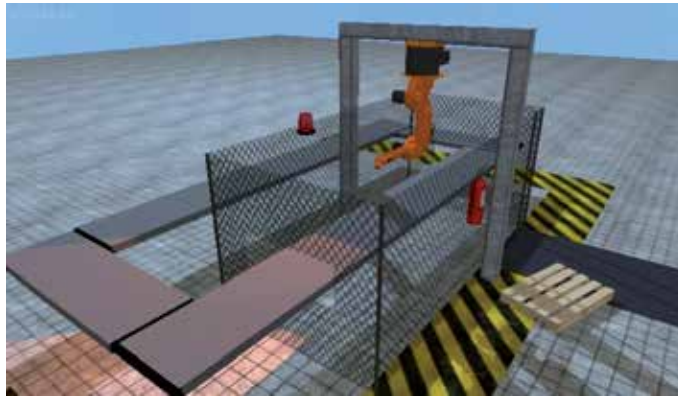


Figure 10.
KUKA KR6 simulation [26].

cards to approximate camera video. In USARSim, the camera is attached to a mobile robot in unknown (virtual) environments, and the user can monitor and control the robot remotely through camera feedback [63]. This scenario can be extended to larger problems of related research for simulating a human-robot interaction and human-robot collaboration. Although the simulation in [63] is not developed in Marilou simulation, the components of devices in USARSim can also be found in Marilou simulation, for instance, the camera sensor (as shown in **Table 2**). Thus, the development of human-robot interaction in Marilou simulation is feasible.

The robot performance for intended industrial application can be evaluated and analyzed if the similar and accurate model of environments can be captured and designed in simulation. For example, as it is given in **Figure 10**, KUKA KR6 robot is placed in a cage for safety reason. This robot can be used for simulating pick-and-place robot tasks, and the users are only concerned with controller design and implementation. Thus, the performance of the robot in specific tasks can be analyzed, for example, to observe the payload, speed response, and accuracy. Of course, the performances of whole dynamic simulation system are depended on sensors used as feedback.

In industry application such as Tesla or BMW, utilizing industrial robots including collaborative robots are still challenging because the robots are not agile enough to keep up the production target [39]. To solve this problem, specific collaborative robot can be developed in computer simulation with real-world simulated environments so that the whole process of production lines can be analyzed and evaluated comprehensively. This means the user can choose which type of robots should be used for specific line of cell to increase productivity, whether it is industrial robot, collaborative robots, or autonomous robots. In spite of the potential advantages of robotic simulation like Marilou to solve real problems, the robot simulation package has limited capability for simulating a large scale of robotic systems running at the same time. This scenario is very important, for example, to simulate robots in automation industry where traditional industrial robot and collaborative robot are existing and used for efficient and productive solution. In fact, this computer simulation of large-scale robots is still rare; unfortunately, this type of simulation can be beneficial toward industry 4.0 paradigm in regard to smart factory and productivity.

4. Humanoid robot

A humanoid robot is a robot having two legs, two arms, the shape of a human body, a trunk, and a head. Usually, it is associated as the robot with the appearance of

a full human body and has the ability to walk, for example, Honda ASIMO, HRP, and HUBO robot. These three examples have similarity with its appearance as well as in mechanical design. The research in humanoid robot was initiated around the 1970s in Japan after the development of “Honda P3” by Honda Motor Co., Ltd. The purpose of this development was to build humanoid robots that can walk stably and mimic how humans walk. Since then, many research groups in humanoid robot pursued developing practical humanoid robot. At that time, Japan and South Korea are probably the leading countries in the research of humanoid robot. However, in literature, it seems the research problems in humanoid robot become broader topics and diverse from control walking, grasping, visual recognition, social interaction, virtual simulation, intelligent robot, and so on, including human-robot collaboration and interaction. Here, the author discusses and highlights humanoid robot toward industry 4.0, in particular human-robot collaboration and human-robot interaction. Other aspects of intelligent robot and virtual robot simulation will be briefly presented.

At present, commonly there are two types of actuators used in humanoid robots: First, motor or servo type with harmonic drives, for example, as in Honda ASIMO [64], DRC-HUBO+ [65], and Valkyrie NASA [66], and second, hydraulic type as in Atlas robot [67] and PETMAN [68]. The significance of the two actuators is very different in the sense that the first group of robots has slower response than the second group. The hydraulic actuator has a greater torque relative to the same size of electric motor, and thus, the robots that use hydraulic system are comparatively free from insufficient joint torque problem, while the robots that use electric motor have some problem with insufficient joint torque [65]. Despite of various actuators being used in humanoid robot, the trend of humanoid robot development is the robot that is lightweight with slim body. This design would make it easier for the robot to maneuver and perform certain tasks.

In industrial application, a semi-humanoid type robot such as Baxter robot is well known as a collaborative robot, and it is used in various industry applications to perform certain tasks. Although this robot is not a full body of a humanoid robot, most of it appears as a human except the fact that the robot has no legs to walk. Indeed, the advantage of full-body humanoid robot is that it can maneuver more easily in a complex terrain. However, in industry application or in other manufacturing industries, the terrain is usually simple with flat terrain, but the obstacles are more complex and dynamic. The general comparison of different robots including humanoid robots is presented in **Table 3**. It is given in **Table 3** that the humanoid robots are commonly used for research, technology demonstrator for specific tasks, or for human-robot interaction. This shows that the humanoid robots so far are not intended for competing with other robots in industrial applications. The use of semi-humanoid robot for collaborative robots in industrial application is more practical than that of a full body of humanoid robots. In fact, the full-body humanoid type of robot is commonly used for research only so far in order to solve practical engineering problems. For example, DCR-HUBO+ in [69] is used to solve the challenging problems of simple tasks such as debris removal, door opening, and wall breaking in the event of the DARPA competition.

The success of humanoid robot in real-world environments is largely dependent on the ability to interact with both humans and its environments [70] in which the humanoid robot has some form of awareness to the real-world context. Hence, the robot’s perception is a key issue for performing high-level tasks such as understanding and learning human-robot interaction. This perception can be detected from the high-level features of human facial expression and body gestures [71]. The perception systems are proposed in [71], but the variety of robotic software architecture and hardware platforms would make the customized solutions hardly interchangeable and adaptable for different human-robot interaction contexts. Another aspect of learning (in control point of view) for the humanoid robot is, for example, in the situation when the robot is falling to the ground. At this circumstance, the robot must be able

Robot name	Developer/manufacturer	Robot type	Application purpose
NAO	SoftBank Robotics	Bipedal humanoid robot	Research, education, and entertainment
Pepper	SoftBank Robotics	Bipedal humanoid robot	Technology demonstrator for social and human interaction
Sanbot robot	Qihan Technology	Wheeled humanoid robot	Retail, hospitality, education, health care, entertainment, security
Enon robot	Fujitsu Frontech Ltd. and Fujitsu Lab	Wheeled humanoid robot	Personal assistant/service robot, technology demonstrator
Toyota Partner Robot	Toyota	Bipedal humanoid robot	Entertainment
Honda ASIMO	Honda	Bipedal humanoid robot	Research, technology demonstrator
HRP	AIST	Bipedal humanoid robot	Research, technology demonstrator
Atlas	Boston Dynamics	Bipedal humanoid robot	Search and rescue, research
TOPIO	Tosy Future Robot	Bipedal humanoid robot	Technology demonstrator
iCUB	Italian Institute of Technology	Bipedal humanoid robot	Research
HUBO, DRC-HUBO+	KAIST	Bipedal humanoid robot	Research, technology demonstrator
Baxter robot	Rethink Robotics	Two-armed robot	Simple industrial jobs, research and education
KR Quantec	KUKA	Manipulator robot	Industrial application
OTTO self-driving vehicle	OTTO Motors	Autonomous mobile robot	Smart transportation/industrial application
MiR100/200/500	Mobile Industrial Robots	Autonomous mobile robot	Industrial application
KUKA youBot	KUKA	Mobile manipulator robot	Research, industrial application
FANUC collaborative robot	FANUC	Mobile manipulator robot	Industrial application
Bosch APAS	Bosch	Mobile manipulator robot	Industrial application
ABB FlexPicker	ABB Group	Parallel Manipulator	Industrial application
FANUC iRPickTool	FANUC	Parallel manipulator	Industrial application
ABB IRB YuMi	ABB Group	Robotic arm	Industrial application
FANUC CR-35iA	FANUC	Robotic arm	Industrial application
UR10	Universal Robots	Robotic arm	Industrial application
Omron TM Series collaborative robot	Omron	Robotic arm	Industrial application
LBR iiwa and KR AGILUS	KUKA	Robotic arm	Industrial application
FANUC SR-3iA/SR-6iA	FANUC	SCARA robot	Industrial application
ABB IRB	ABB Group	SCARA robot	Industrial application

Table 3.
General comparison of various robots and its applications.

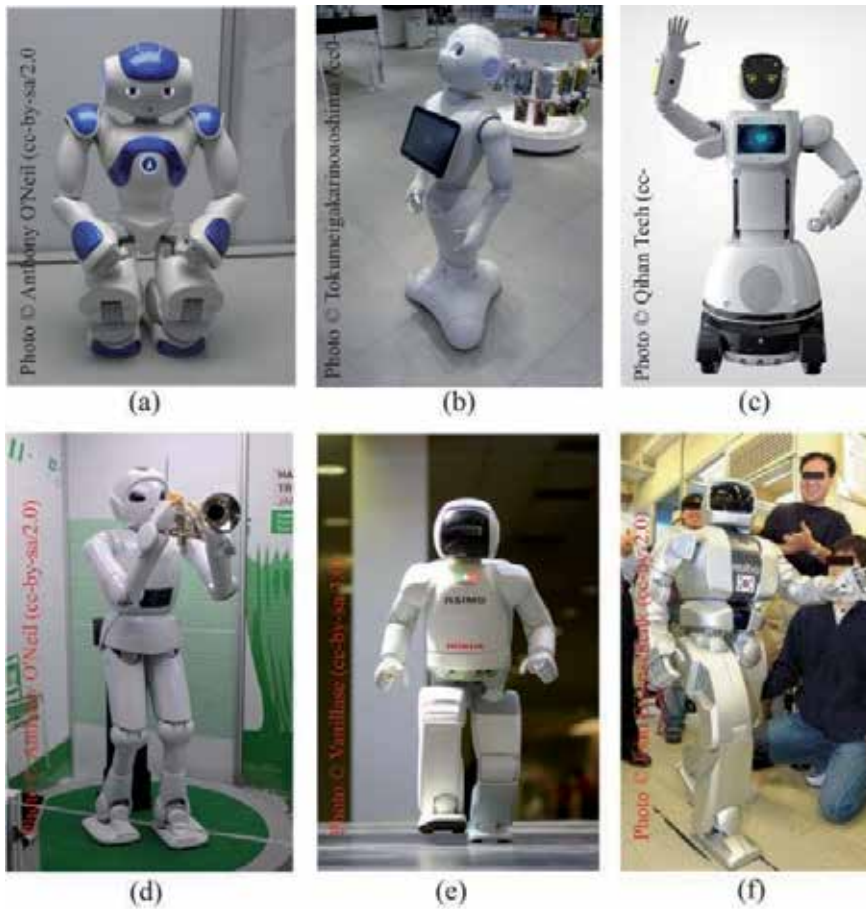


Figure 11. Different types of humanoid robots: (a) NAO humanoid, (b) pepper humanoid robot, (c) Sanbot robot, (d) Toyota partner robot, (e) Honda ASIMO, and (f) HUBO humanoid robot.

to get up immediately with certain self-learning process or automatic learning system. Some of the existing humanoid robots are given in **Figure 11**. They are commonly used for research as in human-robot interaction, control methods of bipedal walks, indoor localization, and navigation. Moreover, some of them are also used for education [72], entertainment [73], and for home service.

The Cloud technology is one of the key components in the new industrial paradigm of industry 4.0. In relation to humanoid robot, one of the potential applications of Cloud technology is to provide collective robot learning, that is, robot sharing trajectories, control policies, and outcome [74]. One good practical example of Cloud technology application in humanoid robot is in the development of simulation of humanoid robot to complete certain tasks [75] which is part of the DARPA virtual robotic challenge. In [75], the existing Cloud technology was combined with Gazebo simulator for simulating humanoid robot. This developed robot simulation is not only applied to virtual humanoid robot in action but also to other specific challenging environments that must be handled by the humanoid robot. Another example of robotic simulation in the context of humanoid robots is given in [76] where V-REP robotic simulation was used as a testbed to observe how virtual robots would behave in completing certain tasks from given commands by humans. This research was related to teleoperation method based on human-robot interaction by mimicking human's movement visually for which Baxter robot would learn the movements. Again, robotic simulation would

be a key component in robotic research and development, in particular in the field of humanoid robot. Moreover, this opportunity is due to the new emerging of Cloud computing that can be incorporated with robotic simulation.

5. Conclusions

Research progress in human-robot collaboration and the application of robot simulations toward industry 4.0 have been discussed in this chapter. The key components of collaborative robot in industrial applications are elaborated with various robot types that exist today. Indeed, the collaborative robots can be designed, modeled, and realized in computer simulation using open dynamic engine such as Marilou AnyKode. This virtual robot can serve as a testbed for different purposes from controller design implementation, robot interactions, to validation of robot in specific environment scenarios. Although existing robot simulation packages are equipped with many actuators and embedded sensors that support for application in collaborative robots, the simulation of collaborative robot is still rare to discuss in literature. Since the practical industrial application of full-body humanoid robot in the industry probably still has a long way to go, thus robot simulations can be a better choice for developing different types of robots for future applications, in particular in areas of human-robot collaboration and human-robot interaction for industrial application and home services. Another opportunity lies in virtual reality of human-robot interaction, implementation of artificial intelligence in virtual robots, and synthesizing control algorithm for different robotic configurations.

Conflict of interest

The author declares that there are no conflicts of interest in this work. All works from other resources in the article have been cited carefully.

Author details


Yusie Rizal^{1,2}

1 Department of Engineering Science, National Cheng Kung University, Tainan, Taiwan

2 Department of Electrical Engineering, Politeknik Negeri Banjarmasin, Banjarmasin, Indonesia

*Address all correspondence to: yusie.rizal@poliban.ac.id

IntechOpen

© 2019 The Author(s). Licensee IntechOpen. This chapter is distributed under the terms of the Creative Commons Attribution License (<http://creativecommons.org/licenses/by/3.0>), which permits unrestricted use, distribution, and reproduction in any medium, provided the original work is properly cited. 

References

- [1] Zlajpah L. Simulation in robotics. *Mathematics and Computers in Simulation*. 2008;**79**:879-897
- [2] Niku SB. *Introduction to Robotics: Analysis, Control, Applications*. 2nd ed. New Jersey, USA: John Wiley & Sons, Inc; 2011
- [3] Rohmer E, Singh SPN, Freese M. V-REP: A versatile and scalable robot simulation framework. In: *IEEE International Conference on Intelligent Robots and Systems*. 2013. pp. 1321-1326
- [4] Wilson M. *Implementation of Robot Systems: An Introduction to Robotics, Automation, and Successful Systems Integration in Manufacturing*. London, UK: Elsevier; 2015
- [5] Echeverria G, Lassabe N, Degroote A, et al. Modular open robots simulation engine: MORSE. In: *IEEE International Conference on Robotics and Automation*. 2011. pp. 46-51
- [6] Schluse M, Rossmann J. From simulation to Experimentable digital twins. In: *IEEE International Symposium on Systems Engineering*. 2016. pp. 1-6
- [7] Heginbotham WB, Dooner M, Case K. Robot application simulation. *Industrial Robotics an International Journal*. 1978;**6**:76-80
- [8] McGhee RB, Iswandhi GI. Adaptive locomotion of a multilegged robot over rough terrain. *IEEE Transactions on Systems, Man, and Cybernetics*. 1979;**9**:176-182
- [9] Chan WW, Rathmill K. Digital simulation of a proposed flexible manufacturing system. In: *19th International Machine Tool Design and Research Conference*. 1979. pp. 323-329
- [10] Tikhanoff V, Fitzpatrick P, Nori F, et al. The iCub humanoid robot simulation. In: *IEEE/RSJ 2008 International Conference on Intelligent Robots and Systems*. Nice, France; 2008. pp. 1-2
- [11] Aleksandrov S, Jovanović Z, Antić D, et al. Analysis of the efficiency of applied virtual simulation models and real learning systems in the process of education in mechatronics. *Acta Polytechnica Hungarica*. 2013;**10**:59-76
- [12] Hermann M, Pentek T, Otto B. Design principles for industrie 4.0 scenarios. *Annual Hawaii International Conference on System Sciences (HICSS)*. 2016;**2016**:3928-3937
- [13] Strandhagen JW, Alfnes E, Strandhagen JO, et al. The fit of industry 4.0 applications in manufacturing logistics: A multiple case study. *Advanced Manufacturing*. 2017;**5**:344-358
- [14] Cheng GJ, Liu LT, Qiang XJ, et al. Industry 4.0 development and application of intelligent manufacturing. In: *International Conference on Information System and Artificial Intelligence*. 2017. pp. 407-410
- [15] Drath R, Horch A. Industrie 4.0: Hit or hype? [industry forum]. *IEEE Industrial Electronics Magazine*. 2014;**8**:56-58
- [16] Roblek V, Meško M, Krapež A. A complex view of industry 4.0. *SAGE Open*. 2016;**6**:1-11. Epub ahead of print. DOI: 10.1177/2158244016653987
- [17] Pereira AC, Romero F. A review of the meanings and the implications of the industry 4.0 concept. *Procedia Manufacturing*. 2017;**13**:1206-1214
- [18] Maly I, Sedlacek D, Leitao P. Augmented reality experiments with industrial robot in industry 4.0 environment. In: *IEEE 14th International Conference on Industrial Informatics*. 2016. pp. 176-181

- [19] Wan J, Tang S, Yan H, et al. Cloud robotics: Current status and open issues. *IEEE Access*. 2016;**4**:2797-2807
- [20] Robla-Gomez S, Becerra VM, Llata JR, et al. Working together: A review on safe human-robot collaboration in industrial environments. *IEEE Access*. 2017;**5**:26754-26773
- [21] Mokaram S, Aitken JM, Martinez-Hernandez U, et al. A ROS-integrated API for the KUKA LBR iiwa collaborative robot. *IFAC-PapersOnLine*. 2017;**50**:15859-15864
- [22] Bahrin MAK, Othman MF, Azli NHH, et al. Industry 4.0: A review on industrial automation and robotic. *Jurnal Teknologi*. 2016;**78**:137-143
- [23] Benešová A, Tupa J. Requirements for education and qualification of people in industry 4.0. *Procedia Manufacturing*. 2017;**11**:2195-2202
- [24] Weiss A, Huber A, Minichberger J, et al. First application of robot teaching in an existing industry 4.0 environment: Does it really work? *Societies*. 2016;**6**:20
- [25] Roennau A, Sutter F, Heppner G, et al. Evaluation of physics engines for robotic simulations with a special focus on the dynamics of walking robots. In: 2013 16th Int Conf Adv Robot ICAR. 2013. pp. 1-7
- [26] Ricatti L. Marilou Robotics Studio. Available from: www.anykode.com [Accessed: 03 March 2019]
- [27] Gazebo. Available from: <http://gazebo.org/> [Accessed: 08 May 2019]
- [28] Webots. Available from: <https://cyberbotics.com> [Accessed: 08 May 2019]
- [29] Michel O. Webots TM : Professional Mobile robot simulation. *International Journal of Advanced Robotic Systems*. 2004;**1**:39-42
- [30] Vysocky A, Novak P. Human-robot collaboration in industry. *MM Science Journal*. 2016;**9**:903-906
- [31] Djuric AM, Urbanic RJ, Rickli JL. A framework for collaborative robot (CoBot) integration in advanced manufacturing systems. *SAE International Journal of Materials and Manufacturing*. 2016;**9**:457-464
- [32] Cremer S, Mastromoro L, Popa DO. On the performance of the Baxter research robot. In: 2016 IEEE International Symposium on Assembly and Manufacturing, ISAM 2016. 2016. pp. 106-111
- [33] KUKA Roboter GmbH B. Factory Automation with Industrial Robots for Palletizing Food Products. 2005. Available from: <https://bit.ly/2Qo6ivy> [Accessed: 17 May 2019]
- [34] Helms E, Sehraft RD, Hägele M. Rob@work: Robot assistant in industrial environments. In: 11th IEEE International Workshop on Robot and Human Interactive Communication. 2002. pp. 399-404
- [35] Ding H, Heyn J, Matthias B, et al. Structured collaborative behavior of industrial robots in mixed human-robot environments. In: IEEE International Conference on Automation Science and Engineering. 2013. pp. 1101-1106
- [36] Goodrich MA, Schultz AC. Human-robot interaction: A survey. *Foundations and Trends in Human-Computer Interaction*. 2007;**1**:203-275
- [37] Teiwes J, Banziger T, Kunz A, et al. Identifying the potential of human-robot collaboration in automotive assembly lines using a standardised work description. In: International Conference on Automation and Computing. 2016. pp. 78-83
- [38] Rießmann M, Lorenz M, Gerbert P, et al. Industry 4.0: The future

of productivity and growth in manufacturing industries. Boston Consulting. 2015;62:40-41

[39] Miller P. Industrial Robots vs. Humans in Manufacturing at Tesla (and Elsewhere). 2018. Available from: <https://www.arcweb.com/blog/industrial-robots-vs-humans-manufacturing-tesla-elsewhere> [Accessed: 19 May 2019]

[40] Flowers L, ABB YuMi IRB. Science Museum Robots Exhibition. 2015. Available from: <https://bit.ly/30iAyu5> [Accessed: 16 May 2019]

[41] Scailyna. Kuka Robotics. Innorobo 2015. 2015. Available from: <https://bit.ly/2JP3iEH> [Accessed: 16 May 2019]

[42] Shi J, Jimmerson G, Pearson T, et al. Levels of human and robot collaboration for automotive manufacturing. In: Workshop on Performance Metrics for Intelligent Systems. 2012. pp. 95-100

[43] Whitsell B, Artemiadis P. Physical human-robot interaction (pHRI) in 6 DOF with asymmetric cooperation. IEEE Access. 2017;5:10834-10845

[44] Mutlu B, Osman S, Forlizzi J, et al. Task structure and user attributes as elements of human-robot interaction design. In: IEEE International Workshop on Robot and Human Interactive Communication. 2006. pp. 74-79

[45] Bischoff R, Huggenberger U, Prassler E. KUKA youBot—A mobile manipulator for research and education. In: IEEE International Conference on Robotics and Automation. 2011. pp. 3-6

[46] Hennessey MP. OTTO 1500 Self-Driving Vehicle (SDV). 2016. Available from: <https://bit.ly/2IqCOIy> [Accessed: 15 June 2019]

[47] Bicchi A, Peshkin MA, Colgate JE. Safety for physical human-robot

interaction. In: Siciliano B, Khatib O, editors. Springer Handbook of Robotics. Berlin, Heidelberg, Germany: Springer-Verlag; 2008. pp. 1335-1348

[48] Kim C-S, Hong K-S, Han Y-S. Welding robot applications in shipbuilding industry: Off-line programming, virtual reality simulation, and open architecture. In: Low K-H, editor. Industrial Robotics: Programming, Simulation and Application. Rijeka, Croatia, Germany: Pro Literatur Verlag; 2006. pp. 537-558

[49] Fitzgerald C. Developing Baxter. In: IEEE Conference on Technologies for Practical Robot Applications, TePRA. IEEE. 2013. pp. 1-6

[50] Cunningham A, Keddy-Hector W, Sinha U, et al. Jamster: A mobile dual-arm assistive robot with Jamboxx control. In: IEEE International Conference on Automation Science and Engineering. IEEE. 2014. pp. 509-514

[51] Kruse D, Radke RJ, Wen JT. Collaborative human-robot manipulation of highly deformable materials. In: Proceedings—IEEE International Conference on Robotics and Automation. IEEE. 2015. pp. 3782-3787

[52] Jurvetson S. Rethink Robotics. 2012. Available from: <https://bit.ly/2YDIDrH> [Accessed: 17 May 2019]

[53] Gomez del Torno P, Alvarez Fres O, Pablos SM. Robotic development. In: Tzafestas SG, editor. Service Robotics within the Digital Home: Applications and Future Prospects. Heidelberg, Germany: Springer Science & Business Media; 2011. pp. 49-88

[54] Datteri E, Schiaffonati V. Robotic simulations, simulations of robots. Minds and Machines. 2019;29:109-125. DOI: 10.1007/s11023-019-09490-x

[55] Harris A, Conrad JM. Survey of popular robotics simulators, frameworks,

and toolkits. In: Conf Proc—IEEE SOUTHEASTCON. 2011. pp. 243-249

[56] Estrada G, Zagal D, Reyes C, et al. Systems engineering as a critical tool in mobile robot simulation. *International Journal of Combinatorial Optimization Problems and Informatics*. 2013;4:25-38

[57] Silva MALL, Dorna I, Bauer J. Simulación Robótica del Ciclo de Marcha Humana. 2015. Available from: http://www.secyt.frba.utn.edu.ar/giar/trabajosviiiijar/jar8_submission_24.pdf [Accessed: 15 June 2019]

[58] Tikhanoff V, Cangelosi A, Fitzpatrick P, et al. An open-source simulator for cognitive robotics research: The prototype of the iCub humanoid robot simulator. In: 8th Workshop on Performance Metrics for Intelligent Systems. 2008. pp. 57-61

[59] Belter D, Kasiński A, Skrzypczyński P. Evolving feasible gaits for a hexapod robot by reducing the space of possible solutions. In: IEEE/RSJ International Conference on Intelligent Robots and Systems. 2008. pp. 2673-2678

[60] Balan L, Bone GM. Real-time 3D collision avoidance algorithm for safe human and robot coexistence. In: IEEE/RSJ International Conference on Intelligent Robots and Systems. 2006. pp. 276-282

[61] Gentiletti GG, Gebhart JG, Acevedo RC, et al. Command of a simulated wheelchair on a virtual environment using a brain-computer interface. *IRBM*. 2009;30:218-225

[62] Schalk G, McFarland DJ, Hinterberger T, et al. BCI2000: A general-purpose brain-computer interface (BCI) system. *IEEE Transactions on Biomedical Engineering*. 2004;51:1034-1043

[63] Lewis M, Wang J, Hughes S. USARSim: Simulation for the study of

human-robot interaction. *Journal of Cognitive Engineering and Decision Making*. 2007;1:98-120

[64] Sakagami Y, Watanabe R, Aoyama C, et al. The intelligent ASIMO: System overview and integration. In: *International Conference on Intelligent Robots and Systems*. 2002. pp. 2478-2483

[65] Jung T, Lim J, Bae H, et al. Mechanism design outline of Hubo. In: Goswami A, Vadakkepat P, editors. *Humanoid Robotics: A Reference*. Dordrecht: Springer; 2017. p. 615-635. DOI: 10.1007/978-94-007-6046-2_93

[66] Radford NA, Strawser P, Hambuchen K, et al. Valkyrie: NASA's first bipedal humanoid robot. *Journal of Field Robotics*. 2015;32:397-419

[67] Feng S, Whitman E, Xinjilefu X, et al. Optimization based full body control for the atlas robot. In: *IEEE RAS International Conference on Humanoid Robots*. 2014. pp. 120-127

[68] Nelson G, Saunders A, Neville N, et al. PETMAN: A humanoid robot for testing chemical protective clothing. *Journal of the Robotics Society of Japan*. 2012;30:372-377

[69] Zucker M, Joo S, Grey MX, et al. A general-purpose system for teleoperation of the DRC-HUBO humanoid robot. *Journal of Field Robotics*. 2015;32:336-351

[70] Romano F, Nava G, Azad M, et al. The CoDyCo project achievements and beyond: Toward human aware whole-body controllers for physical human robot interaction. *IEEE Robotics and Automation Letters*. 2017;3:516-523

[71] Zarakı A, Pieroni M, De Rossi D, et al. Design and evaluation of a unique social perception system for human-robot interaction. *IEEE Transactions on Cognitive and Developmental Systems*. 2017;9:341-355

[72] Tanaka F, Isshiki K, Takahashi F, et al. Pepper learns together with children: Development of an educational application. In: IEEE-RAS International Conference on Humanoid Robots. 2015. pp. 270-275

[73] Kusuda Y. Toyota's violin-playing robot. *Industrial Robot an International Journal*. 2008;**35**:504-506

[74] Kehoe B, Member S, Member SP. A survey of research on cloud robotics and automation. *IEEE Transactions on Automation Science and Engineering*. 2015;**12**:1-11

[75] Agüero CE, Koenig N, Chen I, et al. Inside the virtual robotics challenge: Simulating real-time robotic disaster response. *IEEE Transactions on Automation Science and Engineering*. 2015;**12**:494-506

[76] Shamshiri RR, Hameed IA, Pitonakova L, et al. Simulation software and virtual environments for acceleration of agricultural robotics: Features highlights and performance comparison. *International Journal of Agricultural and Biological Engineering*. 2018;**11**:15-31

Emoji as a Proxy of Emotional Communication

Guillermo Santamaría-Bonfil

and Orlando Grabiél Toledano López

Abstract

Nowadays, emoji plays a fundamental role in human computer-mediated communications, allowing the latter to convey body language, objects, symbols, or ideas in text messages using Unicode standardized pictographs and logographs. Emoji allows people expressing more “authentically” emotions and their personalities, by increasing the semantic content of visual messages. The relationship between language, emoji, and emotions is now being studied by several disciplines such as linguistics, psychology, natural language processing (NLP), and machine learning (ML). Particularly, the last two are employed for the automatic detection of emotions and personality traits, building emoji sentiment lexicons, as well as for conveying artificial agents with the ability of expressing emotions through emoji. In this chapter, we introduce the concept of emoji and review the main challenges in using these as a proxy of language and emotions, the ML, and NLP techniques used for classification and detection of emotions using emoji, and presenting new trends for the exploitation of discovered emotional patterns for robotic emotional communication.

Keywords: emoji, machine learning, natural language processing, emotional communication, human-robot interaction

1. Introduction

Recently, in the episode “Smile” of the popular science fiction television program “Doctor Who,” a hypothetical off-earth colony is presented. This colony is maintained and operated by robots, which communicate and express emotions with humans and its pairs, through the usage of emoji. Sure, one may argue that such technology, besides being mere science fiction, is ridiculous since phonetic communication is much simpler and much easier to understand. While this is true for conventional information (e.g., explaining the concept of real numbers), communicating body emotional responses or gesticulation (e.g., to describe confusion) using only phonograms would require many more words to convey the same message than an emoji (e.g., 😊 or 😞). In this sense, emoji serve as a visual simplified form of (affective) communication that broadens the total amount of information (e.g., cues and gestures), which can be shared between humans and virtual/embodied artificial entities. If we consider that human languages, such as Chinese, Nahuatl [1], or even Sign Language, have evolved from ideographs and pictographs

lexicons, can we expect that in the near future, artificial entities (virtual or embodied) would employ emoji in their emotional communication?

The Japanese word *emoji* (e = picture and moji = word) literally stands for “picture word.” Although recently popularized, its older predecessors can be tracked to the nineteenth century, when cartoons were employed for humorous writing. *Smileys* followed in 1964 and were meant to be used by an insurance company’s promotional merchandise to improve the morale of its employee. The first to employ the emoticon :) in an online bulletin forum to denote humorous messages was Carnegie Mellon researchers in 1982, and 10 years later, the emoticons were already widespread in emails and Websites [2]. Finally, in 1998, Shigetaka Kurita devised emoji to improve emoticons pictorially, and became widespread by 2010. From this moment, the use of emoji has gained a lot of momentum, even achieving that the *word* namely “Face with Tears of Joy” (😄) was chosen by the Oxford Dictionary as the *Word of the Year* [2–4]. This choice was made under the assumption that the pictograph represented the ideas, beliefs, mood, and concerns of English speakers in 2015.

Since its origin, emoji undoubtedly have become a part of the mainstream communication around the globe allowing people, with different languages and cultural backgrounds, to share and interpret more accurately ideas and emotions. In this vein, it has been hypothesized that emoji shall become a *universal* language due to its generic communication features and its ever progressing lexicon [2, 5–7]. Although, this idea is controversial [8, 9] since emoji usage during the communication is influenced by factors such as context, users interrelations, users’ first language, repetitiveness, socio-demographics, among others [2, 5, 8]. This clearly adds ambiguity on how to employ them and its proper interpretation. Nevertheless, in the same fashion as sentiment analysis mines sentiments, attitudes, and emotions from text [10], we can employ billions (or perhaps more) of written messages within the Internet that contains emoji, to generate affective responses in artificial entities. More precisely, using natural language processing (NLP) along with machine learning (ML), we can extract semantics, express beat gestures, emotional states, and affective cues, add personality layers, among other characteristics from text. All this knowledge can be used to build, for instance, emoji sentiment lexicons [10] that will conform the emoji communication competence [2] that will power the engines of the emotional expression and communication of an artificial entity.

In the rest of this chapter, we first review the elements of the emoji code, and how emoji are used in the emotional expression and communication (Section 2). Afterward, in Section 3, we present a review of the state of the art in the usage of NLP and ML to classify and predict annotation and expression of emotions, gestures, affective cues, and so on, using written messages from multiple types of sources. In Section 4, we present several examples on how emoji are currently employed by artificial entities, both virtual and embodied, for expressing emotions during its interaction with humans. Lastly, Section 5 summarizes the chapter and discusses open questions regarding emoji usage as a source for robotic emotional communication.

2. Competence, lexicon, and ways of usage of emoji

To study how emoji are employed and about its challenges, we cannot simply do it without specifying the *emoji competence* [2]. Loosely speaking, competence (either linguistic or communicative) stands for the rules (e.g., grammar) and abilities an individual owns to correctly employ a given language to convey a specific idea [11]. Hence, the emoji competence stands for an adequate usage of emoji within

messages, not only in their representation but also in exact position within the message, to address a specific function (e.g., emotional expression, gestures, maintain interest in the communication, etc.) [2]. Nevertheless, even while the emoji competence has not been formally defined yet, and it can only be developed through the usage of emoji themselves [2, 6], here, we elaborate several of its components.

A key element of the emoji competence is the *emoji lexicon*, which is the standardization of pictograms (i.e., figures that resemble the real-world object), ideograms (i.e., figures that represent an idea) and logograms (i.e., figures that represent a sound or words) into *anime-like* graphical representations that belong to the ever-growing Unicode computer character standard [2, 6, 12]. These are employed within any message in three different ways: adjunctively, substitutively, or providing mixed textuality. In the first case, emoji appear along text within specific points of the written message (e.g., at the end of it) conveying it with emotional tone or adding visual annotations; it requires an overall low emoji competence. In the second case, emoji replace words, requiring a higher degree of competence to understand, not only the symbols per se but also the layout structure of the message, for instance, if we consider *syntagms*, which are symbols sequentially grouped that together conform a new idea (e.g., I love coffee = ☕❤️☕). The third case intertwines text with emoji in a substitutive form rather than adjunctively. This case is the one that requires the highest emoji competence degree, since its decoding requires sophisticated knowledge about rhetorical structures and the proper usage of signs and symbols.

The emoji lexicon possesses generic features such as *representationality*, which allows signs and usage rules to be combined in specific forms to convey a message. Similarly, any person who is well versed with code's signs and rules is capable of interpreting any message based on the code (i.e., *interpretability*). However, messages built using the emoji lexicon are affected by *contextualization*, allowing that references, interpersonal relationships, and other factors affect the meaning of the message [4, 5]. Besides these, the emoji code is composed by a core and peripheral lexicon [2, 5]. As in the *Swadesh list*, the core lexicon stands for those emoji whose meaning and usage is, somehow, universally accepted and used, even while the Unicode supports more than 1000 different emoji [10]. Within this stand, all facial emoji also contain those emoji that stand for Ekman's six basic emotions such as surprise (😮¹) or anger (😡) [2, 13]. On the other hand, the peripheral lexicon is constituted by specialized communication symbols such as the one required for marketing, education [14], promoting national identity, or cultural cues [2], among others. Nevertheless, it is worth mentioning that since emoji may be used as nouns, verbs, or other grammatical structure, even those in the core lexicon can be used as a peripheral element in accordance with users' first language, its position within message, or by concatenating several of them into a syntagm.

2.1 How do we use emoji?

Emoji within any message can have several functions; **Figure 1** summarizes these. As shown by the latter, one of the most important functions an emoji has is *emotivity*, which adds an emotional layer to plain text communication. In this sense, emoji serve as a substitute of face-to-face (F2F) facial expressions, gestures, and body language, to state oneself emotional states, moods, or affective nuances. When used in this manner, emoji take the role of discourse strategies such as intonation or

¹ <https://emojipedia.org/face-screaming-in-fear/>

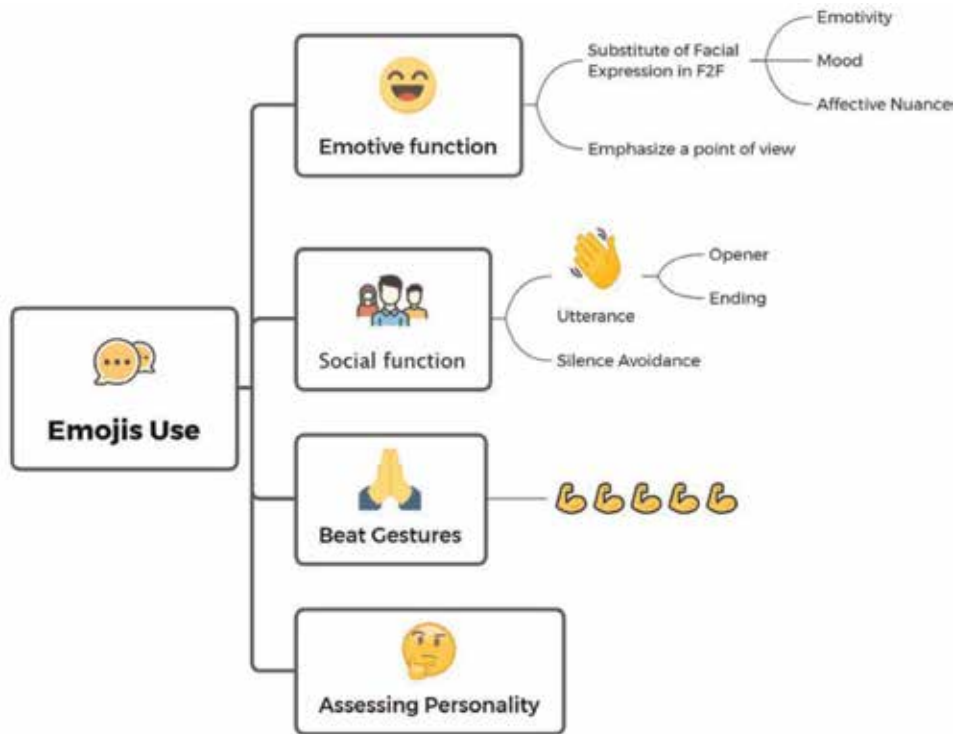


Figure 1.
Emoji functions within the computer-mediated communications.

phrasing [2, 4, 15]. Emoji *emotivity* mostly conveys positive emotions, hence it can be employed to emphasize an specific point of view, such as sarcasm, while softening the negative emotions associated with it (e.g., with respect to the one that is being sarcastic), allowing the receiver of the message to focus on the content instead of the negativity elicited [2, 14].

Another important role of emoji is as phatic instrument during communication [2, 16]. In this sense, they are employed as utterances that allow the flow of the conversation to unfold pleasantly and smoothly. In this sense, emoji serve as an opener or ending utterance (i.e., waving hand) to open or close a conversation, respectively, maintaining a positive dialog regardless of the content. Similarly, emoji can be used to fill uncomfortable moments of silence during a conversation avoiding its abrupt interruption. Beat gestures are another function of emoji; the former can be defined as a repetitive rhythmical co-speech gesture that emphasizes the *rhythm* of the speech [9]. For instance, in the same way that keeping nodding up and down during a conversation emphasizes agreement with the interlocutor, emoji can be repeated to convey the same meaning (e.g., 👏👏👏). Keeping in mind that although emoji, neither as utterance nor as beat gesture, explicitly stands for an emotional reaction, they implicitly convey an emotional (positive) tone to the conversation. Likewise, the other function of emoji, which is also implicitly related to emotion, is personality. The latter stands for basal characteristics that have pre-established effects on thoughts, behaviors, and emotions [17]. Been considered a genetic trait, it suffers less variability over time in contrast to emotions and moods [17]. In this sense, emoji can be used to elucidate the underlying personality traits of individuals, either by data mining or by replacing text-based items by their emoji equivalent in personality tests [18].

3. Studying emoji usage using formal frameworks

Emoji usage has had a deep impact on humans' computer-mediated communication (CMC). With the increasing use of social media platforms such as Facebook, Twitter, or Instagram, people now massively interchange messages and ideas through text-based chat tools that support emoji usage, imbuing these with semantic, emotional, and meaningful meaning. In order to analyze and extract comprehensive knowledge from emoji-embedded message data sets, many methods have been developed through the usage of a multidisciplinary approach, which involves ML along with NLP, psychology, robotics, and so on. Among the tasks developed with ML algorithms for the analysis of emoji usage stand sentiment analysis [5, 19], polarity analysis [10, 20], sentiment lexicon buildage [10], utterance embeddings [21], personality assessment [18], to mention a few. These applications are summarized in **Table 1**.

The following section shows an analysis from the point of view of the use of ML algorithms to support tasks related to the sentiment analysis through the use of emoji, classification, comparison, polarity detection, data preprocessing from tweets with emoji embeddings, and computer vision techniques for video processing to detect facial expression.

3.1 Emoji classification and comparison

In recent years, algorithms such as deep learning (DL) have emerged as a new area of ML, which involve new techniques for signal and information processing. This type of algorithms employ several nonlinear layers for information processing through supervised and unsupervised feature extraction, and transformation for pattern analysis and classification. It also includes algorithms for multiple levels of representation attaining models that can describe the complex relations within data. Particularly, if data sets are considerably large, a deep-learning approach is the best option for reaching a well-trained model regarding if data are labeled or not [25, 26]. Until our days, ML algorithms that use shallow architecture show a good performance and effectiveness for solving simple problems, for instance, linear regression (LR), support vector machines (SVM), multilayer perceptron (MPL) with a single hidden layer, decision trees like random forest or ID3, among others. These architectures have limitations for extracting patterns from a wide complex problem's variety, such as signals, human speech, natural language, images, and sound processing [25]. For this reason, a deep-learning approach allows to solve these limitations showing good results.

Emoji classification and comparison constitute two important tasks for discriminating several kinds of emoji, including those with similar meaning. Deep-learning models have been used for this goal in texts where emoji are embedded, producing better result than softmax methods, such as logistic regression, naive Bayes, artificial neural networks, and others. For example, Xiang Li et al. developed a deep neural network architecture for getting a trained model that could predict the correct emoji for its corresponding utterance [21]. This approach provides the possibility that machines generate an automatic message for humans during a conversation with the use of implicit sentiment and better semantic on ideas.

In Li et al.'s [21] proposal, the system receives as input an utterance set $Y = \{y_1, y_2, \dots, y_n\}$ and an emoji set $X = \{x_1, x_2, \dots, x_n\}$. The main goal is to train a classification model, which could predict the correct emoji for an utterance given.

The architecture used in this work has two parts. The first is a convolutional neural network (CNN) for giving a sentence embedding that represents an

Related papers	Problems addressed	Method	Emoji use	Emoji competence
[21]	Emoji classification correct emoji prediction Matching utterance embeddings with emoji embeddings Emoji for sentiment analysis	One-hot vector Sliding windows CNN Cosine similarity Dynamic Pooling	Emotive Social	Adjunctive
[20]	Sentiment analysis Polarity detection	10-fold cross validation ANN CNN NLP Shallow classifiers: SVM and LR Search-based classifier	Emotive Social	Adjunctive Substitutive Mixed textuality
[22]	Image processing & computer vision to detect facial expression Emoji embeddings	Haar classifier AdaBoost Canny algorithms	Emotive	Adjunctive
[19]	Sentiment analysis Auto-labeling using emoji sentiment Emoji classification Emoticons as a heuristic data Tweets data preprocessing	TF-idf Word2Vec NLP Ensemble classifiers Deep learning	Emotive Social	Adjunctive
[10]	Sentiment analysis Emoji sentiment map & lexicon Polarity detection Emoji sentiment ranking	Discrete probability distribution approximation Welch's t-test Krippendorffs Alpha-reliability	Emotive Social	Adjunctive Substitutive
[5]	Sentiment analysis Automated analysis of social media contents Emoji classification Correlation analysis among languages	Nearest neighbors	Emotive Social	Adjunctive Substitutive
[23]	Emotions detection Emoji classification	LR SVM Adaptive Boosted Decision Trees (ADT) 10-fold cross validation Random Forests (RF)	Emotive Social	Adjunctive Substitutive
[18]	Emotions representation using emoji Big 5 personality assessment test using emoji	Exploratory Factor Analysis (EFA) Confirmatory Factor Analysis (CFA) Bonferroni correction	Emotive Personality assessment	Adjunctive Substitutive
[9]	Emoji as co-speech element Emoji-based measures	NA	Beat gestures Social	Adjunctive Substitutive
[24]	Facial expressions recognition Emoji embeddings Emoji usage for peer communication Emoji as social cues	Haar classifier AdaBoost	Emotive Social	Adjunctive

Table 1.
Comparative table of the articles analyzed.

utterance, and the second one is the embedding of emoji and this part should be trained. In order to join both parts, a matching structure was created due to embeddings in continuous vector space that could well represent emoji, consequently performing better than discrete softmax classifier.

The bottom of CNN is a word embedding layer for tasks of NLP. This provides semantic information about a word using real vector that represents its features. For an utterance that represent a sequence of words, for each word w_i is a one-hot vector of dictionary dimension, a bit from w_i takes value 1 if it corresponds to word on the dictionary and 0 for remaining bits. In Eq. (1), the embedding matrix is defined such that [21]:

$$E_1 \in R^{D \times V}, \quad (1)$$

where D and V are word embedding and word dictionary dimensions, respectively. Each $e_1(w_i) \in E_1$ is the embedding for word in a dictionary. The convolutional layer uses sliding windows to get information from word embeddings; for this process, the following function is used (see the Eq. (2) [21]):

$$Y_1 = f(W_1[e_1(w_1); e_1(w_2); \dots; e_1(w_t)] + b_1), \quad (2)$$

where t is the size of window and b_1 is the bias vector. Hence, the parameter to be trained is W_1 .

Once obtained a series continuous representations of local features from convolutional layer, theory of dynamic pooling is used for sensitizing these embeddings into one vector of the whole utterance. This produces by output the max pooling. The hidden layer uses the sentence embedding of the utterance obtained as y_2 and returns finally the vector to represent the utterance.

Similarly to the word embedding layer, the emoji embedding layer uses a matrix defined as $E_2 \in R^{D \times V}$ to obtain $e_2(x_i)$, where K is the one-hot vector's length that represents each emoji x_i . Each $e_2(x_i)$ of E_2 is one parameter of neural network. The process of training is a forward propagation for computing the matching score between the given utterance and the correct emoji, and matching score between the given utterance and the negative emoji. Backward propagation is used to update model parameters. For calculating the matching score, the cosine similarity measure is used, whereas for training the neural network, the Hinge Loss function was used. It is worth mentioning that the latter is very useful for carrying out pairwise comparison to identify similar emoji types.

Finally, the author obtains an architecture that uses a CNN and a matching approach for classifying and learning emoji embeddings. The importance of the aforementioned work regarding the field of robotics is the possibility of producing a facial gesture as a result of the introduction of a statement, conversation, or idea to a machine, employing the semantic and emotional relation of emoji.

3.2 Emoji sentiment analysis

In the area of decision making, it is being relevant to know how the people think and what they will do in the future. These produce the needs of grouping peoples in accordance with their interaction on Internet and social networks. Sentiment analysis or opinion mining is the study of people's opinions, sentiments, or emotions, using an NLP approach, which includes, but is not limited to, text mining, data mining, ML, and deep learning [20]. For instance, the CNN's usage has been employed to predict the tweets' emoji polarities. These techniques have showed to

be more effective than shallow models in image recognition and text classification where they reach better results [19].

Tweets processing for mining opinion and text analysis tasks play a crucial role for different areas in the industry because these produce relevant result for feedback the design of products and services. As Twitter is a platform where user interactions are very informal and unstructured and people use many languages and acronyms, it becomes necessary to build a model language-independent and non-supervised learning. We can see the use of emoji or emoticons in this scenario through heuristic labels for a system; for this, the feature's extraction process was developed by unsupervised techniques. The emoji/emoticons are the final result that represents a sentiment that a tweet contains. According to Mohammad Hanafy et al. in order to get a trained model for text processing, it is essential to do a data preprocessing for obtaining the data sets, where noisy elements are removed such as hashtags and other stranger characters like "at," reduction of words by removing duplicated words, and very important, reemphasizing the emoticons with their scores. Each emoticon has a raw data that contain a sentiment classified as negative, neutral, or positive. For each classification, a continuous value is recorded. This representation is used in auto-label phase, for generating the training data using the score for determining emoji [19].

Feature extraction stage uses the Tf-idf approach; it indicates the importance of a word in the text through its frequency in the text or text's set. Using Eq. (3), we can calculate this as follows [19, 27]:

$$TfIDF(t, d, F) = tf(t, d) \cdot \log \frac{n_d}{df(d, t) + 1} \quad (3)$$

where t is the word and d is the tweet. Term frequency in the document is tf , df is document frequency where word exists, and n_d is the number of tweets.

Other feature-extracting methods employed were bag-of-words (BOW) and Word2Vec. BOW selects a set of important words in tweets, and then each document is represented as a vector of the number of occurrences of the selected words. Word2Vec uses a two-layer neural network to represent each word as a vector of certain length based on its context. This feature extraction model computes a distributed vector representation of the word, been its main advantage that similar words are close in the vector space. Moreover, it is very useful for named entity recognition, parsing, disambiguation, tagging, and machine translation. In the area of big data processing, the library Spark ML within the Apache Spark engine uses skip-gram-model-based implementation that seeks to learn vector representation that take into account the contexts in which words occur [27].

Skip-gram model learns word vector representations that are good at predicting its context in the same sentence or sequence of training words denoted as $W = \{w_1, w_2, \dots, w_t\}$, where T is $\|W\|$. The objective function is to maximize the average log-likelihood, which is defined by Eq. (4) [27]:

$$\frac{1}{T} \cdot \sum_{t=1}^T \sum_{j=-k}^{j=k} \log p(w_{t+j}|w_t), \quad (4)$$

where k is the size of training windows. Each w is associated with two vectors u_w as word and v_w as context, respectively. Using Eq. (5), given the word w_j , the probability of correctly predicting w_i is computed as [27]:

$$p(w_i|w_j) = \frac{\exp(u_{w_i}, u_{w_j})}{\sum_{l=1}^V \exp(v_l, v_{w_j})}, \quad (5)$$

where V is the vocabulary length. The cost of computing $p(w_i|w_j)$ is expensive; consequently, Spark ML uses hierarchical softmax with computational cost of $O(\log(V))$ [27].

These feature extractor models were used with other classifiers, such as SVM, MaxEnt, voting ensembles, CNN, and LSTM to extend the architecture of recurrent neural network (RNN). As solution proposal, a weighted voting ensemble classifier is used that combines the output of different models and its classification probabilities. For each model, a different weight when voting is assigned. The proposed model reaches a considerable accuracy in comparison with other models. This approach is very important in scenarios where we need no human intervention and any information about the used language; it is very useful to apply a good combination between classical and deep-learning algorithm to achieve better accuracy [19].

3.3 From video to emoji

As consequence of the semantic meaning that emoji carriers, there are some applications and researches that involve the image processing for generating emoji classification or an utterance with emoji embeddings. For that purpose, Chembula et al. have created an application that receives as input a stream of video or images from a person and create an emoticon based on image face. The solution detects the facial expression at the time that message is being generated. Once that facial expression is detected, the device generates a message with the suitable emoticon [28].

This system performs a facial detection, facial feature detection, and classification task to finally identify the facial expression. Although the initial processing proposed by Chembula and Pradesh [22] was not specified on the general description, we can use open source solutions in order to aim this job.

OpenCV is an open source library for computer vision, and it includes classifiers for real-time face detection and tracing like Haar classifiers and Adaptive Boosting (AdaBoost). We can download trained model for performing this task; the model is an XML file that can be imported inside the OpenCV project. For featuring extraction, the library includes algorithm for detecting region of interest in human face like eyes, mouth, and nose. For this propose, drop information from image stream using gray scale convert and afterward using Gaussian Blur for reducing noise is important. Canny algorithms may be used for tracking facial features with more precision than others like Sobel and Laplace [29].

In [24], Microsoft's emotion API is used as a tool to detect facial images from the Webcam image capture of the computer. Once the image is captured, the detected face is classified into seven emotion tags. Although the process is not specified exactly, the API mentioned works on an implementation of the OpenCV library for .NET [30], so the algorithms used for face detection should be the same as those described above.

For classification task, we can use nearest neighbor classifier, SVM, logistic classifier, Parzen density classifiers, normal density Bayes classifiers, and Fisher's linear discriminant [31]. Finally, when the classification is done, the output layer consists a group of types of emoji according to the meaning for each type of emotion detected in the image face. The importance of this contribution lies in the possibility of introducing new forms of human-computer interaction through the use of emotions. This can be useful for intelligent assistants both physical and visual that are able to react or are current according to the mood of people who use a particular intelligent ecosystem.

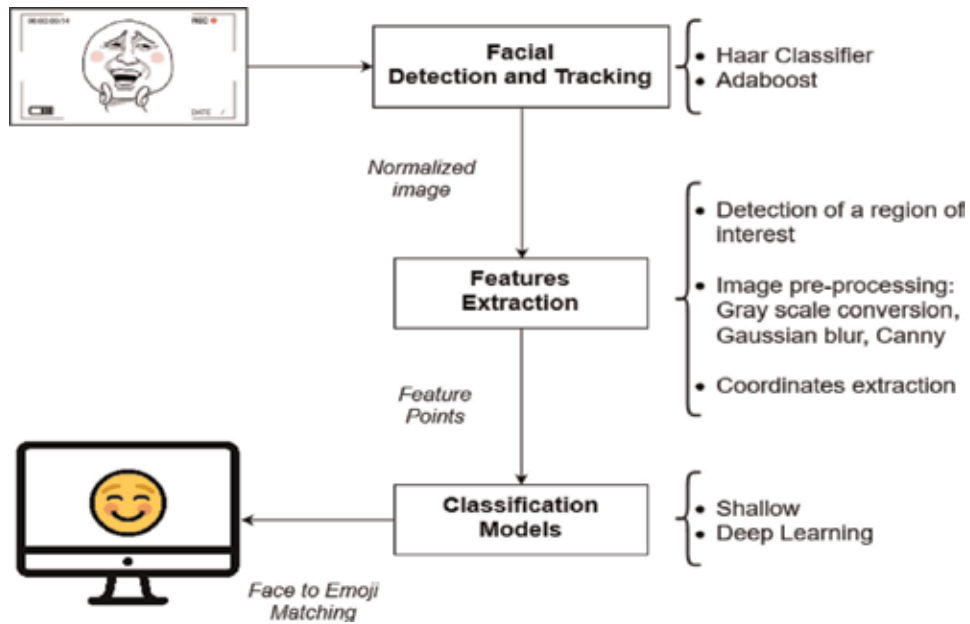


Figure 2. General process of facial detection and its corresponding classification using emoji.

Figure 2 shows in a general way the operation of what has been explained above.

4. Applications to virtual and embodied robotics

As already mentioned, in this work, our intention is to elaborate the elements that will power an artificial intelligent entity, either virtual or physically embodied, with the capacity to recognize and express (R&E) emotional content using emoji. In this sense, we can collect massive amounts of human-human (and perhaps human-machines too) interactions from multiple Internet sources such as social media or forums, to train ML algorithms, which can R&E emotions, utterances, beat gestures, and even assess personality of the interlocutor. Furthermore, we may even reconstruct text phrases from speech in which emoji are embedded to these to obtain a bigger picture of the semantic meaning. For instance, if we asked the robot “are you sure?” while raising the eyebrows to emphasize our incredulity, we may obtain an equivalent expression such as “are you sure? 😬” Once the models are defined and trained, these will be embedded into the artificial entity, which will be interacting with humans. This conceptual framework is displayed in **Figure 3**. While in a virtual entity such as a chatbot, the inference of emotional states or personality, as well as expressing emotions or beat gestures using emoji, is straightforward, in an embodied entity such as a physical robot that requires a little bit more of elaboration. In the latter, an interlocutor’s emotional or personality first requires the humans’ facial expressions and gestures to be transformed into emoji from video streams or speech similarly as shown in [22]. Then, the same pipeline as the one used for a chatbot may be employed, identifying the corresponding emotional state using pretrained sentiment detection algorithm such as in [20]. Therefore, since both, embodied and virtual artificial entities, can employ the same pipeline, we focus on applications to the former. In particular, we discuss some works, which are delved in this direction, and how the cognitive interaction

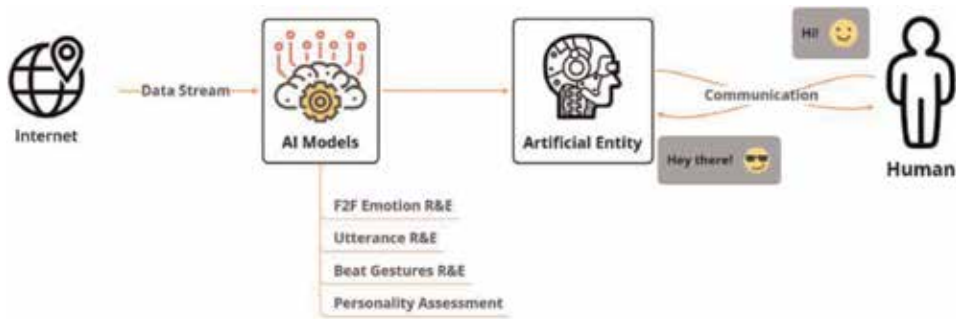


Figure 3.
Emoji emotional communication conceptual framework.

between humans and artificial entities may be improved by modeling the emotional exchange as shaped by emoji usage.

4.1 Embodied service robots study cases

Service robots are a type of embodied artificial intelligent entities (EAIE), which are meant to enhance and support human social activities such as health and elder care, education, domestic chores, among others [32–34]. A very important element for EAIE is improving the *naturalness* of human-robot interactions (HRI), which can provide EAIE with the capacity to R&E emotions to/from their human interlocutors [32, 33].

Regarding the emotional mechanisms of an embodied robot *per se*, a relevant example is the work by [33], which consists in an architecture for imbuing an EAIE with emotions that are displayed in an LED screen using emoticons. Such architecture establishes that a robot's emotions are in terms of long-medium-short affective states suchlike its personality (i.e., social and mood changes), the surrounding ambient (i.e., temperature, brightness, and sound levels), and human interaction (i.e., hit, pat, and stroke sensors), respectively. All of these sensory inputs were employed to determine EAIE emotional state using ad hoc rules, which are coded into a fuzzy logic algorithm, which is then displayed in an LED face. Facial gestures corresponding to Ekman's basic emotions expressions are shown in the form of emoticons.

An important application of embodied service robots is the support of elder's daily activities to promote a healthy life style and providing them with an enriching companion. In such case, a more advanced interaction models for EAIE based on an emotional model, gestures, facial expressions, and R&E utterances are proposed [32, 35–37]. The authors of these works put forward several cost-efficient EAIE based on mobile device technologies namely *iPhonoid*, *iPhonoid-C*, and *iPadrone*. These are robotic companions based on an architecture, which among other features is built upon the informationally structured spaces (ISS) concept. The latter allows to gather, store, and transform multimodal data from the surrounding ambience into a unified framework for perception, reasoning, and decision making. This is a very interesting concept since, not only EAIE behavior may be improved by its own perceptions and HRI but also from remote users' information such as elder's activities from Internet or grocery shopping. Likewise, all these multimodal information can be exploited by any family member to improve the quality of his/her relation with the elder ones [36]. Regarding the emotional model, the perception and action modules are the most relevant. Among the perceptions considered in these frameworks stand the number of people in the room, gestures, utterances,

colors, etc. In the same fashion as [33], these EAIE implements an emotional time-varying framework, which considers emotion, feeling, and mood (from shorter to longer emotional duration states, respectively). First, perceptions are transformed into emotions using expert-defined parameters, then emotions and long-term traits (i.e., mood) serve as the input of *feelings* whose activation follows a spiking neural network model [32, 35]. Particularly, mood and feelings are within a feedback loop, which emphasize the emotional time-varying approach. Once perceptions are turned into its corresponding emotional state, the latter is sent to the action module to determine the robot behavior (i.e., conversation content, gestures, and facial expression). As mentioned earlier, EAIE also R&E utterances, which provide feedback to the robot's emotional state. Another interesting feature of the architecture of these EAIE is its conversational framework. In this sense, the usage of certain utterances, gestures, or facial expressions depends on conversation modes, which in turn depends on NLP processing for syntactic and semantic analyses [32, 37]. Nevertheless, with regard to facial and gesture expressions, these works take them for granted and barely discuss both. In particular, how facial expressions are designed and expressed can only be guessed from figures of these EAIE papers, which closely resemble emoji-like facial expressions.

Embodied service robots are also beneficial in the pedagogical area as educational agents [38, 39]. Under this setting, robots are employed in a *learning-by-teaching* approach where students (ranging from kindergarten to preadolescence) read and prepare educational material beforehand, which is then taught to the robotic peer. This has shown to improve students understanding and knowledge retention about the studied subject, increasing their motivation and concentration [38, 40]. Likewise, robots may enhance its classroom presence and the elaboration of affective strategies by means of recognizing and expressing emotional content. For instance, one may desire to elicit an affective state that engages students in an activity or identify boredom in students. Then, robot's reaction has to be an optimized combination of gestures, intonation, and other nonverbal cues, which maximize learning gains while minimizing distraction [41]. Humanoid robots are preferred in education due to their anthropomorphic emotional expression, which is readily available through body and head posture, arms, speech intonation, and so on. Among the most popular humanoid robotic frameworks stand the *Nao*[®] and *Pepper*[®] robots [38–40]. In particular, Pepper is a small humanoid robot, which is provided with microphones, 3D sensors, touch sensors, gyroscope, RGB camera, and touch screen placed on the chest of the robot, among other sensors. Through the *ALMood Module*, Pepper is able to process perceptions from sensors (e.g., interlocutors' gaze, voice intonation, or linguistic semantics of speech) to provide an estimation of the instantaneous emotional state of the speaker, surrounding people, and ambiance mood [42, 43]. However, Pepper communication and its emotional expression is mainly carried out through speech consequence of limitations such as a static face, unrefined gestures, and other nonverbal cues, which are not as flexible as human standards [44], for instance while we consider **Figure 4**, which is a picture displaying a sad Pepper. Only by looking the picture, it is unclear if the robot is sad, looking at its wheels, or simply turned off.

4.2 Study cases through the emoji communication lens

In summary, in the above revised EAIE cases (emoticon-based expression, iPadrone/iPhonoid, and Pepper), emotions are generated through an ad hoc architecture, which considers emotions and moods that are determined by multimodal data. A cartoon of these works is presented in **Figure 5**, displaying on



Figure 4.
Is Pepper sad or just shutdown?

(a) the work of [33] on (b) the work of [32, 35–37], and on (c) Pepper the robot as described in [42–44].

In these cases, we can integrate emoji-based models to enhance the emotional communication with humans, for some tasks more directly than for others. Take for instance, the facial expressions by itself, in the case of (a) and (b), the replacement of emoticon-based emotional expression by its emoji counterpart is straightforward. This will not only improve visually the robot's facial expression but also allowing more complex facial expressions to be displayed such as sarcasm (🙄) or co-speech gestures as 🤔🤔🤔🤔 after making a joke. Another important feature of replacing emoticon-based faces by emoji is that the latter are used mostly to convey positive emotions even when criticizing or giving negative feedback [2]. Therefore, this feature could be really useful for maintaining a perpetual friendly tone of an elder robotic partner (b) or as an educational agent (c).

Regarding the emotional expression of the discussed EAIE, this is contingent to the emotional model, which in the case of (a) and (b) are expert-design knowledge coded into fuzzy logic behavior rules and more complex neural networks, respectively. In both cases, this not only will bias the EAIE into specific emotional states but also will require vast human effort to maintain it. In contrast, Pepper's framework is robuster, includes a developer kit, which allows modifying robot's behaviors and the integration of third party chatbots, performing semantic and utterance analysis, and is maintained and improved by a robotics enterprise. Yet, Pepper's

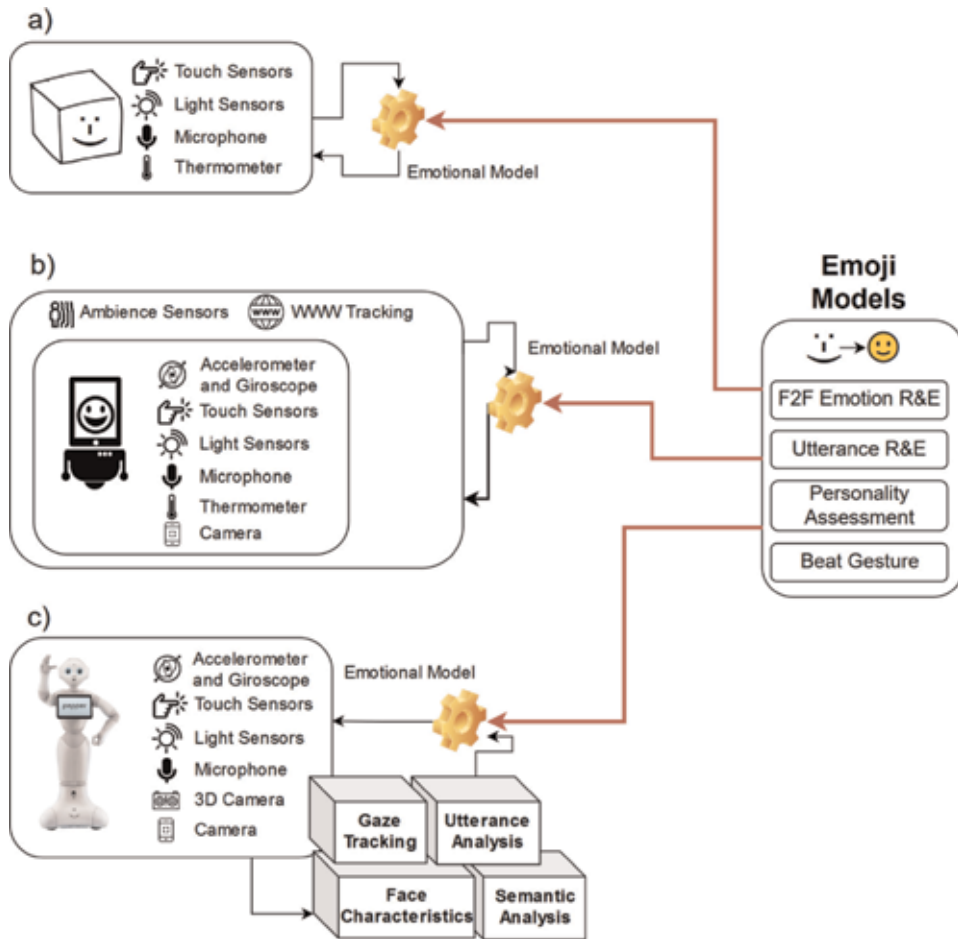


Figure 5. Case studies using emoji-based modules to improve its emotional R&E models.

emotional communication is constrained by a static face, while it can express emotions by changing the color of its led eyes and adopt the corresponding body posture; its emotional communication is mainly done through verbal expressions. Nevertheless, in a pragmatic sense, do we really need to emulate emotions for a robot to have an emotional communication or is enough to R&E emotions so that a human interlocutor cannot distinguish between man and machine? In this sense, NLP and ML can be used to leverage the emotional communication of a robot by first mapping multimodal data into a discourse-like text where emoji are embedded, and then, using emoji-based models to recognize sentiments, utterances, and gestures so the decision-making module can determine the corresponding message along with its corresponding emoji. In the case of (a), the microphone and in the case of (b), the microphone, camera, and ambient sensors will be responsible for capturing speech and facial expressions that will be converted into a discourse-like text. Once the emotional content of the message is identified, the corresponding emoji shall be displayed. In the case of Pepper, F2F communication can be improved directly by displaying emoji in its front tablet. For instance, when Pepper starts waving to a potential speaker, a friendly emoji such as a waving hand 🙌 or a greeting smile 😊 shall be portrayed in the tablet. Likewise, emoji usage as utterances and beat gestures can be employed by Pepper to avoid silences in a goofy manner (🤪), to indicate a lack of knowledge about a particular topic (🤷), or to emphasize politeness when asking an interlocutor for an action (🙏🙏🙏🙏).

5. Discussion

Emotional communication is a key piece for enhancing HRI, after all it will be very useful if our smart phones, personal computers, cars or busses, and other devices could exploit our emotional information to improve our experience and communication. While nowadays, several proposals for robotic emotional communication are undergoing, emoji as a framework for the latter present a novel approach with high applicability and big usage opportunities. Some of the works presented here discussed the linguistic aspects of emoji, as well as the technical aspects in terms of ML and NLP to R&E emotions, utterances, gestures in texts, which contain emoji. Furthermore, we also presented some related works in the area of HRI, which can easily adopt emoji for imbuing an embodied artificial intelligent entity with the capacity for expressing and recognizing emotional aspects of the communication. On the whole, ML models support these issues, but we do not exclude the important task that involves the processing and transformation of data to reach a suitable input representation for training an appropriate model.

On the other hand, there are several open questions regarding the usage of emoji for emotional communication. For instance, are emoji suitable for the communication of every robotic entity? Emoji are mostly employed in a friendly manner and for maintaining a positive communication. If the objective is to model a virtual human, emoji usage will clearly restrain the spectrum of emotions, which may be detected and expressed due to its knowledge base. An important example to consider is the humanoid robot designed by Hiroshi Ishiguro, *the man who made a copy of himself* [45]. Ishiguro's proposal is that in order to understand and model emotions, we must first understand ourselves. Hence, this humanoid robot, namely Geminoid HI-1, is capable of displaying ultrarealistic human-like behaviors. However, do we really want to interact with service robots, which may have bad personality traits such as been unsociable and fickle, or whose mood can be affected by heat and noise like a human does? Do we really want to interact with service robots, which can be *rude* as a real elderly caretaker could? In this sense, emoji usage for the emotional communication may be best suited when the task at hand (e.g., robotic retail store cashier or an educational agent) requires keeping a friendly tone with the human interlocutor. Another question is, should the entire emoji lexicon be used or be restricted only to the core lexicon, which refers to facial expressions? In an ultrarealistic anthropomorphic robot such as Geminoid HI-1, all hand gestures might be carried out by robot's hands itself, thus it should be unnecessary to even fit a screen for displaying a waving emoji (👋) while greeting. On the contrary, more constrained entities such as a Roomba^{®2} or Pepper[®] may clearly be benefited from both core and peripheral emoji lexicons for improving its emotional communication with humans. Also, since most of the emoji knowledge is based on short text messages, multimodal data first need to be converted into their corresponding discourse text message, which is, by itself, an open research question.

Acknowledgements

Author GSB thanks the Cátedra CONACYT program for supporting this research. Author OGTL thanks GSB for his excellent collaboration.

² <https://www.irobot.com/roomba>

Author details

Guillermo Santamaría-Bonfil^{1*} and Orlando Grabiél Toledano López²

1 CONACYT-INEEL, National Institute of Electricity and Clean Energies,
Cuernavaca, Morelos, Mexico

2 University of Informatics Sciences, La Habana, Cuba

*Address all correspondence to: guillermo.santamaria@ineel.mx

IntechOpen

© 2019 The Author(s). Licensee IntechOpen. This chapter is distributed under the terms of the Creative Commons Attribution License (<http://creativecommons.org/licenses/by/3.0>), which permits unrestricted use, distribution, and reproduction in any medium, provided the original work is properly cited. 

References

- [1] Hurlburt G. Emoji: Lingua franca or passing fancy? *IT Professional*. 2018; **20**(5):14-19
- [2] Danesi M. *The Semiotics of Emoji: The Rise of Visual Language in the Age of the Internet*. Bloomsbury Academic: UK; 2016
- [3] Skiba D. Face with tears of joy is word of the year: Are emoji a sign of things to come in health care? *Nursing Education Perspectives*. 2016;**37**(1): 56-57. Available from: <http://insights.ovid.com/crossref?an=00024776-201601000-00015>
- [4] Wiseman S, Gould S. Repurposing emoji for personalised communication. In: 2018 CHI Conference on Human Factors in Computing Systems. Montréal, QC: ACM; 2018. pp. 1-10
- [5] Barbieri F, Kruszewski G, Ronzano F, Saggion H. How cosmopolitan are emojis?: Exploring emojis usage and meaning over different languages with distributional semantics. In: *Proceedings of the 2016 ACM Multimedia Conference*. 2016. pp. 531-535
- [6] Alshenqeeti H. Are emojis creating a new or old visual language for new generations? A socio-semiotic study. *Advances in Language and Literary Studies*. 2016;**7**(6):56-69
- [7] Ai W, Lu X, Liu X, Wang N, Huang G, Mei Q. Untangling emoji popularity through semantic embeddings. In: *Proceedings of the Eleventh International AAAI Conference on Web and Social Media—ICWSM '17* [Internet]. 2017. pp. 2-11. Available from: <https://aiwei.me/files/icwsm2017-ai.pdf>
- [8] Kerslake L, Wegerif R. The semiotics of emoji: The rise of visual language in the age of the internet. *Media and Communication*. 2017;**5**(4):75
- [9] McCulloch G, Gawne L. Emoji grammar as beat gestures. *CEUR Workshop Proceedings*. 2018;**2130**:3-6
- [10] Kralj Novak P, Smailović J, Sluban B, Mozetič I. Sentiment of emojis. *PLoS One*. 2015;**10**(12): e0144296. DOI: 10.1371/journal.pone.0144296
- [11] Chomsky N. *Aspects of the theory of syntax*. The Philosophical Quarterly. MIT press; 2014;**11**:1-8
- [12] Barbieri F, Ballesteros M, Saggion H. Are emojis predictable? In: *Proceedings of the 15th Conference of the European Chapter of the Association for Computational Linguistics: Volume 2, Short Papers* [Internet]. Stroudsburg, PA, USA: Association for Computational Linguistics; 2017. pp. 105-111. Available from: <http://arxiv.org/abs/1702.07285>
- [13] Hussien W, Al-Ayyoub M, Tashtoush Y, Al-Kabi M. On the Use of Emojis to Train Emotion Classifiers. 2019. Available from: <http://arxiv.org/abs/1902.08906>
- [14] Doiron JAG. Emojis: Visual communication in higher education. *PUPIL: International Journal of Teaching, Education and Learning*. 2018;**2**(2):1-11
- [15] Betz N, Hoemann K, Barrett LF. Words are a context for mental inference. *Emotion*. 2019:1-15. DOI: 10.1037/emo0000510
- [16] Guibon G, Ochs M, Bellot P, Guibon G, Ochs M, Bellot P, et al. From emoji usage to categorical emoji prediction. In: *19th International Conference on Computational Linguistics and Intelligent Text*

- Processing (CICLING 2018). Vietnam: Hanoi. p. 2018
- [17] Quereingässer J, Schindler S. Sad but true?—How induced emotional states differentially bias self-rated Big Five personality traits. *BMC Psychology*. 2014;2(1):1-8
- [18] Marengo D, Giannotta F, Settanni M. Assessing personality using emoji: An exploratory study. *Personality and Individual Differences*. 2017;112: 74-78. DOI: 10.1016/j.paid.2017.02.037
- [19] Hanafy M, Khalil MI, Abbas HM. Combining Classical and Deep Learning Methods for Twitter Sentiment Analysis. Switzerland: Springer Nat Switz; 2018. pp. 281-292
- [20] Karthik V. Opinion mining on emoji using deep learning techniques. *Procedia Computer Science*. 2018;132: 167-173
- [21] Li X, Yan R, Zhang M. Joint emoji classification and embedding. *Learning*. 2017;1:48-63
- [22] Chembula AB, Pradesh A. Generating Emoticons Based on an Image of Face. Vol. 2. US Patent; 21 February 2017
- [23] Zhang AX, Igo M, Karger D, Facciotti M. Using Student Annotated Hashtags and Emojis to Collect Nuanced Affective States. London: ACM; 2017
- [24] Liu M, Wong A, Pudipeddi R, Hou B, Wang D, Hsieh G. ReactionBot: Exploring the effects of expression-triggered emoji in text messages. *Proceedings of the ACM on Human Computer Interaction*. 2018;2:1-16
- [25] Deng L, Yu D. Deep learning methods and applications. *Foundations and Trends in Signal Processing*. 2014;7: 197-387
- [26] Bishop CM. *Pattern Recognition and Machine Learning*. Cambridge, UK: Springer Science+Business Media, LLC; 2006. 749 p
- [27] Pentreath N. *Machine Learning with Spark*. Birmingham, UK: Packt Publishing; 2015. 338 p
- [28] Chembula AB, Pradesh A. *Generatin emoticons based on an image of face*. Vol. 2. USA. US 9,576,175 B2. 2017
- [29] Baggio DL. *OpenCV 3.0 Computer Vision with Java*. Birmingham, UK: Packt Publishing; 2015. 174 p
- [30] Larsen L. *Learning Microsoft Cognitive Services*. Birmingham, UK: Packt Publishing; 2017. 484 p
- [31] Pelillo M. *Advances in Computer Vision and Pattern Recognition*. LLC: Springer Science+Business Media; 2013. 293 p
- [32] Tang D, Yusuf B, Botzheim J, Kubota N, Chan CS. A novel multimodal communication framework using robot partner for aging population. *Expert Systems with Applications*. 2015;42(9): 4540-4555. Available from. DOI: 10.1016/j.eswa.2015.01.016
- [33] Daosodsai N, Maneewarn T. Fuzzy based emotion generation mechanism for an emoticon robot. 13th International Conference on Control, Automation and Systems (ICCAS 2013). Gwangju; 2013:1073-1078. DOI: 10.1109/ICCAS.2013.6704075. Available from: <http://ieeexplore.ieee.org/stamp/stamp.jsp?tp=&arnumber=6704075&isnumber=6703852>
- [34] Clabaugh C, Mataric M. Robots for the people, by the people: Personalizing human-machine interaction. *Science robotics*. 2015;3(21):1-2
- [35] Yorita A, Botzheim J, Kubota N. Emotional models for multi-modal communication of robot partners. *IEEE International Symposium on Industrial Electronics*. 2013:1-6

- [36] Obo T, Kakudi HA, Yoshihara Y, Loo CK, Kubota N. Lifelog visualization for elderly health care in informationally structured space. In: 2015 4th Int Conf Informatics, Electron Vision, ICIEV 2015. 2015;(March 2017)
- [37] Woo J, Botzheim J, Kubota N. A socially interactive robot partner using content-based conversation system for information support. *Journal of Advanced Computational Intelligence and Intelligent Informatics*. 2018;22(6): 989-997
- [38] Tanaka F, Isshiki K, Takahashi F, Uekusa M, Sei R, Hayashi K. Pepper learns together with children: Development of an educational application. In: 2015 IEEE-RAS 15th International Conference on Humanoid Robots (Humanoids). 2015. pp. 270-275
- [39] Lehmann H, Rossi G. Social robots in educational contexts: Developing an application in enactive didactics. *Journal of e-Learning and knowledge Society*. 2019;15:27-41
- [40] Jamet F, Masson O, Jacquet B, Stilgenbauer J-L, Baratgin J. Learning by teaching with humanoid robot: A new powerful experimental tool to improve children's learning ability. *Journal of Robotics*. 2018;2018:1-11
- [41] Belpaeme T, Kennedy J, Ramachandran A, Scassellati B, Tanaka F. Social robots for education: A review. *Journal of Robotics*. 2018;3(21): 1-9. Available from: <https://robotics.sciencemag.org/content/3/21/eaat5954>
- [42] Europe SR. {ALMood} {API}. 2019
- [43] Val-Calvo M, Grima-Murcia MD, Sorinas J, Álvarez-Sánchez JR, de la Paz Lopez F, Ferrández-Vicente JM, et al. Exploring the physiological basis of emotional HRI using a BCI Interface. In: Ferrández Vicente JM, Álvarez-Sánchez JR, de la Paz López F, Toledo Moreo J, Adeli H, editors. *Natural and Artificial Computation for Biomedicine and Neuroscience*. Cham: Springer International Publishing; 2017. pp. 274-285
- [44] Europe SR. How to Create a Great Experience with Pepper. September 2017. Available from: <http://doc.aldebaran.com/> [Last accessed: 17 September 2019]
- [45] Guizzo E. Hiroshi Ishiguro: The Man Who Made a Copy of Himself [Internet]. *IEEE Spectrum*. 2010. Available from: <https://spectrum.ieee.org/robotics/humanoids/hiroshi-ishiguro-the-man-who-made-a-copy-of-himself>

Living and Interacting with Robots: Engaging Users in the Development of a Mobile Robot

Valerie Varney, Christoph Henke and Daniela Janssen

Abstract

Mobile robots such as Aldebaran's humanoid Pepper currently find their way into society. Many research projects already try to match humanoid robots with humans by letting them assist, e.g., in geriatric care or simply for purposes of keeping company or entertainment. However, many of these projects deal with acceptance issues that come with a new type of interaction between humans and robots. These issues partly originate from different types of robot locomotion, limited human-like behaviour as well as limited functionalities in general. At the same time, animal-type robots—quadrupeds such as Boston Dynamic's WildCat—and under-actuated robots are on the rise and present social scientists with new challenges such as the concept of uncanny valley. The possible positive aspects of the unusual cooperations and interactions, however, are mostly pushed into the background. This paper describes an approach of a project at a research institution in Germany that aims at developing a setting of human–robot–interaction and collaboration that engages the designated users in the whole process.

Keywords: human–robot–interaction, robotics and society, mobile robotics

1. Introduction

Robots are part of many peoples' everyday life—even if only a few people are in direct contact and interaction, robots are part of production and logistic processes that affect almost all of us. However, the current increase in the development of mobile robots opens up new perspectives for human–robot–interaction processes and possibilities.

At the same time, however, those developments lead to concerns, reservations and questions of safety, ethics as well as the future of communication and society. Therefore, the sole technical development of robots is not enough. There is a high demand for interdisciplinary research in the field of social robotics that is becoming more and more relevant. Due to the sparse immediate contact between humans and robots, the research and development based on research findings is comparatively low. However, there are plenty of project calls and proposals in which robots are meant to perform certain auxiliary functions. However, many of these projects deal with acceptance issues that are due to an unfamiliar type of interaction between humans and robots. These issues partly originate from different types of robot locomotion, limitations in human-like behaviour as well as limited functionalities in general.

At the same time, animal-type robots—robotic quadrupeds such as Boston Dynamic’s WildCat—and underactuated robots are on the rise and present social scientists with new challenges such as the concept of uncanny valley. However, they open up possibilities in many sectors such as in working environments of the industry as well as, e.g., health and geriatric care.

In Germany there are currently about 3.4 million people in need of care. The effects of demographic change affect the care sector in two ways: while the number of people in need of long-term care is constantly increasing, fewer and fewer newcomers to the profession are opting for long-term care; at the same time, older nursing professionals are leaving the profession early due to physical and psychological stress [1]. The majority of people in need of care (73%) are currently in outpatient care [2], 55% of whom are assigned to nursing levels 1 and 2 [3].

These developments require new innovative solutions which contribute to maintaining the independence, self-determination and quality of life of people in need of long-term care. Here, mobile robotic systems offer great potential to maintain and increase mobility as well as an independent participation in social life. However, existing mobile robotic systems show a limitation of mobility to ground-level and structured environments as well as a lack of involvement of user groups during the development process. However, this problem might be solved by a suitable mobile robot system that is developed and tested demand-oriented by including user-centered research approaches. In the following sections, a project at a research institution in Germany will be described. The project aims at developing a setting of human–robot-interaction and collaboration that engages the designated users in the whole process.

2. Shepherd: concept and design of a human–robot-interaction project for geriatric care

The overall objective of the project is the user-centric, iterative development, production and testing of a mobile robotic quadruped to promote and maintain mobility and self-care capability for outpatients of care grade 1 and 2. The system has three modes of support for care grade 1 and 2 patients: autonomous, partial autonomous and hand-guided operation (see **Figure 1**).

The autonomous operation enables the system to automatically navigate under obstacle avoidance indoors and outdoors, whereby unevenness and barriers can also be overcome automatically due to the robotic quadruped design. In semi-autonomous operation, the system can be used as a following system for following the user, e.g., when carrying goods such as groceries or as a navigator system in which



Figure 1.
Use cases for the use of the robotic quadruped for ambulatory care. Assistance in mobility and self-sufficiency of patients in need of care.

the system runs ahead as a navigator. In hand-held operation, the system serves as an additional support for the user. The project pursues a user-centered, participatory and iterative research approach for the development of the robotic system (see **Figure 2**). The active involvement of patients in need of care and outpatient nursing staff in the development process ensures that technical development is demand-oriented and that user acceptance of the robotic system is increased as far as possible. This enables a successful interaction between the patient and the robotic system.

The various assistance functions of the robotic system and the demonstrators to be developed will be subjected to feasibility and effectiveness studies in field trials. Through the accompanying participatory recording of user acceptance and experience, promoting factors for the use of robotic systems are empirically collected, evaluated and translated into recommendations for action using the example of the robotic quadruped. The empirical survey is based on a technographic mixed method approach, which combines quantitative with qualitative methods. Various scientific methods, such as surveys, interviews and observations, are used to provide a dense description of human-machine interaction. In the sense of a common understanding of “good care,” this includes a holistic view of the human, organizational and technical levels with the aim of maintaining the health, well-being and quality of life of those in need of care [4]. The project thus aims at needs-based care and provision, strengthening the well-being of those in need of long-term care and maintaining an independent way of life in the long term. This way, the project contributes to quality care and support in the domestic and familiar living environment of those in need of care.

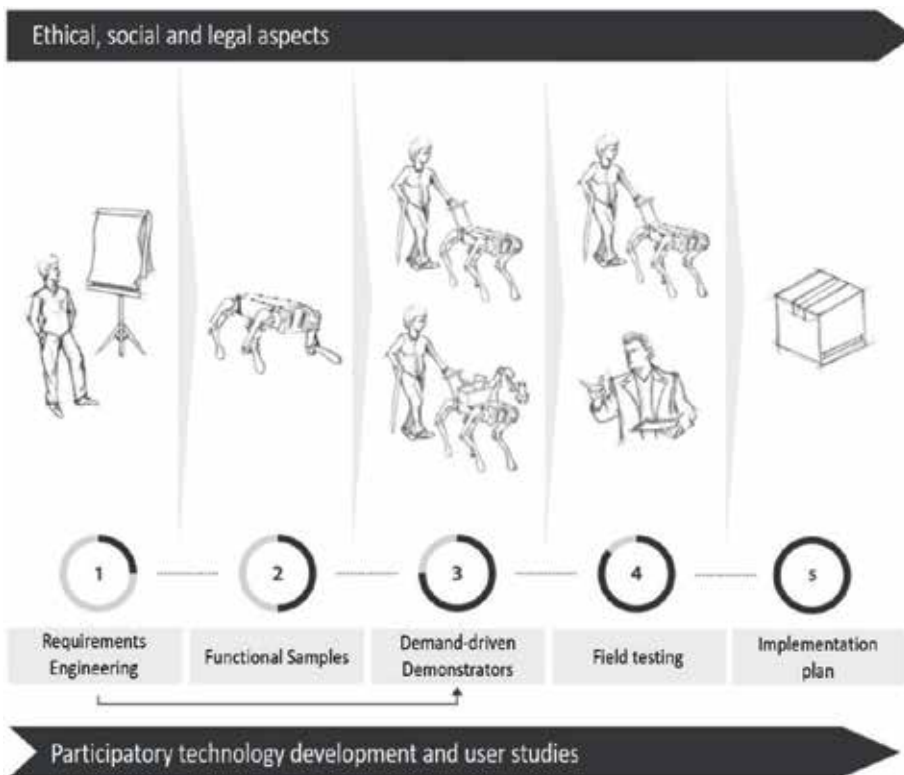


Figure 2.
Project plan of a user-centered, participatory and iterative research approach for the development of the robotic system.

3. State of the art

3.1 User-centered development, technology acceptance, user experience and ethical, legal and social aspects (ELSA)

The development of robotic systems for dependent persons requires a user-centred, iterative approach to ensure acceptance, experience and actual use by dependent persons [5]. Various qualitative and quantitative methods exist for the early involvement of users—often participatory design (PD) methods. The focus here is on the active participation of stakeholders and target groups as well as joint learning [6], the recording of the needs of the target groups and an iterative development through the step-by-step implementation and testing of functions and systems [7]. User-centered methods and techniques of human-robot interaction have already been used in research projects, e.g., in the field of “Comprehensive Geriatric Assessments” [8]. The entire user interface was derived from the requirements and wishes of the target group. A similar procedure was also used in the prototypical development of a service robot for use in geriatric care, in which critical user requirements were collected in a quantitative study and incorporated into the design of the robot [9]. The fact that an early integration of the necessary stakeholders of benefits is shown by the research of the University of Vienna on the prototype assistance robot “Hobbit.” The existing acceptance problems were only eliminated by the use of an “icebreaker team” [10]. In addition, the involvement of users can also help to take into account the fears, hopes and values of future users and thus integrate them into the design phase [11]. For this purpose, a nuanced understanding of the ethical challenges is central [12]. Research in the context of a user-centered development of robotic quadrupeds does not exist yet.

3.2 Mobile robot systems based on quadrupeds

Walking robots (e.g., robotic quadrupeds—see **Figure 3**) are mobile robot systems that can realize biologically inspired gaits agile, fast and balanced by one or more legs [17]. The high degree of mobility of walking robots, in comparison to wheel-based systems, also enables them to overcome obstacles and barriers such as steps, steps or uneven ground with statically and dynamically stable gaits, whereby robotic quadrupeds stand out [18].

The development field of walking robots has experienced a strong upswing in recent years, with the first domestic applications also being presented [19]. Drivers of this development are not least the high-profile ideas of Boston Dynamics Incorporation, which has currently developed heavy-duty quadruped robots (e.g., BigDog or LS3) with a payload of up to 181 kg. The more relevant robotic quadrupeds in the domestic environment are Spot [20] and SpotMini with payloads of 14–45 kg and a dead weight of 30–75 kg. The quadruped robots are electrically and



Figure 3. Robotic quadrupeds. (a) SpotMini [13], (b) Laikago [14], (c) ANYmal [15], (d) ANYmal and Continental [16].

hydraulically actuated and are transformed into an autonomous locomotion by the insertion of, e.g., lidar and depth cameras.

Furthermore, the ANYmal system of the Robotics System Lab (RSL) at ETH Zurich has made significant progress in recent years. With a dead weight of 30 kg and a payload of 10 kg, the system achieves a maximum speed of 1 m/s. The system can be used for a wide range of applications. The system can move autonomously in its environment thanks to the sensors used for this purpose. The Chinese company Unitree Robotics, founded in 2016, developed Laikago. With a total weight of 24 kg, it is capable of overcoming a wide range of uneven surfaces and withstanding kicks in a stable manner. What all systems have in common is that they have not yet been transferred to the area of application of care and therefore do not respond to domain-specific requirements. However, these systems impressively demonstrate the maturity of the technology. This is also underscored by the press releases of Boston Dynamics Incorporation, which is already planning to produce 100 robotic quadrupeds for sale in 2019 [21]. Subcomponents of the ANYbotics AG and Unitree Robotics systems are already available on the market, which were used for the calculation of the components.

Existing systems, however, were developed less along specific user requirements than along technical feasibility. Furthermore, experience shows that, despite press announcements, it remains to be seen whether these systems are actually mature enough to be launched on the market in the near future. In addition, the participatory development of the system along the High-Tech Strategy 2025 enables the Federal Government to both strengthen the competencies of Germany as a science location and contribute to the active shaping of highly innovative systems.

The biologically inspired locomotion of robotic quadrupeds has been the subject of interdisciplinary research for many years [22]. In this area, remarkable successes have been achieved in recent years in stability against external influences (e.g., kicks and jolts by persons) [23], adaptivity on uneven surfaces [24], and safe interaction with humans through the transition from stiff, position-controlled to active, passive and hybrid compliant actuators [25]. Besides the integration of further sensors for environment detection and recognition and the derived motion planning and generation [26], these and other control engineering approaches of whole-body control for the direct adaptation of the system to a changing, uneven terrain are applied [27].

Furthermore, the field of mobile robotic systems with tyres has already produced initial approaches for following persons [28] with medium numbers of persons as well as following systems, e.g., in supermarkets [29], which have so far only been evaluated on a small scale and which have not yet included the aforementioned challenges of robotic quadrupeds. In addition to the technical implementation, the navigation of mobile robot systems outdoors has been the subject of interdisciplinary research for several years [30]. Challenges here are the recognition and classification of passable paths [31], changing lighting situations during the day [32], dynamic obstacles such as people, cyclists or pets [33], intersections and road crossings [34].

4. Scientific and technical objectives of the project

4.1 Requirements analysis and scenario development of robotic quadrupeds

Since the project goal contains a user-centered and demand-oriented development of the demonstrators, the specific requirements of the stakeholders of the care sector—persons in need of care, carers as well as relatives—are collected

in design thinking workshops. On the basis of these user-specific requirements, concrete scenarios and functions for technical implementation are defined, such as, for example, a required seating area on the system or a shopping basket for weekly purchases. The following research questions are addressed within the workshops:

- What requirements do people in need of care, carers and relatives have for mobile robotic systems to maintain and promote the mobility of people in need of care?
- What functionalities must such a system have?
- Which specific application scenarios result from this?

4.2 Participative technology development and user studies accompanied by ELSA

The technical development and implementation of the robotic system follows an iterative, participatory research approach. Together with the users, the project team will develop prototype functions of the system in creativity workshops. In addition, the attitude, usability, user experience and technology acceptance will be recorded in a pre–post design of participative user studies following a technographic mixed-method approach. This approach enables a detailed description of the human–robot interaction for the derivation of scientific and user-oriented findings, which are directly applied in further technical development. The final evaluation of the demonstrators takes place in the context of field tests, which are meant to raise and analyze the effectiveness of the functions in domestic and public environments. The following research questions will be answered:

- How do mobile robotic systems affect technology acceptance and user experience?
- What influence does the user’s attitude have on the handling of robotic systems?

4.3 Development, production and testing of the robotic quadruped

Within the scope of the project, two identical demonstrators will be developed, manufactured and tested in field tests as basic systems of the robotic quadrupeds. A modular approach is chosen, which allows different structures to be determined according to requirements through workshops and surveys on the basic system. The basic system refers to the basic body of the robotic quadruped, which is designed to meet the requirements in terms of load, running speed, motion dynamics and total weight. Further superstructures are used, for example, to carry goods or designate handholds for hand-guided operation. Since the system is used indoors and outdoors, a robust construction and resistance to external influences are taken into account. Lightweight materials are selected to reduce the weight of the platform and maximize the load capacity. The design and selection of suitable drives, battery systems and sensor and computing hardware is based on the components available on the market. In addition to the design and manufacture, the development of the drive controllers and the kinematics of the robotic quadrupeds for the implementation of dynamic and stable gaits takes place.

4.4 Development and testing of locomotion, assistance functions and autonomous navigation

The system has three assistive functions (follow-on, navigator and manual operation) and is able to navigate autonomously indoors and outdoors. The follow-on function allows for the user to be detected and tracked by quadruped sensor systems. This enables the quadruped to be used, for example, as a load carrier. Through the navigator function, it can serve as a “guide” for users to achieve a defined goal. The assistance function for manual operation makes it possible to use the system as a support and control it intuitively. As interaction components, intelligent spacer textiles integrated in the handle of the quadruped are used, which record the user input by means of high-resolution pressure and shear sensors. For this purpose, spacer fabrics are designed with integrated conductive yarns, manufactured on industrial knitting machines and tested for their sensitivity and service life. In autonomous navigation, the system is able to automatically detect its environment, locate itself in it and navigate under collision avoidance, as well as overcome barriers. In order to increase the safety of the user, a contactless connection of the user to the quadruped is established by means of intelligent arm cuffs. The textile-integrated MEMS acceleration sensors and RFID antennas in the cuffs enable the detection of falls, the localization of the affected person and, if necessary, the emission of an emergency signal.

4.5 Social, ethical and legal support for user-centered, iterative development

The responsibility and accountability of technical development and research play a core role in the project. Therefore, the user-centered conception, implementation and testing of the quadruped will be accompanied throughout the entire course of the project, taking social and ethical issues into account. Within the framework of workshops with the project team, ELSA aspects are sensitized and integrated into the technical conception and implementation. Accompanying the technical realization is a first analysis regarding ethical questions towards autonomy and support of autonomy. In addition, the user studies will be carried out and evaluated taking ELSA into account, e.g., in the context of addressing the test persons and data evaluation. Legal challenges, in particular outdoor safety in traffic, data security as well as safety-related aspects are dealt with and analyzed accordingly by subcontracting a lawyer.

5. Conclusions, discussion and outlook

The paper describes the concept and design of a user-centered approach of developing a mobile robot to assist people in need of care. To date, interdisciplinary research on the subject of human–robot interaction is still a field where there is a lack of convincing research methods and results. However, robots are continuously finding their way into our everyday lives and are already indispensable today. Therefore, researchers from the field of humanities as well as robotics and general engineering need to work closer together and develop convincing technologies that are not just functioning on a level of technology but also allow for acceptance and collaboration between robots and humans. One decisive element in this process is that those teams need to work closely together and actively engage the designated users through the whole of the development process.

In order to pursue that goal, a team of researchers from both robotics and humanities has put together a concept and design of a project for the development

of mobile robots that are supposed to assist humans in need of care. The concept shows that not only the technology has to be carefully thought through in order to provide a secure service and show no gap between the robot's appearance and its actions. The social aspects and requirements of people in need of care, the nursing staff as well as relatives need to be taken into consideration and carefully used to develop the technologies. The research questions that have been raised include both human and technology factors that are crucial for the acceptance and success of future interactions between robots and humans.

However, this paper only marks the starting point of the project. It will be subject to further research and publications to show results of the studies and analyses in order to give recommendations on the process of developing social robots of the future. Since technology is continuously developing rapidly, it will not be sufficient to engage the users in just one design process. Rather, interdisciplinarity and user involvement need to become standard requirements in the process of designing technologies that are meant to work at the interface between humans and machines.

Author details

Valerie Varney*, Christoph Henke and Daniela Janssen
Cybernetics Lab of RWTH Aachen University, Aachen, Germany

*Address all correspondence to: valerie.varney@ima-ifu.rwth-aachen.de

IntechOpen

© 2020 The Author(s). Licensee IntechOpen. This chapter is distributed under the terms of the Creative Commons Attribution License (<http://creativecommons.org/licenses/by/3.0>), which permits unrestricted use, distribution, and reproduction in any medium, provided the original work is properly cited. 

References

- [1] Bendel O. *Pflegeroboter*. 2018. DOI: 10.1007/978-3-658-22698-5
- [2] Statistisches Bundesamt. *Pflegestatistik 2015. Pflege im Rahmen der Pflegeversicherung*. Wiesbaden: Deutscherischer-Verlag; 2017
- [3] https://www.bundesgesundheitsministerium.de/fileadmin/Dateien/3_Downloads/Statistiken/Pflegeversicherung/Zahlen_und_Fakten/Zahlen_und_Fakten.pdf
- [4] https://www.zqp.de/wp-content/uploads/ZQP_Ratgeber_GutePflegeerkennen.pdf
- [5] Krishnaswamy K, Moorthy S, Oates T. Survey data analysis for repositioning, transferring, and personal care robots. In: *Proceedings of the 10th International Conference on Pervasive Technologies Related to Assistive Environments (PETRA '17)*; New York, NY, USA: ACM; 2017. pp. 45-51
- [6] Lee HR et al. Steps toward participatory design of social robots: Mutual learning with older adults with depression. In: *Proceedings of the 2017 ACM/IEEE International Conference on Human-Robot Interaction (HRI '17)*; New York, NY, USA: ACM; 2017. pp. 244-253
- [7] Kwon M, Jung MF, Knepper RA. Human expectations of social robots. In: *The Eleventh ACM/IEEE International Conference on Human Robot Interaction (HRI '16)*; Piscataway, NJ, USA: IEEE Press; 2016. pp. 463-464
- [8] Ting KLH et al. Integrating the users in the design of a robot for making comprehensive geriatric assessments (CGA) to elderly people in care centers. In: *2017 26th IEEE International Symposium on Robot and Human Interactive Communication (RO-MAN)*; Lisbon; 2017. pp. 483-488
- [9] Lin X, Chen T. A qualitative approach for the elderly's needs in service robots design. In: *Proceedings of the 2018 International Conference on Service Robotics Technologies (ICSRT '18)*; New York, USA: ACM; 2018. pp. 67-72
- [10] Fischinger D et al. *Hobbit, a care robot supporting independent living at home: First prototype and lessons learned*. *Robotics and Autonomous Systems*. 2016;75:60-78
- [11] van Wynsberghe A. Designing robots for care: Care centered value-sensitive design. *Science and Engineering Ethics*. 2013;19:407. DOI: 10.1007/s11948-011-9343-6
- [12] Sharkey N, Sharkey A. Granny and the robots: Ethical issues in robot care for the elderly. *Ethics and Information Technology*. 2010;14(1):27-40
- [13] <https://robots.ieee.org/robots/spotmini/>
- [14] <https://bit.ly/2X6xAHI>
- [15] <http://www.industrytap.com/anymal-robot-knows-take-elevator/44199>
- [16] <https://www.anybotics.com/2019/01/31/robotic-package-delivery-with-anymal/>
- [17] Raibert MH. *Legged Robots that Balance*. Cambridge, MA, USA: Massachusetts Institute of Technology; 1986
- [18] <https://robotrabi.com/2017/11/20/4legs/>
- [19] <https://www.youtube.com/watch?v=tf7IEVTDjng>
- [20] <https://spectrum.ieee.org/automaton/robotics/robotics-hardware/>

spot-is-boston-dynamics-nimble-new-
quadruped-robot

[21] [https://techcrunch.com/2018/05/11/
boston-dynamics-will-start-selling-its-
dog-like-spotmini-robot-in-2019/](https://techcrunch.com/2018/05/11/boston-dynamics-will-start-selling-its-dog-like-spotmini-robot-in-2019/)

[22] Silva M, José TM. A historical
perspective of legged robots. *Journal of
Vibration and Control*. 2007;**13**:1447-
1486. DOI: 10.1177/1077546307078276

[23] Sparrow R. Kicking a robot dog.
In: 2016 11th ACM/IEEE International
Conference on Human-Robot
Interaction (HRI); Christchurch; 2016.
pp. 229-229

[24] Bellicoso CD et al. Advances in real-
world applications for legged robots.
Journal of Field Robotics. 2018;**35**:1311-
1326. DOI: 10.1002/rob.21839

[25] Buchli J et al. Compliant quadruped
locomotion over rough terrain. In: 2009
IEEE/RSJ International Conference
on Intelligent Robots and Systems; St.
Louis, MO; 2009. pp. 814-820

[26] Fankhauser P et al. Robust rough-
terrain locomotion with a quadrupedal
robot. In: 2018 IEEE International
Conference on Robotics and Automation
(ICRA); Brisbane, QLD; 2018. pp. 1-8

[27] Kalakrishnan M et al. Fast,
robust quadruped locomotion over
challenging terrain. In: 2010 IEEE
International Conference on Robotics
and Automation; Anchorage, AK; 2010.
pp. 2665-2670

[28] Repiso E et al. On-line adaptive
side-by-side human robot companion in
dynamic urban environments. In: 2017
IEEE/RSJ International Conference on
Intelligent Robots and Systems (IROS);
Vancouver, BC; 2017. pp. 872-877

[29] Göller M et al. Sharing of control
between an interactive shopping robot
and its user in collaborative tasks.
In: 19th International Symposium

in Robot and Human Interactive
Communication; Viareggio; 2010.
pp. 626-631

[30] Kümmerle R et al. Autonomous
robot navigation in highly populated
pedestrian zones. *Journal of Field
Robotics*. 2015;**32**:565-589. DOI:
10.1002/rob.21534

[31] Schilling F et al. Geometric
and visual terrain classification for
autonomous mobile navigation. In: 2017
IEEE/RSJ International Conference on
Intelligent Robots and Systems (IROS);
Vancouver, BC; 2017. pp. 2678-2684

[32] Upcroft B et al. Lighting invariant
urban street classification. In: 2014 IEEE
International Conference on Robotics
and Automation (ICRA); Hong Kong;
2014. pp. 1712-1718

[33] Ferrer G, Sanfeliu A. Behavior
estimation for a complete framework
for human motion prediction in
crowded environments. In: 2014 IEEE
International Conference on Robotics
and Automation (ICRA); Hong Kong;
2014. pp. 5940-5945

[34] Radwan N et al. Why did the robot
cross the road?—Learning from multi-
modal sensor data for autonomous
road crossing. In: 2017 IEEE/RSJ
International Conference on Intelligent
Robots and Systems (IROS); Vancouver,
BC; 2017. pp. 4737-4742

Section 2

Robotics Control

Electromechanical Analysis (MEMS) of a Capacitive Pressure Sensor of a Neuromate Robot Probe

Hacene Ameddah

Abstract

The domain of medicine, especially neurosurgery, is very concerned in the integration of robots in many procedures. In this work, we are interested in the Neuromate robot. The latter uses the procedure of stereotaxic surgery but with better planning, greater precision and simpler execution. The Neuromate robot allows in particular the registration with intraoperative images (ventriculographies, and especially angiographies) in order to perfect the planning. In this book, we focus on the contact force measurement system required for the effectiveness of the stimulation between the robot probe and the patient's head and thus ensure the safety of the patient. A force sensor is integrated upstream of the wrist, the pressure sensor is part of a silicon matrix that has been bonded to a metal plate at 70°C. The study was carried out under the software COMSOL Multiphysics, ideally suited for the simulation of applications (Microelectromechanical systems) "MEMS". After electromechanical stationary survey, deflection of the quadrant when the pressure difference across the membrane was 25 kPa, as expected, the deviation was expected to be greatest at the center of the membrane. The proposed sensor structure is a suitable selection for MEMS capacitive pressure sensors.

Keywords: medical robotics, neuromate robot, capacitive pressure sensor, COMSOL, MEMS

1. Introduction

In the past half-century, the Neurosurgery has been undergone tremendous technological innovation. The introduction of the operating microscope, stereotactic surgery, neuro endoscopy, modern neuroimaging, technologically demanding implants and image-guided surgery have enabled advancements while also challenging the limits of human dexterity [1]. Robot-assisted surgical systems can be beneficial for a variety of procedures chirurgical cranial and orthopedic due to their high precision, and ability to access and capacity to integrate various imaging and sensing modalities into the execution of the surgical task [2, 3].

The robot assisted surgical such Neuromate robots helps to ensure that the burr hole is accurately positioned and oriented cantered on the trajectory axis. The trajectory orientation is not restricted due to the variety of configurations to guide

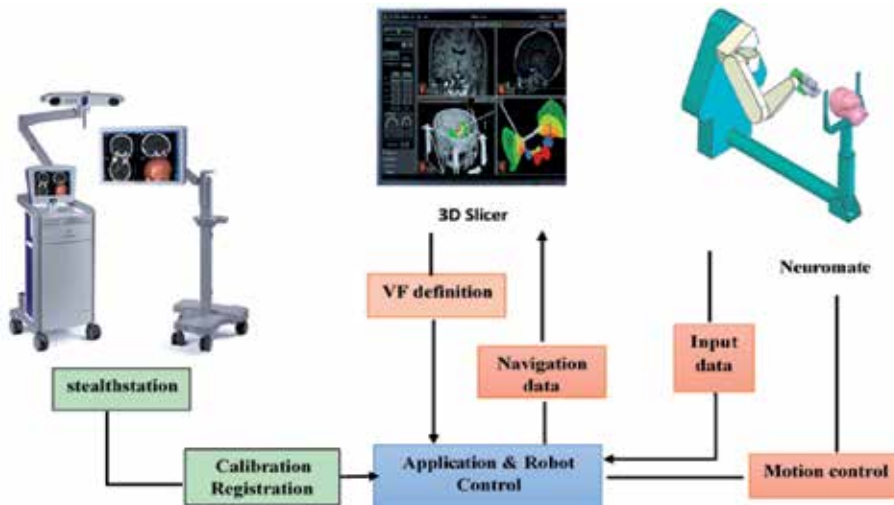


Figure 1. System overview of the image-guided robot for skull base surgery [1].

the surgery tools with a suitable orientation [4]. The current system (see **Figure 1**) consists of the following major components: a modified Neuromate robot.

Since the evolution of Micro-electro-mechanical systems (MEMS) many types of MEMS pressure sensors have been notified. They can be divided MEMS pressure sensors into, capacitive [5], piezoresistive [6], resonant [7]. Capacitive pressure sensing is considered as one of the most sensitive techniques in detecting low pressures [8]. Owing to the fact that the performance is solely a function of the mechanical properties and dimensions of the sensor structure [9]. Capacitive pressure sensors are preferred as they provide high sensitivity to pressure and their performance for most part remains invariant of temperature, this makes it suitable to be used for high pressure and temperature applications [10, 11].

This work addresses the design and modeling of measurement system required the contact force for the effectiveness of the stimulation between the probe and the patient's head, thus ensuring the safety of the patient. However, capacitive pressure sensors are gaining market share over their piezoresistive counterparts since they consume less power, are usually less temperature sensitive and have a lower fundamental noise floor. This model performs an analysis of a capacitive pressure sensors as discussed below using the electro mechanics interface. The effect of a rather poor choice of packaging solution on the performance of the sensor is also considered. The results emphasize the importance of considering packaging in the MEMS (micro-electro mechanical system) design process (**Figure 1**).

2. Neuromate robotic device and surgical procedure

Stereotactic biopsy is a standard procedure in neurosurgery. In addition to or even replacing frame based stereotaxy, some centers also use frameless imaging-based techniques and more recently robotic systems. Here, Yasin et al. [12] report a retrospective analysis of experience with 102 consecutive biopsies performed in his institution using the Neuromate robotic device.

The Neuromate robotic device is a platform designed for robot assisted stereotactic neurosurgery. It consists of a robotic arm with 5 degrees of freedom and a planning station (**Figure 2A**) and can be used for frame-based surgery as well as in frameless mode.

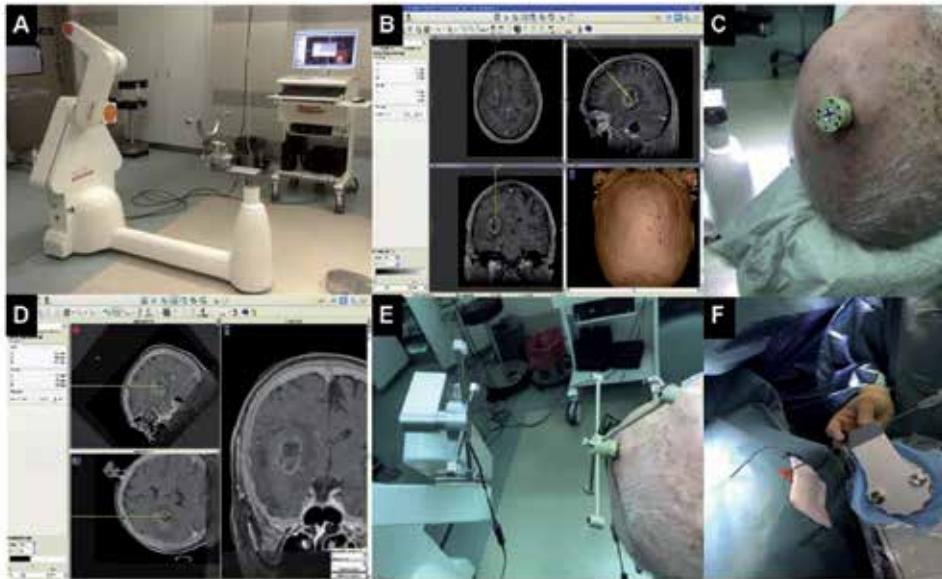


Figure 2. Images of the Neuromate robot and surgical workflow [12]. (A) Robot and planning station. (B) Trajectory plan. (C) The base of the localizing device is mounted to the skull. (D) The preoperative magnetic resonance imaging including the trajectory is fused to the computed tomography reference scan. (E) Patient registration using the ultrasonic tracking system. (F) Positioning the biopsy needle through the instrument holder along the trajectory [12].

The Neuromate device has been employed for a wide variety of stereotactic applications in neuro endoscopy, biopsy, epilepsy surgery, functional neurosurgery, and even convection-enhanced delivery.

All patients included in his study [12] had frameless biopsies. Biopsy trajectories were planned in advance using VoXim neuromata software (**Figure 2B**).

The localizing device consisted of a base mounted to the skull using a bone screw under local anesthesia and a helicopter-shaped ultrasonic localizing device and corresponding computed tomography (CT) localizers (**Figure 2C**). A CT reference scan was obtained and the data were uploaded on the planning station.

Next, the biopsy trajectory and the preoperative MR scan were fused to the reference scan (**Figure 2D**). Verifying trajectories were planned based on the reference scan data.

The second part of the procedure was performed in all patients under general anesthesia. Patients were placed in the supine, lateral, or prone position as required. The head was fixed in the head holder of the robot with 4–6 pins. Patient registration was performed using the ultrasound tracking system (**Figure 2E**).

Accuracy was tested using the verifying trajectory and a laser pointer mounted to the robot.

Next, the robotic arm with the instrument holder was moved into the planned biopsy position using a remote control. A Sedan side cutting aspiration needle (1.8 mm) was introduced manually through the instrument holder, and standard serial biopsies were taken as indicated (**Figure 2F**).

Biopsies through separate trajectories were obtained after simply repositioning the robotic arm.

3. Configuration of the neuromate robot

Nowadays, the use of robots in medicine becomes usual. One of the problems widely dealt in this area is the trajectory planning and contact force control.

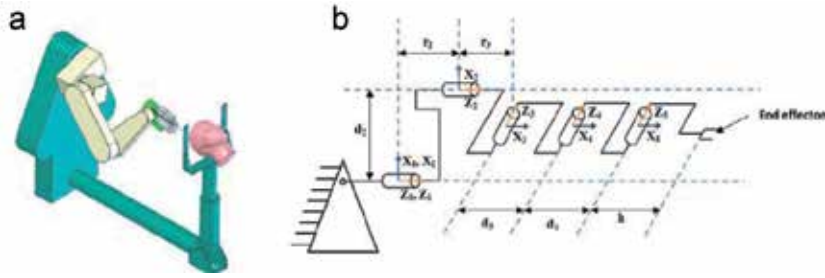


Figure 3. The Neuromate robot [13]. (a) Representation of the robot. (b) Geometric configuration of the robot.

In Menasria et al.'s (2015) works [13], a novel trajectory planning approach is proposed for redundant manipulators in the case of several obstacles. They use the property to find the best configuration that allows to avoid obstacles and singularities of the robot. The proposed method is based on a bi-level optimization formulation of the problem and bi-genetic algorithm to solve it.

The Neuromate robotic device is a platform designed for robot assisted stereotactic neurosurgery. It consists of a robotic arm with 5 degrees of freedom and a planning station (**Figure 3**) and can be used for frame-based surgery as well as in frameless mode. The Neuromate device has been employed for a wide variety of stereotactic applications in neuro endoscopy, biopsy, epilepsy surgery, functional neurosurgery, and even convection-enhanced delivery. Next, the assigned coordinate frames are followed to fill out the parameters as shown in **Tables 1** and **2** below.

Geometric and kinematic modeling was carried out under the symbolic software MapleSim (**Figure 4**) in order to simulate the trajectory of the probe.

3.1 Neuromate inverse kinematics analysis

Numerically, Inverse kinematic analysis is done by multiplying each inverse matrix of T matrices on the left side of above equation and then equalizing the corresponding elements of the equal matrices of both ends.

DH parameters	T_0^1	T_1^2	T_2^3	T_3^4	T_4^5
d_i	0	d_2	0	d_4	d_5
d	0	0	r_3	0	0
r_i	0	r_2	r_3	0	0
θ_i	θ_1	θ_2	θ_3	θ_4	θ_5

Table 1. Denavit Hartenberg table of the robot [13].

Joints	Mint (rad)	Max (rad)
θ_1	$-\pi$	π
θ_2	$-\pi$	π
θ_3	$-\pi/2$	$\pi/2$
θ_4	$-\pi/2$	$\pi/2$
θ_5	$-\pi/2$	$\pi/2$

Table 2. Angular rangers of the rotary articulations [13].

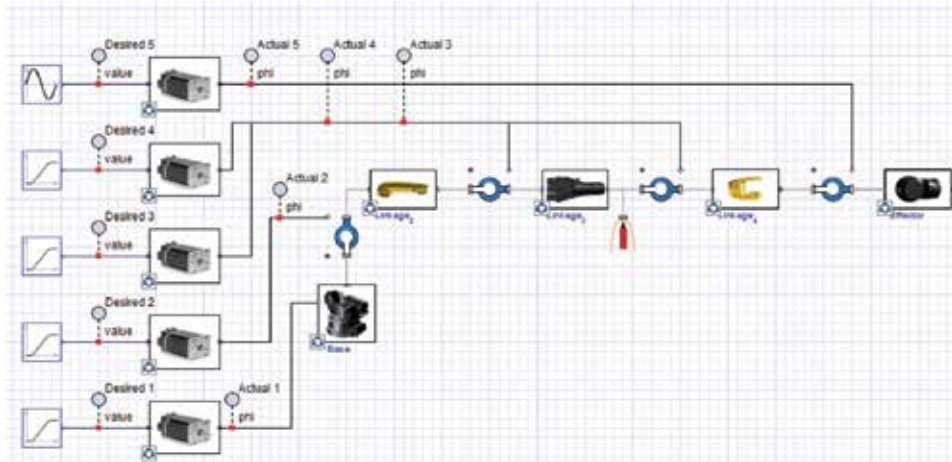


Figure 4.
Modelization of the Neuromate robot in MapleSim.

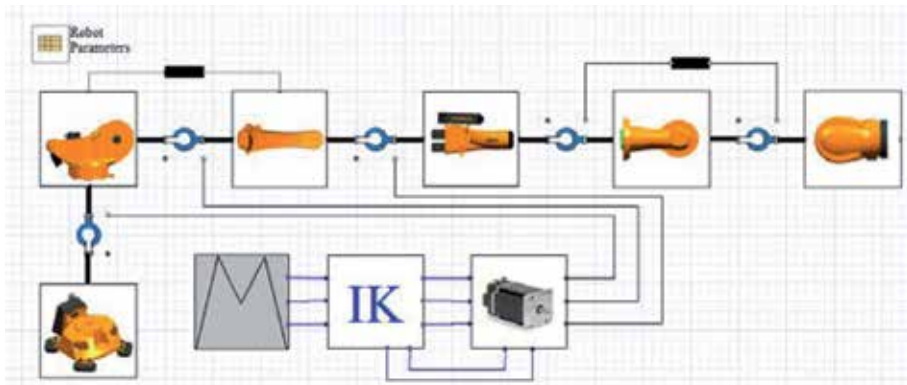


Figure 5.
Inverse kinematics of the Neuromate robot in MapleSim.

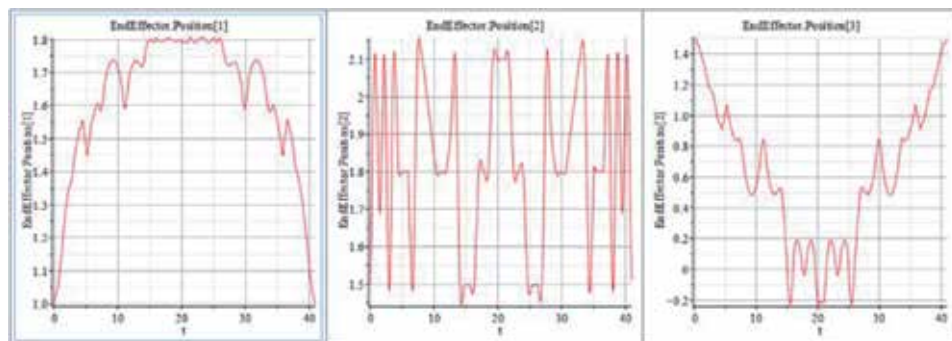


Figure 6.
End effector positions of the Neuromate robot.

With inverse kinematic solutions, the value of each joint can be determined in order to place the arm at a desired position and orientation. In our case, inverse kinematics is done under MapleSim software (**Figure 5**).

Based on relevant theories on robotic arms movement, a forward and an inverse kinematic model are successfully developed with the application of Neuromate with 5 dof in MapleSim software.

A simple trajectory is carried out in order to investigate the forward and inverse kinematics models of Neuromate. A movement flow planning is designed and further developed into the MapleSim programming.

A summary of the calculation is obtained for tree position of end effector (**Figure 6**).

4. Robotic pressure sensor control

In robotic applications, position control of manipulators can only be effective if the task is precisely described. For this reason, there is a clear need to integrate force information to the control loop. The interaction control between the effector and the patient's head can be through the robot's position control algorithms in the direction of the task space while the environment imposes natural position constraints.

Pressure control has many advantages. It can provide the necessary Cartesian compliant behavior of a robot, enable robust and fast manipulation in contact with unknown surfaces, and provide safety and dependability in interaction with humans.

Surgical robots with pressure control the pressure information collected in one of the above described ways may be used to control the servos of the robot. In medical robotics, the fundamental methods of force control have been widely applied as usually there is interaction with patient, interaction with surgeon and the procedures mostly deal with soft and deformable tissues with variable stiffness. The realized control architecture can depend on the bandwidth of the force sensor (the frequency of sensor measurements) [14–16].

The following section presents an example of the field of surgical robotics performing pressure control by a force control MEMS probe described above.

5. Geometry and material properties of pressure sensor

Newly Micro electro mechanical system (MEMS) capacitive pressure sensor gains more advantage over micro machined piezo resistive pressure sensor due to high sensitivity, low power consumption, free from temperature effects, etc.

Geometry of Pressure sensor made of piezoelectric silicon layer and graphene substrate at 70°C, with high-pressure sensitivity of 120 pF/Pa.

Since the geometry is symmetric, only a single quadrant of the geometry needs to be included in the model, and it is possible to use symmetry boundary condition. **Figure 7** shows the total sensor geometry.

As extensively reported in Mechanics books and scientific papers, the governing differential equation for the deflection of a thin plate in Cartesian coordinates can be expressed as follows:

$$\Delta C = C - C_0 = \epsilon A \frac{\Delta d}{d(d - \Delta d)} \quad (1)$$

D is referred as the flexural rigidity of the plate and can be defined as follows:

$$D = \frac{Et_m^3}{12(1 - \nu^2)} \quad (2)$$

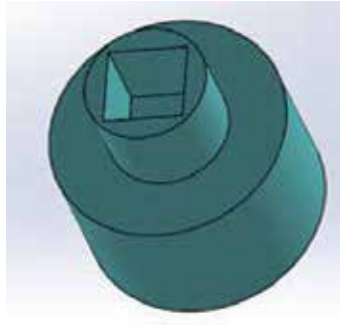


Figure 7.
 The geometry of the total sensor.

With E and ν being the modulus of elasticity and Poisson's ratio of the plate material, respectively.

The mechanical deformation under compression for the pressure sensitivity of such a pressure sensor:

$$\Delta C = C - C_0 = \epsilon A \frac{\Delta d}{d(d - \Delta d)} \quad (3)$$

ΔC is the change of capacitance under compression, C_0 is the initial capacitance value of the sensor, A is the surface area of the overlapping plates, ϵ is the permittivity of dielectric medium between the two plates, d is the initial overall thickness of the medium and Δd is the amount of compression.

The designed MEMS capacitive pressure sensors are composed of a square silicon diaphragm of 500 μm side length and 500 μm thickness that deflects because of pressure and acts as the movable plate of a differential capacitor, and a fixed Graphene substrate that acts as the other half of the pressure-dependent capacitor.

5.1 Mechanical properties

The material properties of graphene and Silicon are defined in the model and are shown in **Table 3**.

	Symbol	Silicon	Graphene
Young's modulus (GPa)	E	170	1000
Poisson's ratio	ν	0.6	0.17
Density (Kg m^{-3})	ρ	2330	2000
Relative permittivity	ϵ	11.7	2.14
Coefficient of thermal expansion (1/K)		2.6e-6	8e-6

Table 3.
 Material constants for silicon and graphene.

6. Results and discussion

The deformation surface of the membrane when a pressure of 25 kPa is applied to it, in the absence of packaging stresses, the maximum deflection is 3.64×10^{-8} m and the minimum deflection is 2.58×10^{-8} m (**Figure 8**).

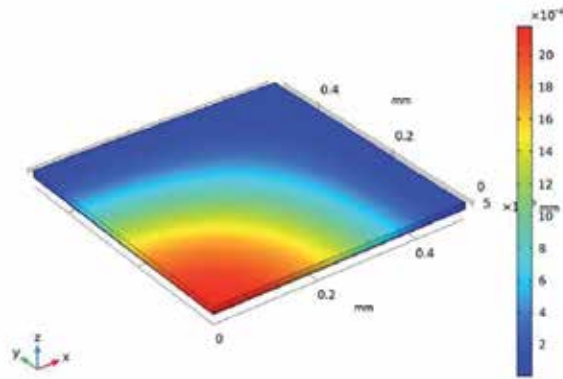


Figure 8.
Surface of the deformation membrane when applied voltage is 25 kPa.

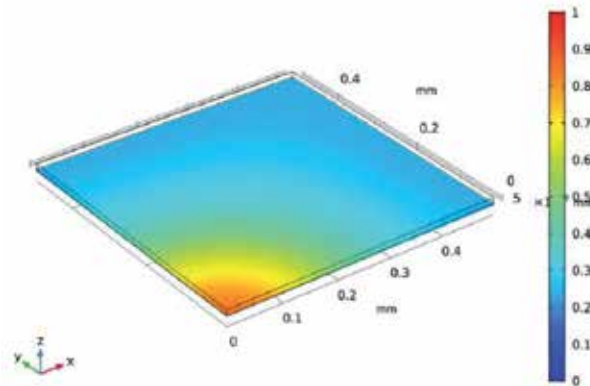


Figure 9.
Electric potential in the sealed chamber, plotted on a slice between the two plates of the capacitor.

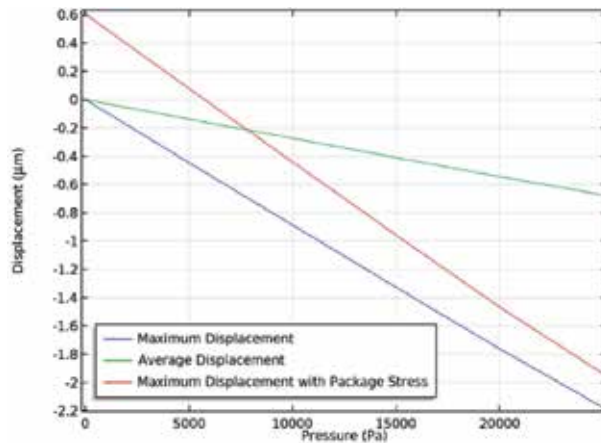


Figure 10.
Displacement of the membrane as a function of the applied pressure.

Figure 9 shows the surface potential on a plane located between the plates. The potential is almost uniform and the value is near to 0.3 V.

In **Figure 10**, the simulated median and maximum displacements of the membrane as a function of applied pressure. At an applied pressure of 10 kPa, the

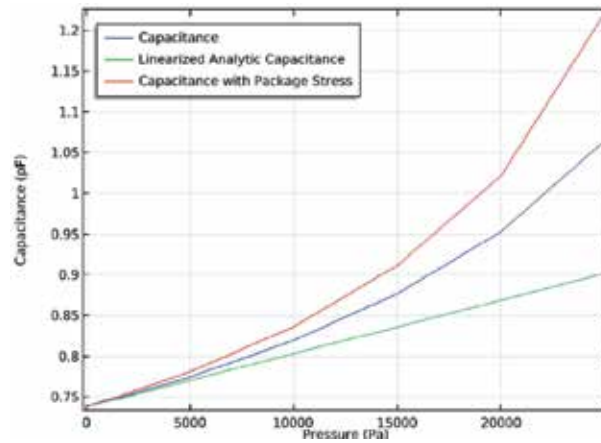


Figure 11.
Capacitance of the membrane as a function of applied pressure.

diaphragm displacement in the center is $0.15 \mu\text{m}$. The mean displacement of the diaphragm is $0.5 \mu\text{m}$. These results indicate the mean diaphragm and the maximum diaphragm results are very close which increases the stability of the sensor.

Figure 11 shows that the capacitance of the device increases nonlinearly with applied pressure.

At zero applied pressure the sensitivity of the model (quarter of the whole sensor) is $7.4 \times 10^{-6} \text{ pF/Pa}$. The device sensitivity is therefore $7.4 \times 10^{-6} \text{ pF/Pa}$.

The capacitance without package stress is less than the analytic capacitance but the capacitance with package stress is greater than the analytic capacitance.

7. Conclusion

In this work, a symbolic modeling under MapleSim is presented for the purpose of trajectory generation. In addition, we presented a simulation and analysis of the MEMS capacitive pressure sensor for robot Neuromate probe using COMSOL Multiphysics. The results show that the slotted MEMS capacitive pressure sensor realizes good sensitivity and large operating pressure range. Furthermore, as the ease of designing and fabricating these devices continues to improve, researchers will increasingly turn towards MEMS as standard tools for Neurosurgery.

Author details

Hacene Ameddah
Laboratory of Innovation in Construction, Eco-design, and Seismic Engineering
(LICEGS), University of Batna 2, Batna, Algeria

*Address all correspondence to: hacamed@gmail.com

IntechOpen

© 2019 The Author(s). Licensee IntechOpen. This chapter is distributed under the terms of the Creative Commons Attribution License (<http://creativecommons.org/licenses/by/3.0>), which permits unrestricted use, distribution, and reproduction in any medium, provided the original work is properly cited. 

References

- [1] Xia T et al. An integrated system for planning, navigation and robotic assistance for skull base surgery. *The International Journal of Medical Robotics and Computer Assisted Surgery*. 2008;**4**(4):321-330
- [2] Dillon NP, Siebold MA, Mitchell JE, Blachon GS, Balachandran R, Fitzpatrick JM, et al. Increasing safety of a robotic system for inner ear surgery using probabilistic error modeling near vital anatomy. In: Webster RJ III, Yaniv ZR, editors. *Proceedings of SPIE*. CCC code: 1605-7422/16/\$18. *Medical Imaging 2016—Image-Guided Procedures, Robotic Interventions, and Modeling*. International Society for Optics and Photonics. 2016;**9786**:97861G-1. DOI: 10.1117/12.2214984
- [3] Taylor RH et al. Medical robotics and computer-integrated surgery. In: Siciliano B, Khatib O, editors. *Springer handbook of robotics*. Berlin, Heidelberg: Springer; 2008. pp. 1199-1222. Available from: https://doi.org/10.1007/978-3-540-30301-5_53 2008
- [4] Kajita Y et al. Installation of a Neuromate robot for stereotactic surgery: Efforts to conform to Japanese specifications and an approach for clinical use—Technical notes. *Neurologia Medico-Chirurgica*. 2015;**55**(12):907-914
- [5] Bakhom EG, Cheng MH. Capacitive pressure sensor with very large dynamic range. *IEEE Transactions on Components and Packaging Technologies*. 2010;**33**(1):79-83
- [6] Liu C. *Foundations of MEMS*. 2nd ed. New Jersey, CA, USA: Prentice Hall; 2010. pp. 231-233
- [7] Welham CJ, Greenwood J, Bertoli MM. A high accuracy resonant pressure sensor by fusion bonding and trench etching. *Sensors and Actuators, A: Physical*. 1999;**76**(1-3):298-304
- [8] Maheshwari V, Saraf R. Tactile devices to sense touch on a par with a human finger. *Angewandte Chemie (International Edition, in English)*. 2008;**47**:7808-7826
- [9] Mitrakos V et al. Design, manufacture and testing of capacitive pressure sensors for low-pressure measurement ranges. *Micromachines*. 2017;**8**(2):41
- [10] Kirankumar BB, Sheeparamatti BG. A critical review of MEMS capacitive pressure sensors. *Sensors and Transducers*. 2015;**187**(4):120-128
- [11] Marsi N et al. The mechanical and electrical effects of MEMS capacitive pressure sensor based 3C-SiC for extreme temperature. *Journal of Engineering*. 2014;**2014**:8. Article ID: 715167. Available from: <http://dx.doi.org/10.1155/2014/715167>
- [12] Yasin H, Hoff H-J, Blumcke I, Simon M. Experience with 102 frameless stereotactic biopsies using the Neuromate robotic device. *World Neurosurgery*. 2019;**123**:e450-e456. DOI: 10.1016/j.wneu.2018.11.187
- [13] Menasria R, Nakiba A, Daachia B, Oulhadja H, Siarry P. A trajectory planning of redundant manipulators based on bilevel optimization. *Applied Mathematics and Computation*. 2015;**250**:934-947
- [14] Haidegger T, Benyó B, Kovács L, Benyó Z. Force sensing and force control for surgical robots. In: *Proceedings of the 7th IFAC Symposium on Modelling and Control in Biomedical Systems*; 12-14 August 2009; Aalborg, Denmark; 2009
- [15] Taylor RH, Kazanzides P. Medical robotics and computer integrated

interventional medicine. In:
Feng DD, editor. Biomedical
Information Technology. Elsevier
Inc., Academic Press; 2007:393-416.
Available from: [https://doi.org/10.1016/
B978-012373583-6.50022-0](https://doi.org/10.1016/B978-012373583-6.50022-0)

[16] Taylor RH, Menciassi A,
Fichtinger G, Dario P. Medical robotics
and computer-integrated surgery.
In: Siciliano B, Kathib O, editors.
Springer Handbook of Robotics. Berlin:
Springer; 2008

Physical Interaction and Control of Robotic Systems Using Hardware-in-the-Loop Simulation

Senthil Kumar Jagatheesa Perumal and Sivasankar Ganesan

Abstract

Robotic systems used in industries and other complex applications need huge investment, and testing of them under robust conditions are highly challenging. Controlling and testing of such systems can be done with ease with the support of hardware-in-the-loop (HIL) simulation technique and it saves lot of time and resources. The chapter deals on the various interaction methods of robotic systems with physical environments using tactile, force, and vision sensors. It also discusses about the usage of hardware-in-the-loop technique for testing of grasp and task control algorithms in the model of robotic systems. The chapter also elaborates on usage of hardware and software platforms for implementing the control algorithms for performing physical interaction. Finally, the chapter summarizes with the case study of HIL implementation of the control algorithms in Texas Instruments (TI) C2000 microcontroller, interacting with model of Kuka's youBot Mobile Manipulator. The mathematical model is developed using MATLAB software and the virtual animation setup of the robot is developed using the Virtual Robot Experimentation Platform (V-REP) robot simulator. By actuating the Kuka's youBot mobile manipulator in the V-REP tool, it is observed to produce a tracking accuracy of 92% for physical interaction and object handling tasks.

Keywords: hardware-in-the-loop, control algorithms, robotic manipulators, mobile robots, physical interaction

1. Introduction

Robotics have been flourished as a platform with its extensive set of applications, which once was thought as a night mare, and now have started dominating the industrial sector. Because of its expanded domain of applications, it can even start ruling humans in near future. Robotic systems have been turned into very powerful essentials of today's industrial sector. It is often anticipated to synthesis certain features of human tasks in huge scale by using actuators, sensors, and personal computers or on-board computers. Designing and controlling of such robotic systems requires combining the concepts from various classical fields of science [1].

Robotic manipulators are a class of robotic systems with mechanical-articulated arm along with a static base. On the other hand, mobile robots belong to another different class of robotic systems with mobile base. Currently, most of the automation tasks in industries also depend on hybrid variant of robotic systems, which

have both manipulator and mobile base [2]. Usage of robots mainly aims to reduce man power in control appliances for industrial and other household or commercial appliances, by enabling accuracy in processing and performing physical interactions. Actions performed by robotic systems are relatively faster than humans and also deliver reliability and robustness in the system.

Various robotics research domains are available with their potential paths that work together with human beings in households and workplaces as useful and capable agents based on the ability of robots. Another most essential objective of robotic systems are interacting with the physical environment toward specific applications domains, tracking the objects, and moving the gripper with accuracy [3]. Also precision in trajectory tracking of robotic systems, grasping of objects, stabilizing the grip and force control are all challenging research issues, which in turn may seriously affect the production in industrial sector if they are not properly addressed [4].

For performing physical interaction with the help of robotic systems, handling of objects in industries and other applications are becoming predominant. It is driven by proper motion control accomplished by fixing global, joint, and object's reference frames in the physical environment [5]. The choice of workspace of the robotic systems also plays a major role for physical interaction. Workspaces are the collection of points that can be reached by the robot based on its configuration, size of links, type of joints, and also defined by its own limitations.

For establishing the physical link of the robot with the environment, tactile sensors along with force sensors and vision sensors can be deployed based on the variety of applications. Sensing of the handled objects and force applied on the particular object based on dexterous capability of the objects are vital parameters in physical interaction. Controlling the force applied on the objects and stabilizing the grasping potential of the grippers are crucial challenges while performing interaction with the environment. Various controllers were proposed by researchers for reducing the control effort with reduced noise in control torque. Also for operating the robotic systems under unknown external environments, certain adaptive techniques were also proposed by researchers. Accuracy in driving of the end-effectors of the robots can be accomplished by tracking the desired path for each joint of robots by choosing the best closed loop controllers. In this chapter, systematic solutions are provided for the design of grasp and force control along with the support of visual servoing for controlling the hybrid robotic systems with the physical environment [6].

2. Physical interaction of robotic systems

Robotic systems can interact physically in its workspace by first establishing a contact with the environment with appropriate configuration. Subsequently, the robots are fed with required force for motion of its physical parts to perform certain desired tasks. Interaction by means of grasping of objects in workspace and the desired motion control constrained to tasks are dealt. Since, the early inception of robotic research, manipulation of robots with its environment has been dealt by different researchers.

2.1 Interaction with environments

Robotic systems grasping objects in the environment can be implemented based on either contact level method or knowledge-based method. Contact level method applies force torque to the objects handled by the robot. Few of the variants of the contact-based methods include frictionless contacts, soft contact, and with

frictional contact forces applied. Reliability of grasping potential can be estimated using force closure property, by compensating external disturbances. Other possible forces of contact can also be random potential grasps, which may not be optimal but manages vector space that includes all feasible contact forces.

The limitation of contact-based approach is that it never considers the constraints imposed on the hand of the robotic systems. This may result in target points that may not be reachable by the hand. Knowledge-based method considers the hand post postures that are already predefined. This provides a qualitative method for planning for grasping objects by adapting to the workspace geometry. Control algorithms based on task-oriented grasping consider requirements of tasks in the workspace of the robots. This method requires minimum number of contacts than other conventional methods. So, the number of fingers in the workspace of the robotic systems can be minimized. For any given task, the efficiency of task-oriented approach is reasonably better, and it also increases the versatility of the robot for performing different tasks.

2.2 Role of sensors for physical interaction

Usage of tactile sensors are one of the best choice for performing physical interactions of robots with the environment. They are also used for estimating the contact information and detecting the slippery of objects during grasping. Force sensors on the other hand estimates the impact of forces applied on the objects and studies the dexterous capability of the object under test. Vision sensors are one of the best choices for observing the impact of physical interaction of the robot with the environment [7]. However, it also challenges the designer with series of preprocessing stages during implementation. Model-based pose estimation techniques can simultaneously observe the position as well the orientation of the hand and the objects under manipulation.

Best and robust estimation of environmental parameters during physical interaction of the robotic systems can be availed by implementing sensor fusion techniques. Sensor fusion provides mechanisms for combining different sensor outputs for better observation about the environment. Accurate prediction of environmental parameters is possible only if the information acquired from multiple sensors is combined for decision making. Popular approaches such as Kalman Filter and Extended Kalman Filter can be better choices for sensor fusion processes, particularly in robotic applications.

2.3 Planner for physical interaction

The requirements of physical interaction and tasks can be defined with the support of interaction planning algorithms. Physical interaction tasks can be automatically specified, by feeding the description of objects and tasks to be handled at workspace to planning algorithms. Choice of ideal gripper, gripper pre-shapes, and gripper adaptors provides generic task-based planning algorithms for the end-effectors of robots with good versatility. Also, the planning algorithm may also be environmental specific based on the dexterous capability of the objects for grasping and tasks performed on the environment.

Vast category of objects may limit the physical interaction tasks supported by the planner. Coupling the planner with vision-based sensors for physical interaction with strange objects in the environment provides perfect versatility and autonomy for the robotic systems. Approximating the shapes of the strange objects, the planning algorithms generate suitable velocity and force references for the end-effectors to actuate the joint actuators.

2.4 Application of force and feedback during interaction

During physical interaction of the robot with the environment, even a minimum change in the positioning may lead to generate unwanted interaction forces by the planner. Choice of active and passive stiffness methods can be employed to regulate the application of the forces on the end-effectors. Based on the requirements of task, the active stiffness method controls the desired end-effector stiffness. Passive method enables to deform the mechanical body of the gripper based on the external forces applied.

3. Control of physical interaction

During physical interaction using the robot's gripper with the objects, usage of tactile sensors enables to acquire the contact force and pressure information. Forces from the hand can be observed by placing a force sensor in the wrist of the robot [8]. It ensures to give force feedback always, whenever some kind of forces at any part of the hand is sensed. Force feedback is a vital observation in physical interaction to detect jointly the object contact at the end effector and the motion of the hand simultaneously. **Figure 1** shows the generic control scheme imparted for physical interaction using force and tactile sensors for feedback. For the improved manipulation, vision-based sensors can be combined with tactile sensors.

3.1 Grasp and force control for object positioning and handling

To stipulate few dynamic behaviors of robot in its environmental workspace, its contact with the objects can be controlled using impedance control method coupled with active stiffness. Position of the gripper with respect to the contact force can be obtained using reconfigurable mechanical impedance in the workspace. It can be derived based on second order transfer function equivalent to mass spring damper. **Figure 2** shows how the desired impedance can be used to modify the position by generating appropriate position control signals. The impedance transfer function generates a position error with respect to the difference between the reference force and the force feedback from the robot. The position controller uses the error feedback computed from the reference position and current Cartesian position of the robot, to generate the control signal for moving the robot's gripper actuators.

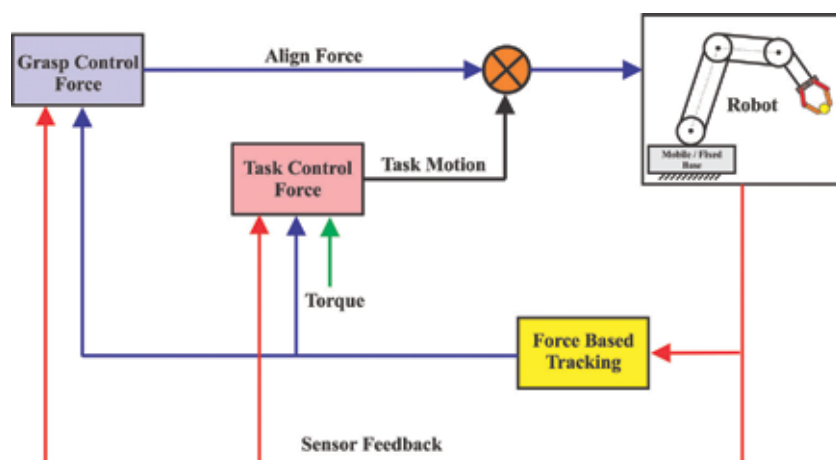


Figure 1.
The general force control mechanism for physical interaction of the robots.

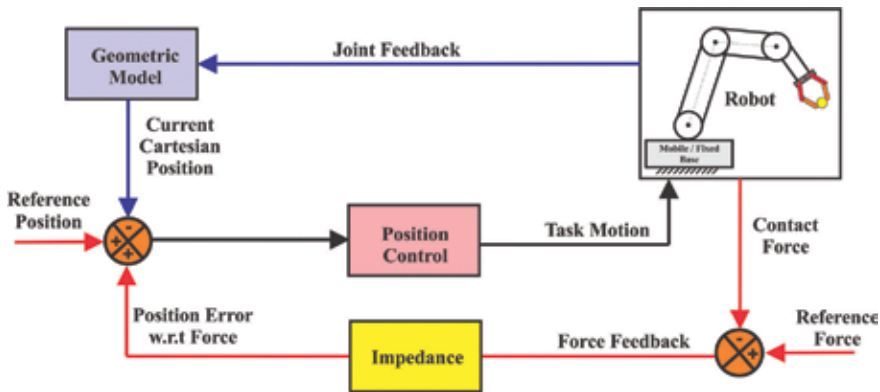


Figure 2.
 General control approach of the position based on impedance.

The interaction forces and its control can be performed using indirect method by controlling the contact forces explicitly or by implementing hybrid techniques. Those hybrid approaches combine the force control and position control on the same directions. **Figure 3** shows the generic method of the hybrid position force control by including position and force error filters. A frame fixed to the task handling part of the end-effector can be specified using a matrix in which the value of 1 represents axis of force control direction and value of 0 indicates the axis of position control. This particular very spontaneously allows the control law implementation for the physical interaction tasks. With precise knowledge of the frame and the environment, it ensures that no disturbance appears between the directions of position and force [9]. If the physical interaction is deployed on unstructured type of environment, this kind of control will be quite challenging. This approach utilizes a position error filter and force error filter, which filters the unwanted errors to drive the position and force controller. Generated hybrid signal from the deployed control law drives the gripper actuator for task handling.

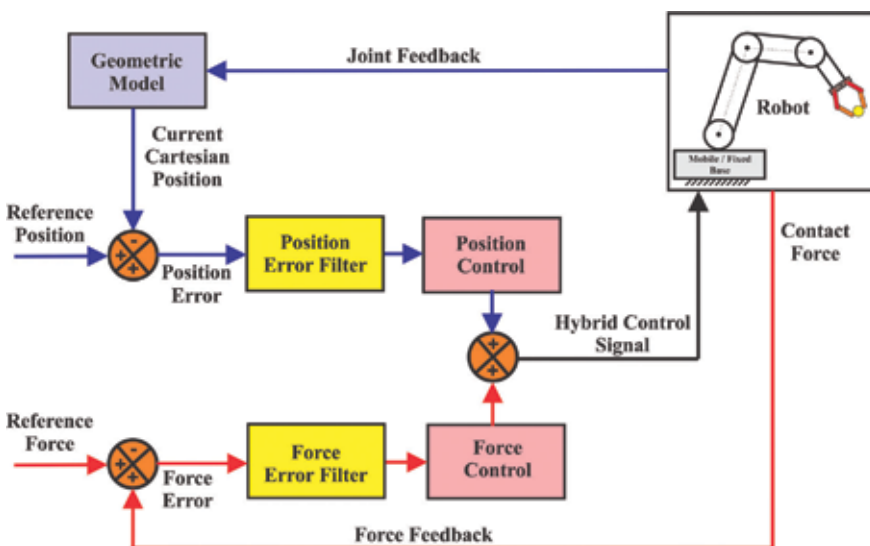


Figure 3.
 General approach of the hybrid position force control.

Simultaneous control of position and force along the same direction can be achieved with the support of hybrid external position force control in physical interactions tasks. In this architecture, the inner position control loop will be driven by an outer force control loop as shown in **Figure 4**. The new reference position is computed from the force control signal estimated through the reference force and feedback force error. The force error is added to the existing reference of the position [10]. This provides simplicity in the architecture and implemented above the existing position controller of the robot. The hybrid control law is finally based on the position control signal generated in the control system using computed position error [11].

3.2 Visual control for object positioning and handling

Vision-based sensors play a most vital role during the physical interaction phase. When the robot does not interact with the environment, information from force and tactile sensors will not be available. In such circumstances, vision sensor data can be acquired in order to trace the target object in the environment. This enables to guide the robot's hand toward the object in the robot's workspace. For grasping the objects in the workspace, pose estimation methods can offer an approximate position and orientation of the target object. The adopted algorithm complexity is of polynomial time, for which the accuracy varies with the chosen optimization techniques [12]. The physical look-based pose estimation method does not need familiarity about the 3D model of the object. In model-based methods, the pose accuracy is better than physical look-based pose estimation, but it usually needs a suitable initial estimate in addition to the model of the object. The task programmer has to choose the most suitable approach depending on the available previous knowledge.

During physical interaction phase, vision-based pose estimation algorithms can be used to investigate the properties of the physical interaction on the object. When the robotic system executes the task motion, desired vital measures can be detected, such as the angle of gripper opening, reachability of the object, failure of grasping, and many more. However, the chief impact of vision sensors during physical interaction tasks, is that it is promising to track the progress of the frames fixed in the environment. This can be accomplished by a direct observation on the hand and the object in the workspace. This completely avoids the necessity of force-based techniques for object tracking. Grasping of objects can be detected directly with

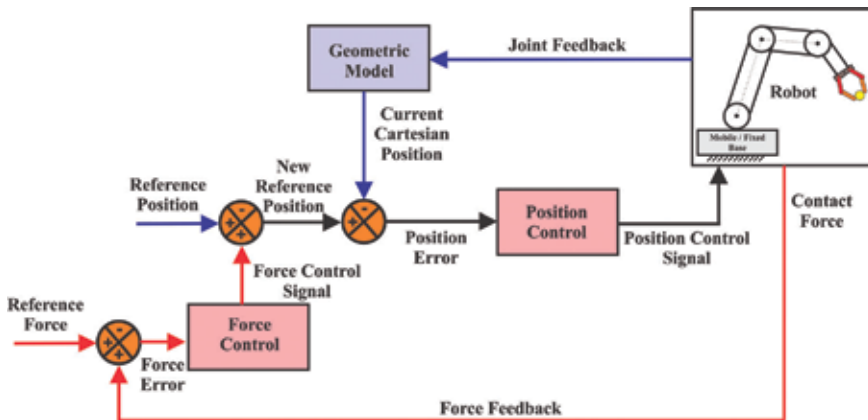


Figure 4. General approach of the hybrid external position and force control.

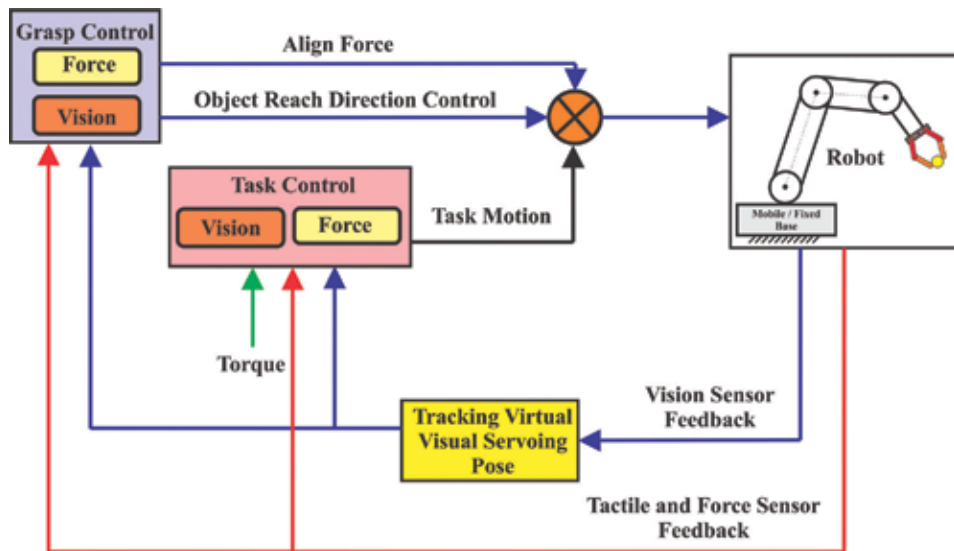


Figure 5.
The general vision and force control scheme for the physical interaction.

the aid of vision sensors, by detecting a specific sequence, without formulation of a predefined path for the arm and gripper. It is absolutely mandatory to perform sensor fusion of the visual signal with force feedback, to manage unforeseen forces due to vision sensor calibration and preprocessing errors.

Figure 5 outlines the main impact of vision sensors combined with tactile and force sensors for grasping objects during physical interaction. They together can trace the objects in the physical environment, thus empowering accurate reaching and alignment between the object and robotic hand, before and after physical contact. After physical contact, alignment task needs to be performed with the support of force controller, in order to consistently handle and stabilize the misalignments caused between object and hand due to deployment of vision sensors.

4. Hardware-in-the-loop simulation

Certain physical systems are prone to possess complex design, unsafe to test in real time, subjected to operate in certain real time systems, and not economical. Robots also belong to one such category of physical systems. For such robotic systems, development of the embedded control system and testing are made feasible with the support of HIL simulation technique [1].

As a robotic system design requires multidisciplinary mastering, partitioning the design tasks into various subsystems simplifies their analysis and synthesis. So, by utilizing the real hardware modules in the loop of real time simulation enables the detailed analysis of sensor noises and actuator limitations of robotic systems [2]. This can be accomplished by HIL technique, where the control algorithms are implemented in the actual hardware, and it controls the simulated model of the robotic system.

In the adopted HIL methodology, complexity of the robots to be controlled is modeled by including all its related dynamics by equivalent mathematical representation of the systems included in test and development. The embedded target runs the control algorithm for the control of joint actuators and they interact with the simulated model of the robot. **Figure 6** shows the HIL simulation setup of the

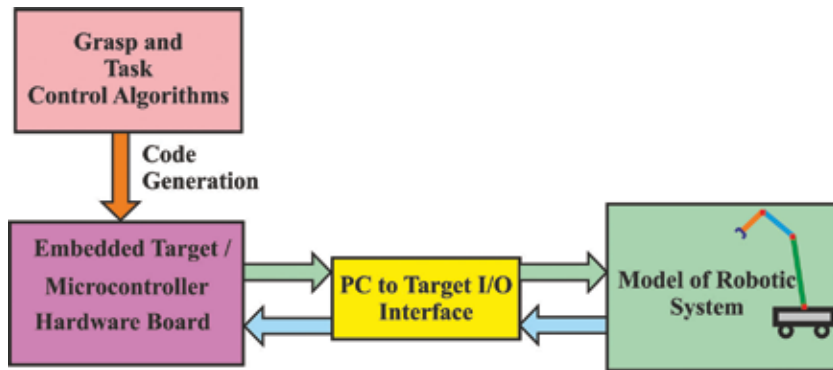


Figure 6.
Hardware-in-the-loop simulation setup of the robotic systems.

robotic systems [3]. It is implemented with the control algorithms running on the embedded target board. The board is interfaced to the PC, which runs a model of robotic system via Input/Output interface. Certain modeling tools possess simulation of the complex mechanisms in the robotic systems.

The usage of HIL simulation techniques increases the safety in operating the robots and enhances the production quality after analyzing the performance in HIL platform and later on switching to actual physical robotic system. Another striking feature of using HIL is that it saves time and money to a larger extent.

4.1 Steps in HIL simulation

The core steps in HIL simulation of the robotic system carried out are as follows:

1. Developing the mathematical model of the actual physical robotic systems using the tools such as MATLAB, LabVIEW, or other open source platforms. It must also be ensured that the developed model can be accessed by the hardware devices with appropriate communication.
2. Developing the control algorithms for robotic systems using the open source or proprietary tools for the core embedded target board. It acts as a heart of the system running the task and grasp control algorithms.
3. Configuration of the environment variables in the software environment based on the appropriate compiler choice, bios setup, device support form control suite, and flashing utilities, etc.
4. The target preferences in the embedded coder of software environment need to be configured by choosing the appropriate target processor by mapping the developed algorithms to the input, output pins of the controller.
5. Perform the HIL simulation by testing the implemented control algorithms on the embedded target board along with simulated mathematical model of the robotic system.

These sets of tasks investigate the crucial awareness of performing the HIL simulation using embedded target controller, modeling, and simulation tools. Initial step on this process is to work on the virtual model of the simulated plant under test

using the software tool. Followed by, testing of the implemented control algorithms running in the embedded hardware on the simulated model of the robotic system is performed. Finally, these test analyses give the confidence for driving the actual robotic system using the grasp and task control algorithms.

5. Case study using Kuka's youBot mobile manipulator

The KUKA's youBot is a mobile robot manipulator that was designed targeting the scientific research and training community as an open source platform. **Figure 7** shows the picture of KUKA's youBot mobile manipulator with a mobile base and manipulator mounted on top of it [13]. Since, youBot can be used for development and validation of mobile robot platform as well as for fixed manipulation tasks, youBot is considered in our case study for physical interaction with the environment.

5.1 Specifications of KUKA's youBot

KUKA's youBot consists of an omnidirectional mobile platform along with 5-degree of freedom (DOF) manipulator that possess two finger gripper, which can be controlled independently. The omnidirectional base of the robot has a payload of 20 kg and it is driven by four omni wheels, which allows the movement of wheels in all directions without any external mechanical steering. Each wheel consists of a series of rollers mounted at a 45° angle. The wheels are driven by brushless DC motors with built-in gearbox, relative encoder and joint bearing. Wheel motion is controlled independently through drives using commands. The lowest level of command being pulse width modulation (PWM) and higher level control commands are: current control (CC), velocity control (VC), and position control (PC).

Youbot's arm can manipulate a load of up to 0.5 kg in any position in three dimensions. The distributed axis controllers are connected via the EtherCAT backplane bus EBUS. Each joint in youbot arm has its own servo controller, which contains: ARM Cortex-M3 microcontroller, hall sensors, EtherCAT interface, position, velocity, and current PID-controllers. Using predefined positions provided



Figure 7. KUKA's youBot mobile manipulator (image courtesy: <http://www.youbot-store.com/>).

over WLAN or Ethernet as input, the PC calculates moment, speed or position instructions for each axis and handles their interpolations individually.

Youbot's arm wrist is equipped with a two finger parallel gripper with a 20 mm stroke. There are multiple mounting points for the gripper fingers that user can choose based on the size of the objects to pick up [14]. In the standard gripper, the jaws are operated by two stepper motors.

Operation of the robot is possible with both connected power supply unit and the batteries. The power controller features separate charging controls for the two maintenance-free lead-acid batteries (24 V, 5 Ah) when the charger (200 W) is connected. If no charger is connected, the two batteries can supply power for up to 90 minutes. In addition, the power controller features individually switchable power supplies for the computer and the motors. Battery current is monitored via the on-board computer.

5.2 V-REP and MATLAB interface for youBot

V-REP is an open source robot simulation tool that possesses various features, relatively independent functions and more elaborate application program interfaces (APIs). It is one of the stable platforms than other open source tools with easy plugin and configuration of robotic systems [15]. Each object/model in V-REP scene can be individually controlled via an embedded script, a plugin, a Robot Operating System (ROS) node, a remote API client, or a custom solution. Control algorithms can be written in C/C++, Python, Java, Lua, MATLAB, and Octave or Urbi.

Remote API can be implemented by blocking function calls, non-blocking function calls, data streaming, and synchronous operation. In this research, we used MATLAB as the remote API because it provides a very convenient and easy way to write, modify, and run. This also allows controlling a simulation or a model with the exact same code as the one that runs the real robot. The remote API functionality relies on the remote API plugin and the remote API code on the client side. Both programs are open source and can be found in the "programming" directory of V-REP's installation. Robot HIL control system is connected with V-REP robot simulator through MATLAB remote API function as shown in **Figure 8**.

Simulation scene in V-REP robot simulator contains several elemental objects that are assembled in a tree-like hierarchy and operate in conjunction with each other to achieve physical interactions. In addition, V-REP also possesses several calculation modules that can directly operate on one or several objects in a scene. Major objects and modules used in the simulation scene include (i) sensors, (ii) CAD models of the plant and robot manipulator, (iii) inverse kinematics, (iv) minimum distance calculation, (v) collision detection, (vi) path planning, and (vii) visual servo control. Other objects that were used as basic building blocks are: dummies, joints, shapes, graphs, paths, lights, and cameras.

V-REP supports different vision sensors (orthographic and perspective type) and proximity sensors (ray-type, pyramid-type, cylinder-type, disk-type, and

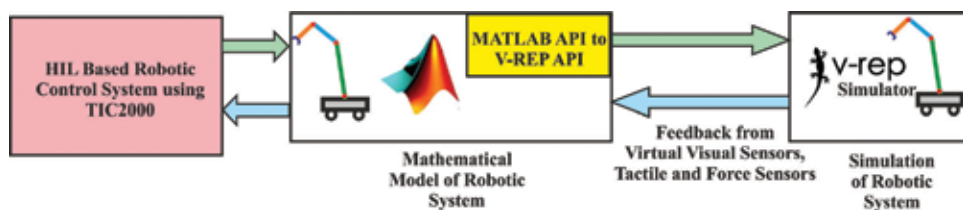


Figure 8. Schematic diagram for robot HIL system with V-rep through MATLAB API.

cone- or randomized ray-type proximity sensors). In this study, we used tactile sensors, force sensors, camera, RGB sensor, XYZ sensor, and laser range finder.

Following are the steps to be followed for interfacing V-REP with MATLAB.

1. Load the virtual model of Kuka's youBot in to V-REP environment by selecting youbot from the mobile robot model available in Model browser tab.
2. To enable control from MATLAB API, call the function `simRemoteApi.start` (port address) with specific port address in the V-REP script.
3. To establish link to the MATLAB API calls, place the two supporting MATLAB files (`remApi` and `remoteApiProto`) and `remoteApi.dll` file to your currently working folder. Those files can be located in V-REP's installation directory, in the directory `programming/remoteApiBindings/matlab`. Also make sure that MATLAB uses the same bit-architecture as the `remoteApi` library: 64bit MATLAB needs 64bit `remoteApi` library
4. Then run the MATLAB script code ensuring that V-REP simulator is already running.
5. Observe the animation of the virtual model of Kuka's youBot in to V-REP environment for object handling based on the control signals from the C2000 microcontroller.

5.3 HIL-based control law implementation

Commands to the actual physical youBot drives are sent from an Intel Atom on-board computer running on a real-time Linux kernel for the Simple Open EtherCAT Master (SOEM). A real-time communication is established between drives and on-board computer using EtherCAT, a technology used in KUKA's industrial robots.

The KUKA youBot drive protocol is open source, which encourages the users to develop their own applications and control systems. This flexible feature enables us to deploy the control algorithm in Texas Instruments C2000 microcontroller. Since, we deploy HIL-based control law and virtual model of the youBot, we eliminate the Intel Atom on-board system and use the TI C2000 hardware target board for deploying the grasp and task control algorithms. **Figure 9** shows the HIL setup for the robotic systems using TI C2000 real time controller, which runs the vision and force control scheme for the physical interaction along with the model of the youBot developed using MATLAB. The animated actions of the youBot are observed using V-REP robot simulator for object handling controlled using the HIL setup.

MATLAB Simulink environment has the support for deploying the developed algorithm, model of environment in the real time target boards, thereby providing support for HIL. MATLAB also possess the capability to interface Texas Instruments C2000 microcontroller board. With those extended support, the control algorithms are deployed in the C2000 microcontroller board.

For carrying out those tasks, following steps are done:

1. First, the kinematic and dynamic model of Kuka YouBot mobile manipulator was developed in the MATLAB Simulink Environment.
2. Control algorithms for physical interaction of the robot for prescribed environmental characteristics are developed using MATLAB Simulink Environment.

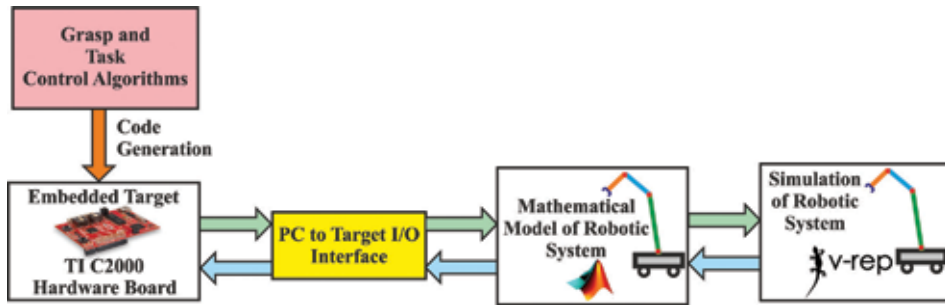


Figure 9. Hardware-in-the-loop simulation setup of the robotic system.

3. Executable model of the control algorithms is downloaded in the C2000 microcontroller board for building a HIL simulation platform.
4. The control algorithms run on the hardware board, which replaces the developed software.
5. Testing of the model is done in conjunction with the developed model of the Kuka YouBot mobile manipulator.

Repeated testing of the control algorithms are performed until meeting desired performance. Steps 4 and 5 are repeated for gaining confidence of real time implementation of the control algorithms in the physical Kuka YouBot mobile manipulator.

These testing phases enable to deploy the algorithm in real time. This was demonstrated using the model of Kuka YouBot mobile manipulator in V-REP robot simulation environment. Sensors data are taken from the V-REP environment as input to the HIL systems. Performance of the robot was assessed for the implemented control algorithms and the results are presented as shown in **Figures 10–12**.

5.4 Physical interaction of youBOT

Commands to the actual physical youBot drives are sent from an Intel Atom on-board computer running on a real-time Linux kernel for the Simple Open EtherCAT Master (SOEM). A real-time communication is established between drives and on-board computer using EtherCAT, a technology used in KUKA's industrial robots. The KUKA youBot drive protocol is open source, which encourages the users to develop their own applications and control systems. This flexible feature enables us to deploy the control algorithm in Texas Instruments C2000 microcontroller. Since, we deploy HIL-based control law and virtual model of the youBot, we eliminate the Intel Atom on-board system and use the TI C2000 hardware target board for deploying the grasp and task control algorithms.

Figure 10 shows the snapshot of the animated Kuka's youBot performing physical interaction with the objects in the environment simulated using V-REP robot simulator. The trajectory taken by the robotic arm, and the force exposed for grasping of objects are commands from the HIL-based robot control algorithms implemented using TI C2000 microcontroller board. The force and tactile feedbacks along with visual feedback are acquired from robot deployed in the V-REP environment. Those signals are given as an input to the control algorithms executing in the C2000 controller through the MATLAB environment.

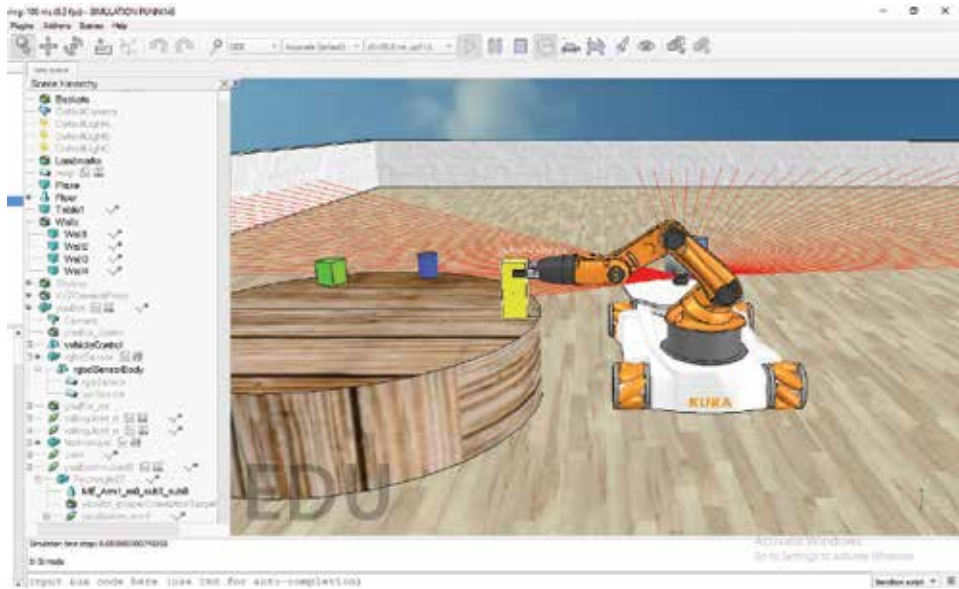


Figure 10. Kuka's youBot performing physical interaction with the objects in the environment simulated using V-REP robot simulator.

Range of sensors monitoring the environment during the physical interaction of the robot, gives the acquired environmental parameters to the MATLAB environment through the APIs. **Figure 11** shows the 2D visual range of the youBot feedback along x and y axis from the virtual physical environment acquired from the V-REP robot simulator.

Based on the acquired information and additional sensor feedback to the MATLAB environment, sensor fusion is done using Kalman filter. The probabilistic range of output of Kalman filter, data are fed to the C2000 real time controller through the target PC connector. The vision and force control algorithm running on the C2000 board, generate control signals based on the required tasks and grasp forces for dynamic range of objects in the physical environment. This process ensures to give the required force, maintains the stability of the grasped objects, and avoids slippery of the objects in the robot's hand. Initially, the tracking characteristics of the youbot are tested for a circular trajectory for object handling. From **Figure 12**, the plot shows the deviation of the actual trajectory from the desired

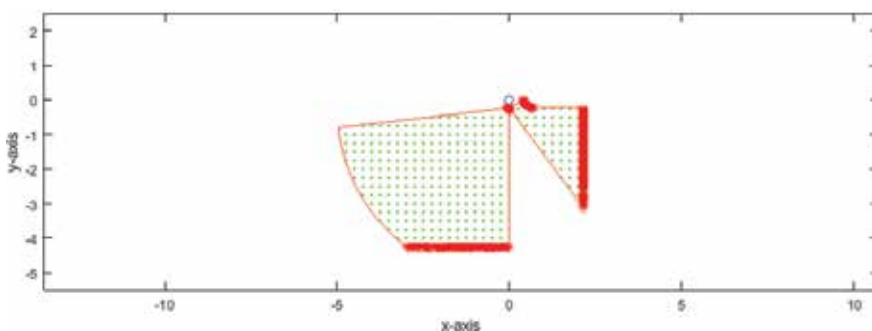


Figure 11. 2D visual range of Kuka's youBot feedback to the MATLAB environment from V-REP along x and y axis.

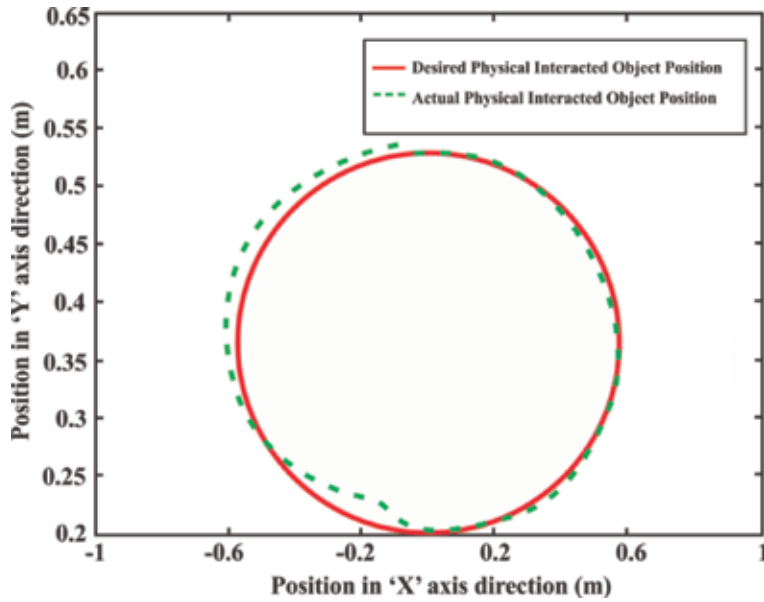


Figure 12. Circular trajectory tracking characteristics of Kuka's youBot for the vision and force control algorithm implemented in TI C2000 real time controller.

trajectory. For different observations, it was evident that the deviation is around 8% for the proposed algorithm.

Based on the satisfactory performance observed from tracking the circular trajectory, the youbot was configured with the application toward object handling. It was engaged in pick and place of an object using the proposed vision and force control algorithm implemented as in the HIL setup shown in **Figure 6** using TI C2000 real time controller. **Figure 13** shows the tracking of desired trajectory

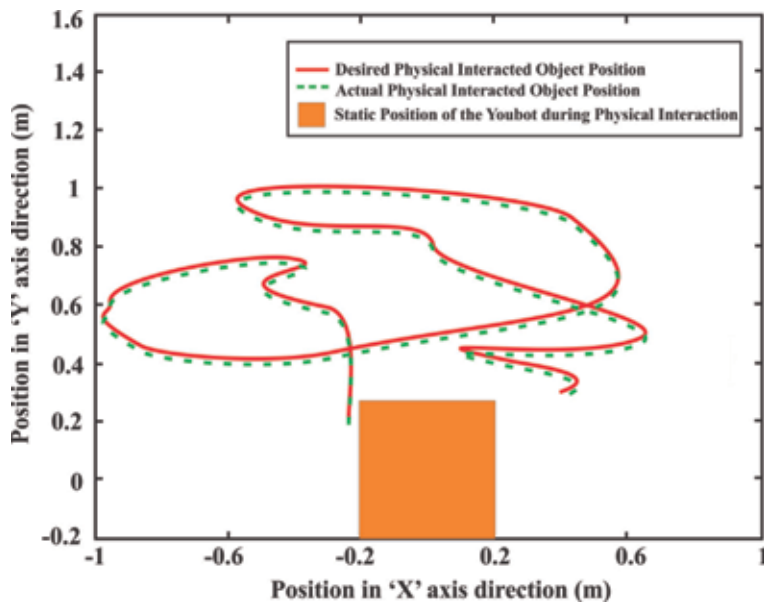


Figure 13. Object handling trajectory of static Kuka's youBot for the vision and force control algorithm implemented in TI C2000 real time controller.

during the physical interaction of the youbot with the environment. It is observed that the youbot in a static position engaged in physical interaction with the objects. The actual trajectory is deviated by 8% from the desired trajectory for the physical interaction of objects in the environment. This ensures better tracking accuracy of 92% in the implemented control algorithm using the proposed HIL setup and TI C2000 hardware for robotic applications. Further improvement can be ensured with the choice of appropriate adaptive sensor fusion techniques, control algorithms, and optimization techniques for fine tuning the system parameters.

6. Conclusion

The goal of this chapter is to implement HIL-based grasp and task control algorithms supported by using the vision-based sensors, tactile, and force sensors. The objective was to test the performance of the youBot arm for physical interaction with an environment and control its manipulation using the algorithms implemented in C2000 real time controller based on HIL simulation technique. HIL-based control algorithms actuate the joints of virtual youBot model implemented with appropriate scenario in V-REP robot simulator driven by the model of the robot implemented using MATLAB. After the analysis of performance of HIL-based grasp and task control algorithms youBot arm and a study of the pre-existing control and hardware, we proposed a new decentralized control architecture. The control algorithms are tested first using C2000 controller on a V-REP robot simulator, then by observing satisfactory performance of the algorithms they can be ported to real youBot arm. The HIL-based results of the vision and force controller give confidence level of 92% to deploy them on real youBot mobile manipulator. It can be further improved with more adaptive and optimization techniques.

Acknowledgements


The authors gratefully acknowledge the support of the Management of Mepco Schlenk Engineering College, Sivakasi, Tamil Nadu, India, the Principal and Head of Electronics and Communication Engineering Department for their constant support and encouragement.

Author details

Senthil Kumar Jagatheesa Perumal* and Sivasankar Ganesan
Department of Electronics and Communication Engineering, Mepco Schlenk Engineering College, Sivakasi, Tamil Nadu, India

*Address all correspondence to: senthilkumarj@mepcoeng.ac.in

IntechOpen

© 2019 The Author(s). Licensee IntechOpen. This chapter is distributed under the terms of the Creative Commons Attribution License (<http://creativecommons.org/licenses/by/3.0>), which permits unrestricted use, distribution, and reproduction in any medium, provided the original work is properly cited. 

References

- [1] Huang S, Tan KK. Hardware-in-the-loop simulation for the development of an experimental linear drive. *IEEE Transactions on Industrial Electronics*. 2010;57(4):1167-1174. DOI: 10.1109/TIE.2009.2038408
- [2] Martin A, Emami MR. Dynamic load emulation in hardware-in-the-loop simulation of robot manipulators. *IEEE Transactions on Industrial Electronics*. 2011;58(7):2980-2987. DOI: 10.1109/TIE.2010.2072890
- [3] Pouria S, Samereh Y. State of the art: Hardware in the loop modelling and simulation with its applications in design, development and implementation of system and control software. *International Journal of Dynamics and Control*. 2015;3(4):470-479. DOI: 10.1007/s40435-014-0108-3
- [4] Robin C, Emami MR. A holistic concurrent design approach to robotics using hardware-in-the-loop simulation. *Mechatronics*. 2013;23(3):335-345. DOI: 10.1016/j.mechatronics.2013.01.010
- [5] Senthil Kumar J. Investigation of adaptive controllers for precise trajectory tracking of three link planar rigid robotic manipulator employing hardware-in-the-loop simulation [thesis]. Chennai: Anna University; 2017
- [6] Maass J, Kohn N, Hesselbach J. Open modular robot control architecture for assembly using the task frame formalism. *International Journal of Advanced Robotic Systems*. 2006;3(1):1-10. DOI: 10.5772/5763
- [7] Tegin J, Wikander J. Tactile sensing in intelligent robotic manipulation—A review. *Industrial Robot*. 2005;32(1):64-70. DOI: 10.1108/01439910510573318
- [8] Baeten J, Bruyninckx H, De Schutter J. Integrated vision/force robotic servoing in the task frame formalism. *International Journal of Robotics Research*. 2003;22(10-11):941-954. DOI: 10.1177/027836490302210010
- [9] Bicchi A, Kumar V. Robotic grasping and contact: A review. In: *IEEE International Conference on Robotics and Automation*. San Francisco, CA; 2000. pp. 348-353
- [10] Borst C, Ott C, Wimbock T, Brunner B, Zacharias F, Bauml B, et al. A humanoid upper body system for two handed manipulation. In: *IEEE International Conference on Robotics and Automation*. 2007. pp. 2766-2767
- [11] Gunji D, Mizoguchi Y, Teshigawara S, Ming A, Namiki A, Ishikawaand M, et al. Grasping force control of multi-fingered robot hand based on slip detection using tactile sensor. In: *IEEE International Conference on Robotics and Automation*. Pasadena, CA, USA; 2008. pp. 2605-2610
- [12] Han L, Trinkle JC, Li Z. Grasp analysis as linear matrix inequality problems. *IEEE Transactions on Robotics and Automation*. 2000;16:1261-1268. DOI: 10.1109/70.897778
- [13] Enea S, Markus K, Tinne DL, Herman B, Marcello B. Intelligent Robots and Systems (IROS) Preview coordination: An enhanced execution model for online scheduling of mobile manipulation tasks. In: *IEEE/RSJ International Conference*. 2013. pp. 5779-5786
- [14] Timothy J. Mobile manipulation for the KUKA youBot platform [thesis]. Worcester Polytechnic Institute; 2013
- [15] Di Napoli G, Filippeschi A, Tanzini M, Avizzano CA. A novel control strategy for youBot arm. In: *IECON—42nd Annual Conference of the IEEE Industrial Electronics Society*. Florence, Italy; 2016. pp. 482-487

Toward Dynamic Manipulation of Flexible Objects by High-Speed Robot System: From Static to Dynamic

*Yuji Yamakawa, Shouren Huang, Akio Namiki
and Masatoshi Ishikawa*

Abstract

This chapter explains dynamic manipulation of flexible objects, where the target objects to be manipulated include rope, ribbon, cloth, pizza dough, and so on. Previously, flexible object manipulation has been performed in a static or quasi-static state. Therefore, the manipulation time becomes long, and the efficiency of the manipulation is not considered to be sufficient. In order to solve these problems, we propose a novel control strategy and motion planning for achieving flexible object manipulation at high speed. The proposed strategy simplifies the flexible object dynamics. Moreover, we implemented a high-speed vision system and high-speed image processing to improve the success rate by manipulating the robot trajectory. By using this strategy, motion planning, and high-speed visual feedback, we demonstrated several tasks, including dynamic manipulation and knotting of a rope, generating a ribbon shape, dynamic folding of cloth, rope insertion, and pizza dough rotation, and we show experimental results obtained by using the high-speed robot system.

Keywords: dynamic manipulation, flexible object, high-speed robot, high-speed vision

1. Introduction

Typical flexible object manipulation by robots has been performed in a static state or a quasi-static state [1–7]. In these methods, dynamical deformation of the flexible object is not considered, making it easier to manipulate the flexible object. However, the robots have to wait until the deformation converges to the steady state, which results in the manipulation time being very long, and the working efficiency is not good. Moreover, although it is desired to manipulate the flexible object while observing its deformation with cameras, the working efficiency becomes even worse because of the low speed of the cameras and image processing for recognizing the deformation. In addition, a deformation that changes momentarily cannot be recognized in real time by general-purpose cameras and image processing, and appropriate feedback control may not be carried out because of the latency from the recognition to the robot motion.

Recently, dynamic manipulations and nonprehensile manipulations of objects have been actively investigated with the goal of developing new manipulation techniques [8]. Our goal has been to achieve high-speed flexible object manipulation by handling the flexible object in a “dynamic,” nonprehensile state. As a result, we succeeded in simplifying the deformation model of flexible objects by using the high-speed motion of a high-speed robot, and we were able to perform appropriate real-time visual feedback control with a high-speed vision system. This dynamic manipulation technique may enable rapid realization of flexible object manipulation tasks.

In this chapter, we review the proposed method based on high-speed motion and visual feedback, and we demonstrate several tasks carried out by a high-speed robot system using the proposed method.

2. Concept of dynamic manipulation of flexible object

The key difficulties in the dynamic manipulation of a flexible object include:

- A. Deformation of the flexible object during manipulation
- B. Prediction of its deformation

In order to solve these problems as easily as possible and to enable dynamic manipulation of flexible objects, we proposed an entirely new method. In the proposed method, the robot moves with a tip velocity that decreases the effect of undesirable deformation of the flexible object; as a result, the model and motion planning can be simplified. **Figure 1** shows the basic concept of dynamic rope manipulation. The proposed method can be understood by picturing the manipulation of a rhythmic gymnastics ribbon, in which the ribbon deforms according to the tip motion.

From the above discussion, the rope deformation depends on the high-speed robot motion. In addition, we can assume that the rope deformation can be derived algebraically from the robot motion. Thus, the rope deformation model can be described as a simple deformation model derived from the robot motion. Also, since the rope deformation can be calculated algebraically from the robot motion in the model, the rope deformation model can be made more simple than typical models that use matrix differential equations as a multi-link model or partial differential equations as a continuous body model [9, 10].

Moreover, if the dynamic manipulation is performed in slow motion, gravity has a non-negligible effect on the rope. In that case, the algebraic equation does not hold, and we have to consider a differential equation, making dynamic

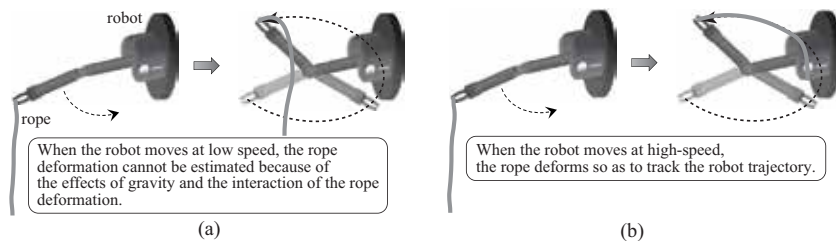


Figure 1. Basic concept. (a) Low-speed motion and (b) High-speed motion.

manipulation in slow motion extremely difficult as a result. Thus, high-speed robot motion is required in order to achieve dynamic manipulation.

Dynamic manipulation enables faster manipulation, high efficiency of task realization, and shorter task completion time and working time.

3. Dynamic manipulation method using high-speed robot motion

First, this section describes a theoretical analysis of a dynamical deformation model of flexible objects. We deal with a flexible rope as one example of such flexible objects. Then, we obtain a condition for dynamic manipulation based on the analysis. Next, we propose a simple deformation model that can be expressed by an algebraic equation. We also suggest a robot motion planning method using this simple model [11].

In the analysis, we assume that gravity is basically ignored, but we briefly describe the handling of gravity in Appendix-A.2, and we also assume that the flexible object does not exhibit elasticity.

3.1 Theoretical analysis for dynamic manipulation

3.1.1 Equation of motion of rope

Let us consider the equation of motion of the rope when the rope deformation is restricted to a given curve and a constraint force acts on the rope, as shown in **Figure 2**. The constraint force is R [N/m], the rope position is w [m], the position of the inside of the rope is σ [m], the line density of the rope is μ [kg/m], the tension is T [N], and the curvature is ρ [m]. Considering a length $\delta\sigma$ [m] of the curve, the difference between the tensions in the tangential direction becomes δT [N]. Since the angle of the part $\delta\sigma$ from the center of curvature is assumed to be $\delta\theta$ [rad], the equation $\delta\sigma = \rho\delta\theta$ holds. Thus, the tension in the normal direction at both ends of this part can be described as:

$$(T + \delta T) \cos \frac{\delta\theta}{2} - T \cos \frac{\delta\theta}{2} \approx \delta T. \quad (1)$$

$$2T \sin \frac{\delta\theta}{2} \approx T\delta\theta = \frac{T\delta\sigma}{\rho}. \quad (2)$$

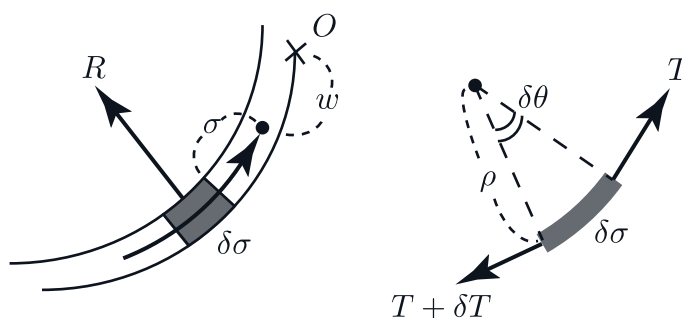


Figure 2.
 Rope mechanics.

Since the force R is the constraint force, the direction of the force is perpendicular to the curve. Then, the equations of motion in the tangential and normal directions of the part $\delta\sigma$ become

$$\begin{cases} (\mu\delta\sigma)\ddot{w} = \delta T \\ (\mu\delta\sigma)\frac{\dot{w}^2}{\rho} = \frac{T\delta\sigma}{\rho} + R\delta\sigma \end{cases} \quad (3)$$

Eq. (3) leads to

$$\begin{cases} \mu\ddot{w} = \frac{dT}{d\sigma} \\ \mu\frac{\dot{w}^2}{\rho} = \frac{T}{\rho} + R \end{cases} \quad (4)$$

Eq. (4) represents the rope dynamics under the condition that the rope behavior is restricted to the given curve. Next, we derive conditions for the robot motion in order to simplify the rope dynamics.

3.1.2 Condition for restricting rope on reference trajectory

When the constraint force R is equal to zero, the rope can deform so as to track the given curve. Therefore, the condition that $R = 0$ be satisfied can be obtained from Eq. (4):

$$T = \mu\dot{w}^2. \quad (5)$$

This equation is a function of the rope velocity. Substituting Eq. (5) into Eq. (4) yields

$$\mu\ddot{w} = \frac{d}{d\sigma} (\mu\dot{w}^2). \quad (6)$$

Since the part inside the brackets on the right-hand side is a function of the rope velocity, the right-hand side is equal to zero. This leads to

$$\mu\ddot{w} = 0. \quad (7)$$

As a result,

$$\dot{w} = \text{const.} \quad (8)$$

holds. In addition, the tension T can be obtained from Eq. (5):

$$T = \mu\dot{w}^2 = \text{const.} \quad (9)$$

And the tension T thus becomes constant. From this discussion, the necessary and sufficient condition that the rope can move along the reference trajectory in the absence of gravity and with the constraint force $R = 0$ can be summarized as

$$\dot{w} = \text{const.} \quad \text{and} \quad T = \mu \dot{w}^2 \quad (10)$$

This result means that when the rope moves along the rope reference trajectory, the velocity in the tangential direction of the rope is constant and a uniform force is applied to each joint of the rope. On the contrary, if the condition that the velocity and tension of the rope be constant is satisfied, the rope can move along the reference trajectory of the rope. Manipulating the rope at a constant velocity can be achieved by moving the robot arm in the tangential direction at a constant velocity. It is impossible to control the tension to be constant in the case of the free end of the rope. However, assuming that the rope is sufficiently long and that the rope tracks the reference configuration, the condition that the tension be constant approximately holds.

As a result, the robot motion conditions necessary to simplify the rope model are as follows:

- A. Constant-velocity motion: the rope deformation can be restricted to the reference trajectory.
- B. High-speed motion: the effects of gravity can be reduced under the gravity condition.

Thus, by manipulating the rope with this strategy, the rope can deform so as to track the robot motion. Since the robot is moved at a constant speed, each joint of the rope tracks the robot motion with a constant time delay. This time delay depends on the location of the joint.

In this analysis result, another solution ($\rho = \infty$) can also be obtained. The details are explained in Appendix-A.1.

3.2 Simple deformation model

3.2.1 Robot motion

First we consider the kinematics in order to derive the tip position of the robot arm. The joint angles and the tip position of the robot arm are defined by θ and r , respectively. In general, the relationship between the tip position and the joint angles can be obtained by the following equation:

$$\mathbf{r}(t) = \mathbf{f}(\boldsymbol{\theta}(t)). \quad (11)$$

Although the details of the derivation are omitted, the tip position is derived by using the Denavit-Hartenberg description.

3.2.2 Algebraic deformation model of rope

In general, a rope model is described by a distributed parameter system represented by partial differential equations. As another model, the rope is approximated by a multi-link system, and an equation of motion expressed by matrix differential equations is derived. In this research, we apply the multi-link system to the rope model. Then, the equation of motion can be replaced by an algebraic equation under the condition of constant, high-speed motion of the robot.

Based on the analysis described in the previous section, the following facts can be introduced in the rope deformation model:

- The rope behavior tracks the robot motion.
- The distance between two joint coordinates of the rope is not variable.
- Twisting of the rope is not taken into account.

The first assumption holds by ensuring constant, high-speed motion. This means that the rope deformation model can be described by the robot motion. The second assumption is that the rope does not have elasticity. Thus, the link distance in the multi-link model does not change.

From the above discussion, we propose a simplified rope deformation described by the following equation:

$$s_i(t) = r(t) + \sum_{i=1}^{N-1} l e_i, \quad (12)$$

where t is time, i is the joint number of the rope ($i = 0, 1, \dots, N - 1$), N is the number of particles in the multi-link rope model, s_i is the i -th joint coordinate of the rope, l is the distance between two joint coordinates (viz., the link length in the multi-link model), and e_i is a unit vector that represents the direction from the $(i - 1)$ -th joint to the i -th joint ($i = 1, \dots, N - 1$). In the case of $i = 0$, $s_0(t) = r(t)$ holds. This means that the location of the end point of the rope is the same as the tip position of the robot. **Figure 3** shows an overview of the proposed simple model. As shown in **Figure 3**, the rope deforms so as to track the tip of the robot arm.

Since the proposed model does not include an inertia term, Coriolis and centrifugal force terms, or a spring term, we do not need to estimate the dynamic model parameters. The advantage of the proposed model is that the number of model parameters is lower than in typical models. Therefore, the proposed model itself is robust. Moreover, since the rope model can be algebraically calculated, the simulation time becomes much shorter.

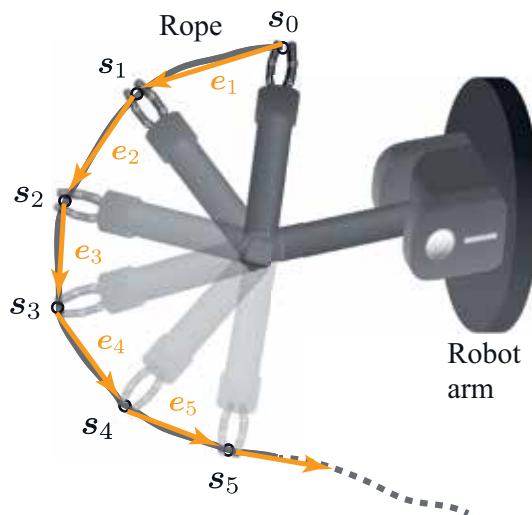


Figure 3.
Overview of simple model.

3.3 Motion planning

This section explains the motion planning for deriving the trajectory of the robot arm from the rope configuration. The procedure for the motion planning of the robot is the following:

- A. The desired rope configuration (s_r) is defined by a user; that is, the user gives the control points, as shown in **Figure 4**. Here, there exists a case where the link distance between two joint coordinates on the given rope configuration is not equal to l . Therefore, the rope configuration is corrected so that the link distance is equal to l .
- B. The trajectory of the tip position (r) of the robot arm is calculated from the rope configuration (s_r). The trajectory (r) of the robot arm can be obtained to track the given coordinate of each joint of the rope, as shown in **Figure 4**. Namely, we have the following equations:

$$r(t = 0) = s_{r_{N-1}}, \quad r(t = \Delta T) = s_{r_0}. \quad (13)$$

The trajectory is determined so as to linearly move from the N -th link to the first link during the motion time ΔT .

- C. The joint angles (θ) of the robot arm can be obtained by solving the inverse kinematics.

3.4 Features of proposed method

The advantages of the proposed method can be summarized as follows:

- The rope can be controlled so as to trace the robot trajectory in the absence of gravity.
- In contrast, any reference shape of the rope can be obtained by moving the robot so as to trace the reference shape of the rope in the absence of gravity.
- The deformation model of the rope can be represented by an algebraic equation with the constant-velocity motion of the robot in the absence of gravity.

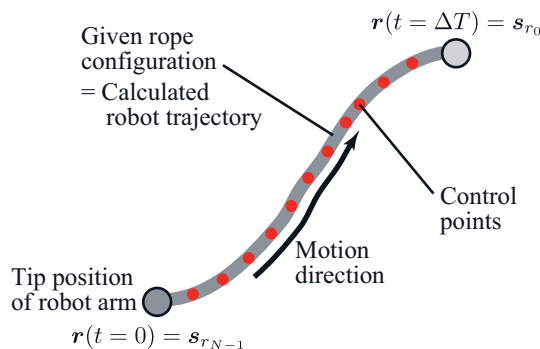


Figure 4.
 Inverse problem.

- A reference shape of the ribbon can be produced at a certain timing in the presence of gravity.

On the other hand, the disadvantages are as follows:

- There is a possibility that the deformation around the end of the rope may be out of alignment.
- The time during which a reference shape of the ribbon can be produced and maintained is limited to a short period. Moreover, since there is a possibility that the error between the reference shape and the actual shape may increase when the motion time is long, high-speed motion of the robot is required.
- The error in a rope with high rigidity or stretching properties may increase.

3.5 High-speed visual feedback control

The proposed method with the simple deformation model includes a modeling error, and the error may affect the dynamic manipulation of the flexible object. In order to correspond to the modeling error, we introduce a high-speed visual feedback control using a high-speed vision system and a high-speed image processing technique. A block diagram of the high-speed visual feedback control is shown in **Figure 5**.

By appropriately setting the extraction of the image feature and applying the self-window method, it is possible to speed up the image processing. As a result, a high-speed visual feedback is realized. In our method, the sampling rate of the visual feedback control is set at 1 kHz which is the same as the sampling rate of the robot control.

4. Task realization

In this section, we explain our high-speed robot system. Then, based on the proposed dynamic manipulation method, we describe proposed strategies for realizing various tasks such as dynamic knotting of a flexible rope, a generation of ribbon shape, and a dynamic folding of a cloth. The experimental results will be shown in Section 6.

4.1 High-speed robot system

The high-speed robot system consists of a high-speed robot arm (four degrees of freedom, manufactured by Barrett Technology Inc.), two high-speed robot hands ($180^\circ/0.1$ s) [12] mounted on two sliders (2 m/s), a high-speed vision system (1000 frames per second), and a real-time controller (1 kHz). The high-speed vision system is used for high-speed visual feedback, including real-time image processing. The joint angles of the robot system (arm, hands, and sliders) are controlled by a proportional-derivative law to the reference joint angles every 1 ms (corresponding to a sampling rate of 1 kHz).

4.2 Dynamic knotting of a flexible rope

As a first example, we explain a dynamic knotting of a flexible rope. **Figure 6** shows a strategy of the dynamic knotting. Firstly, we produce the circle shape on

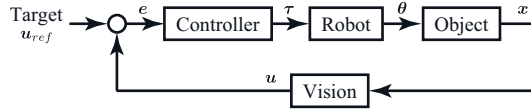


Figure 5.
 Block diagram of high-speed visual feedback control.

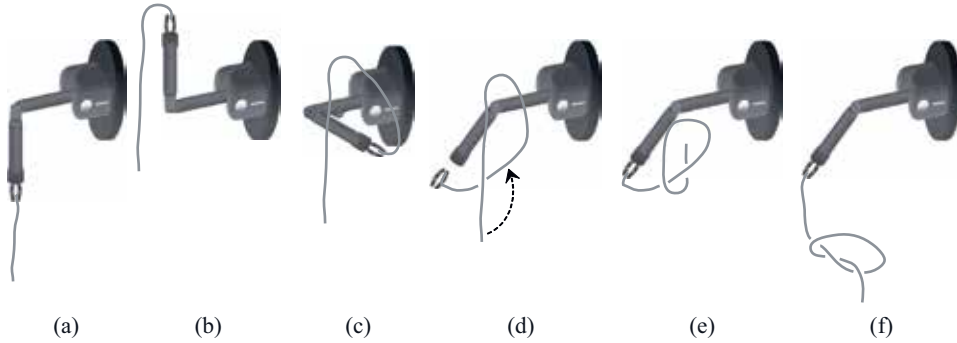


Figure 6.
 Strategy of dynamic knotting of flexible rope.

the rope as shown in **Figure 6(a)–(d)**. Then we perform the impact phenomenon on the intersection of the circle as shown in **Figure 6(d)–(f)**. After the impact, the end of the rope passes through the circle. As a result, the dynamic knotting can be completed.

4.3 Generation of ribbon shape

This section describes circular shape control of a ribbon based on the proposed method [13]. **Figure 7** shows a strategy of ribbon shape generation. Using constant, high-speed motion described above and air drag, we achieve the circle shape generation as shown in **Figure 7**.

For this task, we extended the simplified model of the rope to a belt-like flexible object, taking into account the effects of drag and gravity [13].

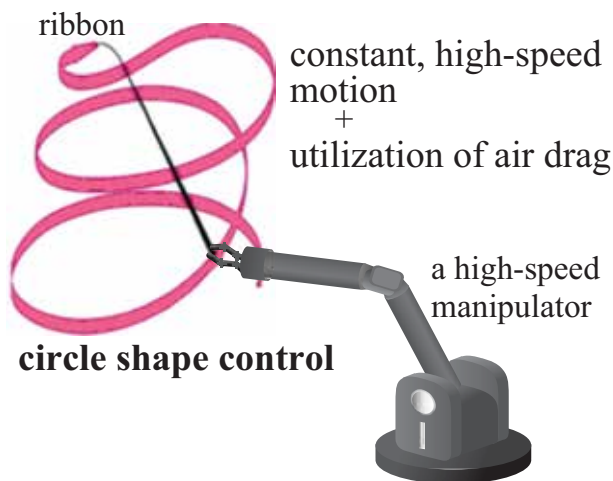


Figure 7.
 Strategy of generation of ribbon shape.

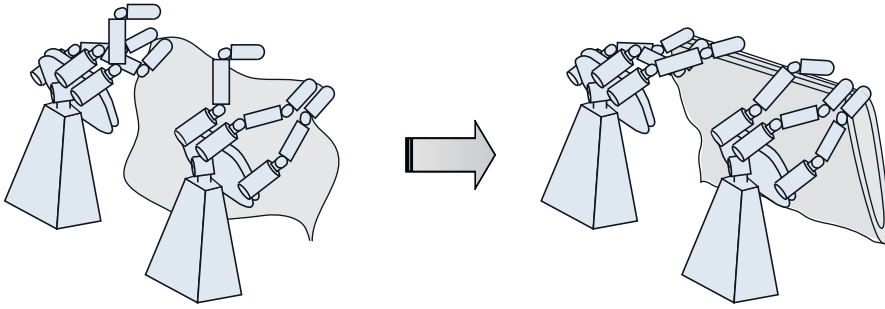


Figure 8.
Strategy of dynamic folding of cloth.

4.4 Dynamic folding of a cloth

Next, we explain a dynamic folding of a cloth, as shown in **Figure 8**, which is an application of two-dimensional flexible object. In the initial state, two robot hands grasp a cloth. Then, based on the proposed method, we obtained the joint trajectories of the robot system in order to appropriately deform the cloth using the high-speed motion. Finally, the robot hands grasp the end of the cloth using the high-speed visual feedback.

In this task, we extended the simplified model of the rope to a sheet-like flexible object. We constructed a two-dimensional model [14].

5. Rotational motion system

Here we describe the realization of additional tasks with a rotational motion system, including robotic rope insertion and pizza dough spinning. First, we briefly discuss analysis of the rotational motion system using high-speed rotational motion. Then, based on the results, we describe proposed strategies of rope insertion and pizza dough spinning using real-time visual feedback. The experimental results will be shown in Section 6.

5.1 Discussion

In this section, we explain a simple theoretical analysis of the high-speed rotational motion system. Using high-speed rotational motion, the flexible characteristics of an object to be manipulated may be effectively decreased, allowing us to consider only the rigid characteristics of the object.

Considering the forces acting on a part of the object as shown in **Figure 9**, the following equations can be obtained:

$$\begin{cases} T \cos \theta = \Delta m r \omega^2, \\ T \sin \theta = \Delta m g, \end{cases} \quad (14)$$

where T is the tension, Δm is the mass of a part of the object, r is the radius from the rotational center to the part, ω is the angular velocity, and θ is an approximate angle at the part, as shown in **Figure 9**. From these equations, we can get

$$\tan \theta = \frac{\Delta m g}{\Delta m r \omega^2} = \frac{g}{r \omega^2}. \quad (15)$$

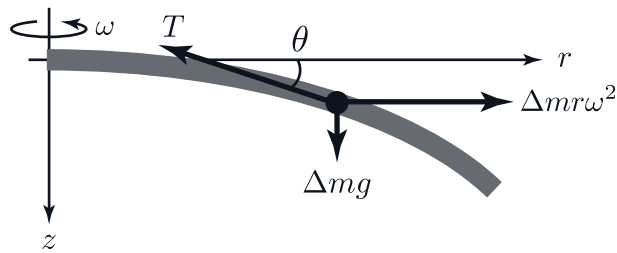


Figure 9.
 Model of rotational motion (side view).

From this result, we found that the angle θ decreases when the angular velocity ω increases. Thus, the deformation in the gravitational direction (z direction) can be ignored. In addition to this result, assuming that the elastic characteristics of the rope can be neglected, we can consider that the rotational system of the flexible object can be boiled down to the rotational system of a rigid body. This analysis result can be also applied to the dynamics of the flexible object in the radial direction.

5.2 Rope insertion

We briefly explain a rope insertion task as the first application [15]. **Figure 10** shows a strategy of the rope insertion. The rope deformation is restricted to a linear shape by using high-speed rotation, and visual feedback positioning control, as shown in **Figure 5**, between the tip position of the rope and the position of a hole is performed using the high-speed robot system. At the time when the tip position and the hole position are the same, the rope insertion is achieved by using the motion of a linear actuator (maximum speed is 2.4 m/s).

5.3 Pizza dough spinning

Next, we describe spinning of pizza dough [16]. **Figure 11** illustrates a strategy of the pizza dough spinning. In this task, the pizza deformation is restricted to a

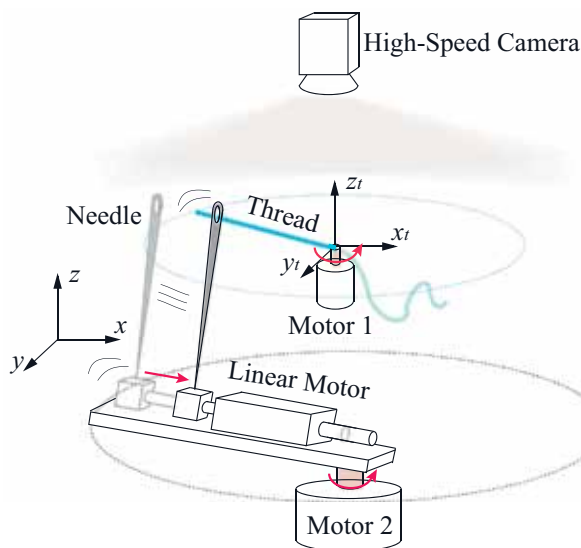


Figure 10.
 Strategy of rope insertion.

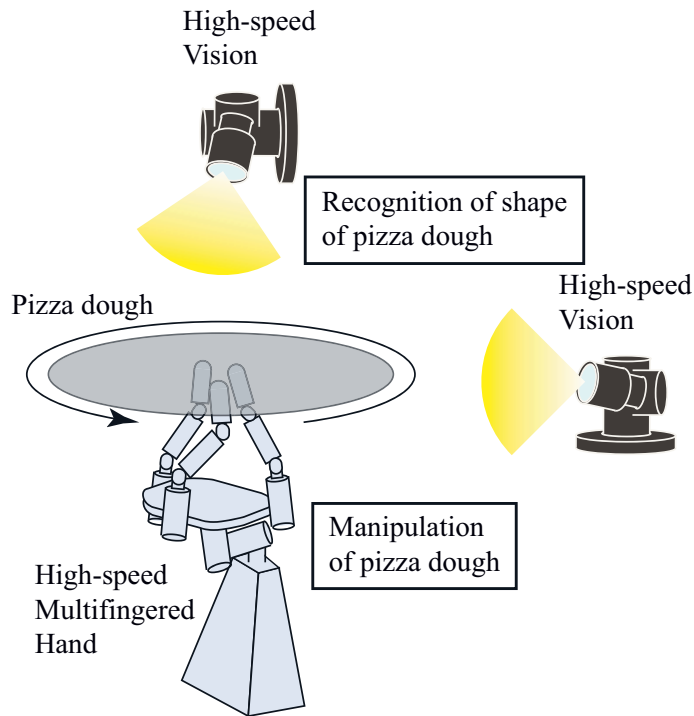


Figure 11.
Strategy of pizza dough spinning.

planar shape by using the proposed method. Angular acceleration of the rotation was achieved by high-speed finger motion. The contact control was carried out by using high-speed visual feedback.

6. Experimental results

Here we show experimental results of the dynamic knotting of a rope, the generation of ribbon shape, the dynamic folding of a cloth, the rope insertion, and the pizza dough spinning, respectively.

6.1 Result of dynamic knotting of a rope

Figure 12 shows the experimental result for dynamic knotting with the high-speed robot arm [17]. Also, **Figure 13** show a desired rope configuration for producing the circle shape and the joint trajectories of the high-speed robot arm solved by the inverse kinematics. In this experiment, the diameter and the length of the rope are 3 mm and 0.5 m, respectively. It can be seen from **Figure 12** that dynamic knotting of the flexible rope was achieved. Since the execution time is 0.5 s, the knotting can be carried out at high speed.

6.2 Result of generation of ribbon shape

The starting configuration was with the ribbon hanging straight down. **Figure 14** shows a composite photograph in which the circle shape was produced. In **Figure 14**, the dotted white line depicts the reference shape of the ribbon (i.e., the robot trajectory), and these pictures were taken at intervals of 0.067 s. **Figure 15**

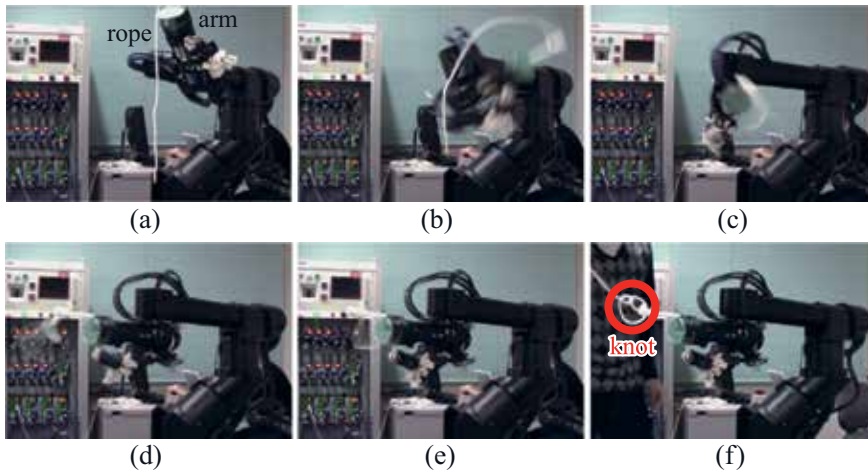


Figure 12. Continuous sequence of photographs of dynamic knotting. (a) $t = 0.00$ [sec], (b) $t = 0.16$ [sec], (c) $t = 0.32$ [sec], (d) $t = 0.48$ [sec], (e) $t = 0.64$ [sec] and (f) $t = 3.20$ [sec] [17].

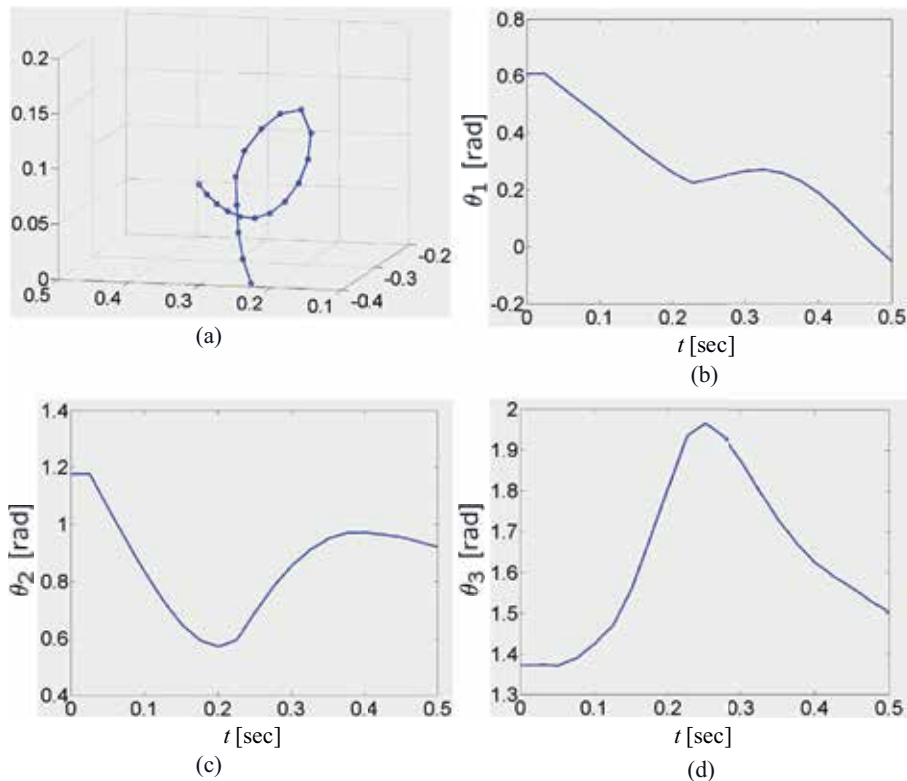


Figure 13. Desired rope configuration and joint trajectories of the robot arm. (a) Desired rope configuration, (b) Rotation axis of the upper arm, (c) Circulation axis of the upper arm and (d) Rotation axis of the lower arm [17].

shows an error between the reference circle shape and the actual ribbon shape. The error is calculated by a square root of sum of square error of each direction. As can be seen from these figures, the circle shape of the ribbon was successfully produced. We also produced a figure-eight shape, a wave shape, and a crank shape in the ribbon [18].

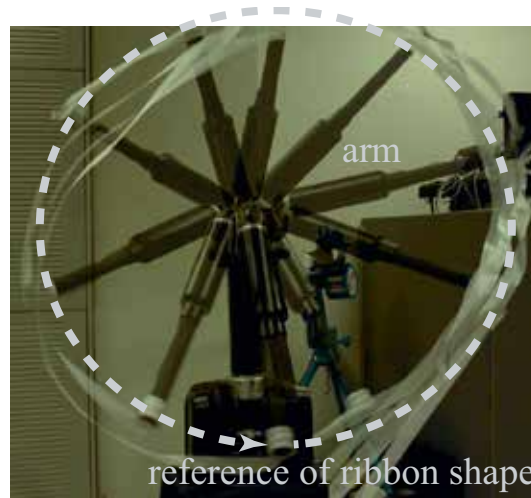


Figure 14.
Composite photograph of shape generation [13, 18].

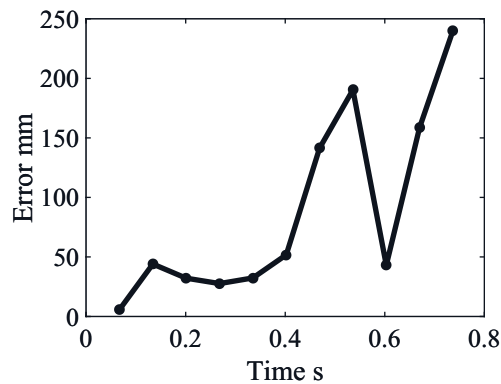


Figure 15.
Error between reference and actual shapes [13, 18].

The error between the reference shape and the obtained shape was evaluated for each reference shape.

6.3 Result of dynamic folding of a cloth

Next, we show the experimental result for dynamic folding of a cloth [14] shown in **Figure 16**. **Figure 17** shows the trajectories of the slider and hand wrists, and **Figure 18** shows the experimental data (visual information). **Figure 16(a)** represents the initial condition of the experiment, where the two hands grasp the cloth. **Figure 16(b)–(c)** shows the cloth being pulled toward the grasp position using the hand and slider motions. **Figure 16(d)** shows that when the hand and slider motions stop, the free end (the point far from the grasp position) of the cloth is folded by inertial force. **Figure 16(e)–(f)** shows grasping of the free end of the cloth using high-speed visual feedback [19]. As can be seen from the experimental results, dynamic folding of the cloth can be achieved by the two high-speed multi-fingered hands and two high-speed sliders. In addition, since the action time of the dynamic folding performed by the robot system is 0.4 s, high-speed folding can be achieved.

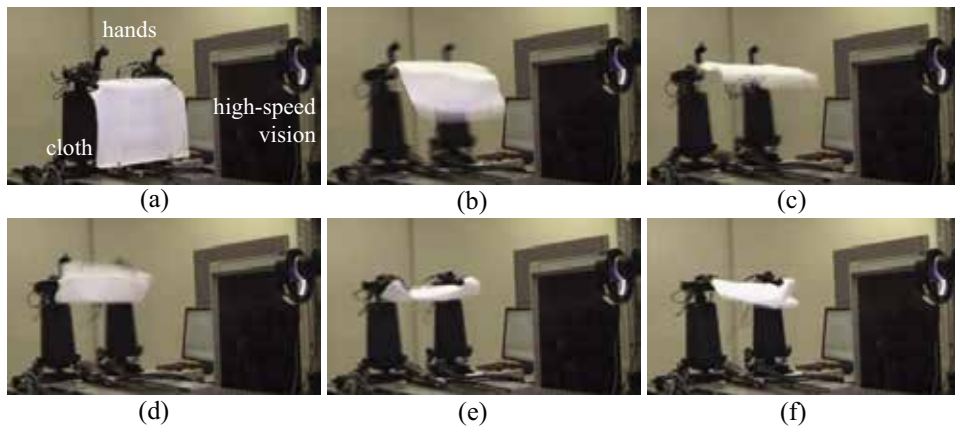


Figure 16. Continuous sequence of photographs of dynamic folding. (a) Time = 0.0 [sec], (b) Time = 0.1 [sec], (c) Time = 0.2 [sec], (d) Time = 0.3 [sec], (e) Time = 0.4 [sec] and (f) Time = 0.5 [sec] [19].

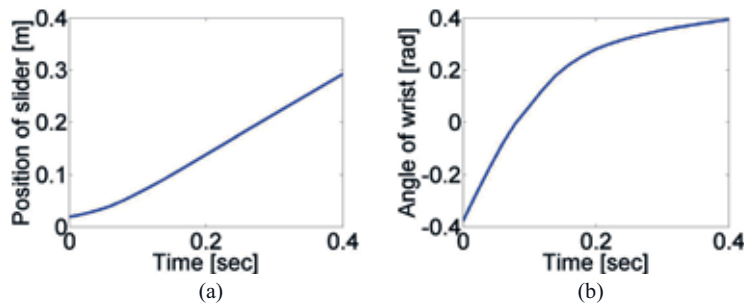


Figure 17. Trajectories of slider and hand wrist. (a) Trajectory of slider and (b) Trajectory of wrist of hand [19].

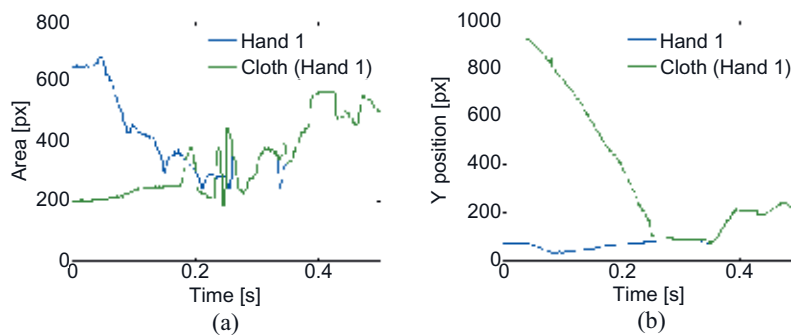


Figure 18. Experimental data of dynamic folding. (a) Area of markers and (b) Y position of markers [19].

6.4 Result of rope insertion

Figures 19 and 20 show the experimental result and data during rope insertion experiment. From the experimental results, the rope is deformed by the effect of gravity in the initial state as shown in Figure 19(a), but the rope deformation could be successfully controlled to a linear shape using the high-speed rotation motion.

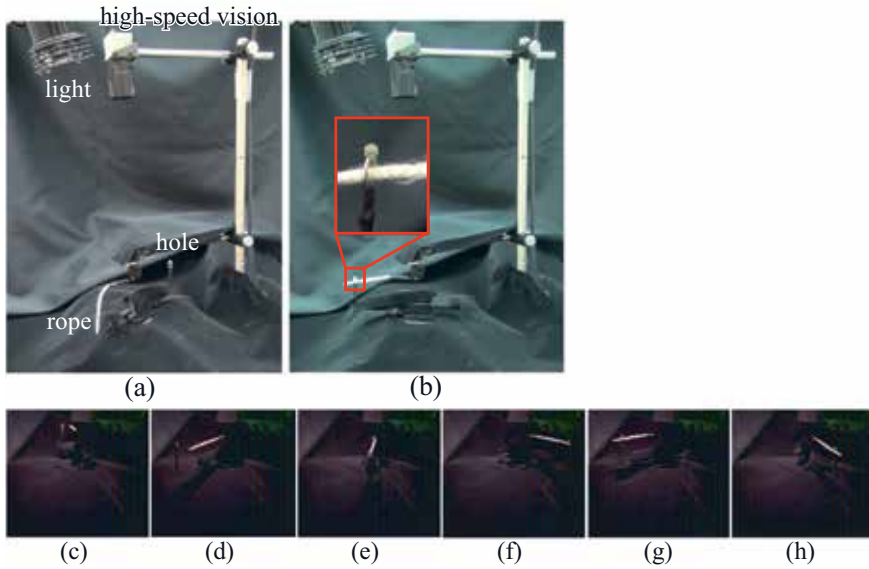


Figure 19. Continuous sequence of photographs of rope insertion task. (a) Initial state, (b) Finish state, (c) 2.0 [s], (d) 2.40 [s], (e) 2.75 [s], (f) 2.82 [s], (g) 2.90 [s] and (h) 2.95 [s] [15].

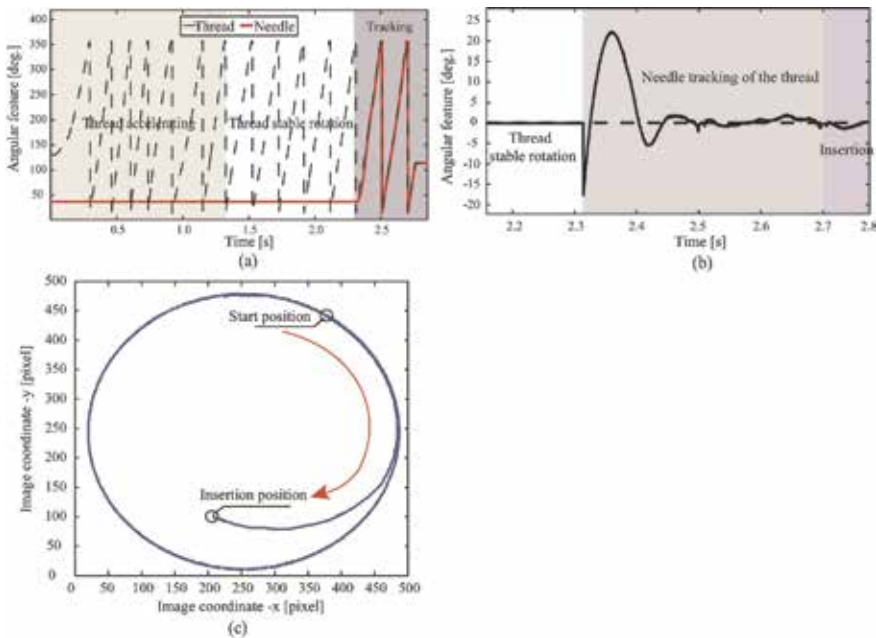


Figure 20. Experimental data of rope insertion. (a) Angular feature, (b) Angular feature error and (c) Image coordinate x - y [15].

Consequently, we achieved the rope insertion task with the proposed method, as shown in **Figure 19(b)**.

6.5 Result of pizza dough spinning

Figures 21 and **22** show the experimental result and data during pizza dough spinning experiment. It can be seen that the deformation of the pizza dough could

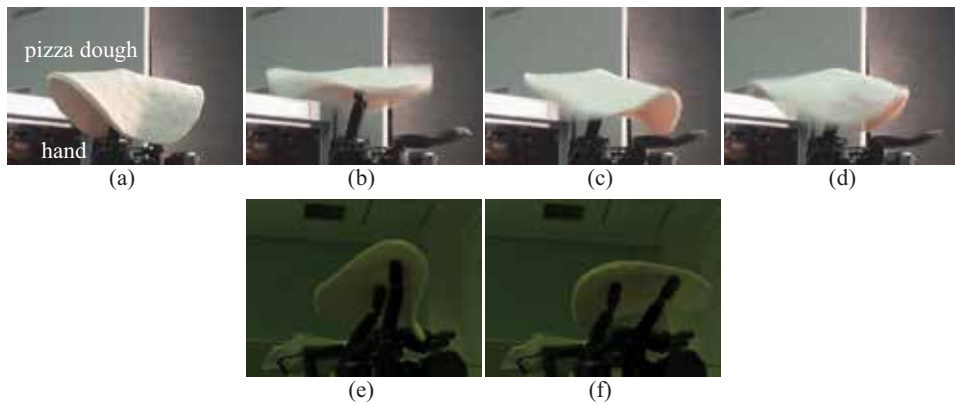


Figure 21. Continuous sequence of photographs of pizza dough spinning. Normal camera; (a) $t = 0.00$ [s], (b) $t = 0.33$ [s], (c) $t = 0.67$ [s], (d) $t = 1.00$ [s], High-speed camera; (e) $t = 0.04$ [s] and (f) $t = 0.12$ [s] [16].

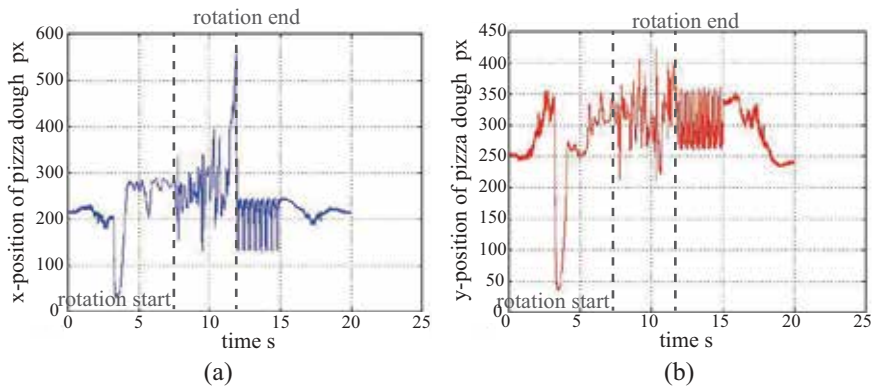


Figure 22. Experimental data of pizza dough spinning. (a) x -position of pizza dough and (b) y -position of pizza dough [16].

be controlled to approximately a planar shape by the proposed method, and the angular acceleration of the rotation could be achieved using the high-speed finger motion with contact control by high-speed image processing.

Summarizing this section, high-speed motion and real-time visual feedback allowed us to perform dynamic manipulation of flexible objects in a rotational motion system.

7. Conclusion

We have proposed a new method for dynamic and high-speed manipulation of flexible objects. The proposed method includes constant, high-speed robot motion and real-time visual feedback control. The findings described in this chapter can be summarized as follows:

- A. The constant, high-speed robot motion contributed to the construction of a simple deformation model of flexible objects (expressed by an algebraic equation).

- B. High-speed visual feedback also allowed for compensation of the modeling error, in order to increase the success rate and robustness for task realization.
- C. Dynamic, high-speed manipulations of flexible objects, such as dynamic knotting, shape generation, dynamic folding, rope insertion, and pizza dough spinning, could be achieved successfully by using the proposed method and a high-speed robot system.

Our proposed method will bring about a paradigm shift in which the flexible object strategy changes from static or quasi-static to dynamic.

In the future, we plan to demonstrate dynamic manipulations of flexible objects other than the tasks we explained in this article.

Conflict of interest

The authors declare no conflict of interest.

Supplementary materials

The experimental results can be seen on our YouTube channels and web sites [20–23].

A. Appendices

A.1 Another solution in the theoretical analysis: $\rho = \infty$

As another solution from Eq. (4), we can obtain the following condition so that $R = 0$ holds:

$$\rho = \infty \quad (16)$$

This is also a necessary and sufficient condition that the rope can move along the reference trajectory in the absence of gravity and with the constraint force $R = 0$. This means that the reference shape of the rope is a straight line, and therefore, it is trivial that the rope moves with straight-line motion.

Thus, we do not adopt this solution ($\rho = \infty$) in this research.

A.2 Case in which effects of gravity are considered

Here, we briefly explain a case in which the effects of gravity are considered in the simple deformation model and the motion planning [17].

In the calculation of the rope deformation, since the robot moves at high speed, the effects of gravity ($G(t)$) can be approximated as

$$G(t) = -\frac{1}{2}gt^2, \quad (17)$$

and then this term is added to z direction in Eq. (12).

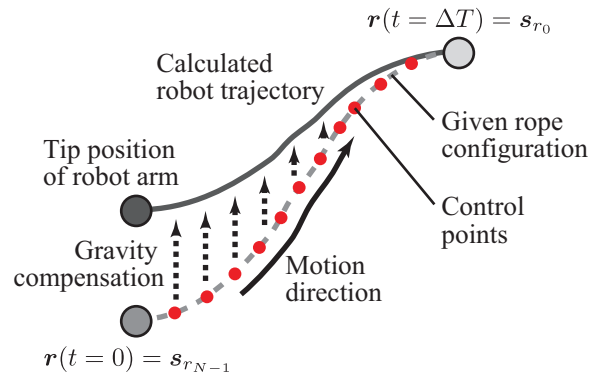


Figure 23.
 Inverse problem with consideration of effects of gravity.

In the motion planning, compensation for the effects of gravity,

$$G(\Delta T - t) = \frac{1}{2}g(\Delta T - t)^2 \quad (18)$$

is also considered, and this term is added to the given control points, as shown in **Figure 23**.

After that, the inverse kinematics are calculated in order to obtain the reference joint angles of the robot.

Author details

Yuji Yamakawa^{1*}, Shouren Huang², Akio Namiki³ and Masatoshi Ishikawa²


1 Interfaculty Initiative in Information Studies, The University of Tokyo, Tokyo, Japan

2 Graduate School of Information Science and Technology, The University of Tokyo, Tokyo, Japan

3 Department of Mechanical Engineering, Chiba University, Chiba, Japan

*Address all correspondence to: y-ymkw@iis.u-tokyo.ac.jp

IntechOpen

© 2019 The Author(s). Licensee IntechOpen. This chapter is distributed under the terms of the Creative Commons Attribution License (<http://creativecommons.org/licenses/by/3.0>), which permits unrestricted use, distribution, and reproduction in any medium, provided the original work is properly cited. 

References

- [1] Inoue H, Inaba M. Hand-eye coordination in rope handling. In: *Robotics Research: The First International Symposium*; MIT Press; 1984. pp. 163-174
- [2] Matsuno T, Fukuda T, Arai F. Flexible rope manipulation by dual manipulator system using vision sensor, In: *Proc. IEEE/ASME Int. Conf. on Advanced Intelligent Mechatronics*; 2001. pp. 677-682
- [3] Wakamatsu H, Morinaga E, Arai E, Hirai S. Deformation modeling of belt object with angles. In: *Proc. IEEE Int. Conf. on Robotics and Automation*; 2009. pp. 606-611
- [4] Asano Y, Wakamatsu H, Morinaga E, Arai E, Hirai S. Deformation path planning for belt object manipulation. In: *Proc. 2010 Int. Symp. on Flexible Automation*; 2010
- [5] Tanaka K, Kamotani Y, Yokokohji Y. Origami folding by a robotic hand. In: *Proc. Int. Conf. on Intelligent Robot Systems*; 2007. pp. 2540-2547
- [6] Balkcom DJ, Mason MT. Robotic origami folding. *The International Journal of Robotics Research*. 2008; 27(5):613-627
- [7] Shepard JM, Towner MC, Lei J, Abbeel P. Cloth grasp point detection based on multiple-view geometric cues with application to robotic towel folding. In: *Proc. Int. Conf. on Robotics and Automation*; 2010. pp. 2308-2315
- [8] Lynch KM, Mason MT. Dynamic nonprehensile manipulation: controllability, planning, and experiments. *The International Journal of Robotics Research*. 1999;18(1):64-92
- [9] Suzuki T, Ebihara Y, Shintani K. Dynamic analysis of casting and winding with hyper-flexible manipulator. In: *Proc. IEEE Int. Conf. on Advanced Robotics*; 2005. pp. 64-69
- [10] Mochiyama H, Suzuki T. Kinematics and dynamics of a cable-like hyper-flexible manipulator. In: *Proc. IEEE Int. Conf. on Robotics and Automation*; 2002. pp. 3672-3677
- [11] Yamakawa Y, Namiki A, Ishikawa M. Simple model and deformation control of a flexible rope using constant, high-speed motion of a robot arm. In: *Proc. IEEE Int. Conf. on Robotics and Automation*; 2012. pp. 2249-2254
- [12] Namiki A, Imai Y, Ishikawa M, Kaneko M. Development of a high-speed multifingered hand system and its application to catching. In: *Proc. Int. Conf. Intelligent Robots and Systems*; 2003. pp. 2666-2671
- [13] Yamakawa Y, Namiki A, Ishikawa M. Dexterous manipulation of a rhythmic gymnastics ribbon with constant, high-speed motion of a high-speed manipulator. In: *Proc. 2013 IEEE Int. Conf. on Robotics and Automation*; 2013. pp. 1888-1893
- [14] Yamakawa Y, Namiki A, Ishikawa M. Motion planning for dynamic folding of a cloth with two high-speed robot hands and two high-speed sliders. In: *Proc. 2011 IEEE Int. Conf. on Robotics and Automation*; 2011. pp. 5486-5491
- [15] Huang S, Yamakawa Y, Senoo T, Ishikawa M. Robotic needle threading manipulation based on high-speed motion strategy using high-speed visual feedback. In: *Proc. 2015 IEEE/RSJ Int. Conf. on Intelligent Robots and Systems*; 2015. pp. 4041-4046
- [16] Yamakawa Y, Nakano S, Senoo T, Ishikawa M. Dynamic manipulation of a thin circular flexible object using a high-speed multifingered hand and

high-speed vision. In: Proc. 2013 IEEE Int. Conf. on Robotics and Biomimetics; 2013. pp. 1851-1857

[17] Yamakawa Y, Namiki A, Ishikawa M. Motion planning for dynamic knotting of a flexible rope with a high-speed robot arm. In: Proc. IEEE/RSJ 2010 Int. Conf. on Intelligent Robots and Systems; 2010. pp. 49-54

[18] Yamakawa Y, Namiki A, Ishikawa M. Simplified deformation model and shape generation of a rhythmic gymnastics ribbon using a high-speed multi-jointed manipulator. Mechanical Engineering Journal. 2016;3(6. Paper No. 15-00510)

[19] Yamakawa Y, Namiki A, Ishikawa M. Dynamic manipulation of a cloth by high-speed robot system using high-speed visual feedback. In: Proc. 18th IFAC World Congress; 2011. pp. 8076-8081

[20] Dynamic Manipulation of a Linear Flexible Object with a High-speed Robot Arm [Internet]. 2017. Available from: <http://www.youtube.com/watch?v=hZJ5qrfRS90> [Accessed: 08 August 2018]

[21] Dynamic Cloth Folding [Internet]. 2011. Available from: <http://www.youtube.com/watch?v=Bkt01ZWniGY> [Accessed: 08 August 2018]

[22] Robotic Needle Threading Manipulation based on High-Speed Motion Strategy [Internet]. 2015. Available from: <http://www.k2.t.u-tokyo.ac.jp/fusion/NeedleThreading/threading.mp4> [Accessed: 08 August 2018]

[23] Rotational Holding of Thin Circular Flexible Object using a Multifingered Hand [Internet]. 2013. Available from: <http://www.k2.t.u-tokyo.ac.jp/fusion/PizzaSpinning/PizzaSpinning.wmv> [Accessed: 08 August 2018]

Trajectory Tracking Using Adaptive Fractional PID Control of Biped Robots with Time-Delay Feedback

*Joel Perez Padron, Jose P. Perez, C.F. Mendez-Barrios
and V. Ramírez-Rivera*

Abstract

This paper presents the application of fractional order time-delay adaptive neural networks to the trajectory tracking for chaos synchronization between Fractional Order delayed plant, reference and fractional order time-delay adaptive neural networks. For this purpose, we obtained two control laws and laws of adaptive weights online, obtained using the fractional order Lyapunov-Krasovskii stability analysis methodology. The main methodologies, on which the approach is based, are fractional order PID the fractional order Lyapunov-Krasovskii functions methodology, although the results we obtain are applied to a wide class of non-linear systems, we will apply it in this chapter to a bipedal robot. The structure of the biped robot is designed with two degrees of freedom per leg, corresponding to the knee and hip joints. Since torso and ankle are not considered, it is obtained a 4-DOF system, and each leg, we try to force this biped robot to track a reference signal given by undamped Duffing equation. To verify the analytical results, an example of dynamical network is simulated, and two theorems are proposed to ensure the tracking of the nonlinear system. The tracking error is globally asymptotically stabilized by two control laws derived based on a Lyapunov-Krasovskii functional.

Keywords: biped robot, fractional time-delay adaptive neural networks, fractional order PID control, fractional Lyapunov-Krasovskii functions, trajectory tracking

1. Introduction

Fractional calculus is a generalization of differential and integral calculus which involves generalized functions. The first to work this new branch of mathematics was Leibniz. Due to the growing interest in the applications of fractional calculation, in this work we obtain conditions that guarantee the tracking of trajectories of nonlinear systems generated by differential equations of fractional order which we will call plants (This term is widely used in engineering), which in our case will be a mechanical arm, a helicopter, a plane or limbs of a humanoid, all of fractional order.

The problem of tracking control of trajectories is very important, since the control function allows the non-linear system to carry out a previously assigned

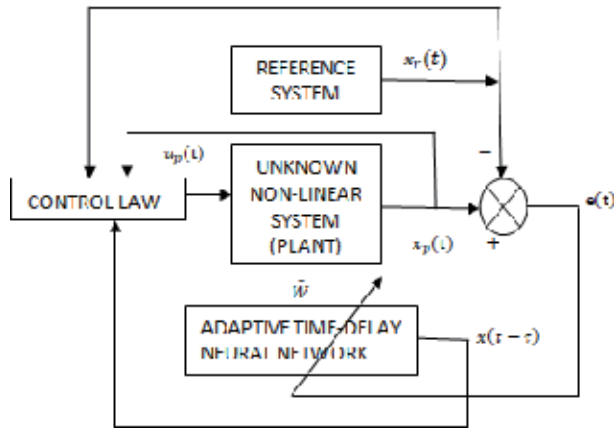


Figure 1.
Adaptive recurrent control diagram.

task, work or trajectory, for example, a mechanical arm and its objective is to cut a piece with a previously generated form, or the coupling of two aircraft in space.

In this chapter we use adaptive recurrent neural networks with time delay, since its use allows us to work with systems whose mathematical model is unknown and with the presence of uncertainties, this is a well-known problem of robust control.

We include mathematical models with time delay, since the processing and transmission of information is important in this type of systems, which depending on the delay, these systems can generate undesirable oscillatory or chaotic dynamics, and cause instability in the mathematical model that describes the trajectory tracking error.

The chapter is organized as follows: first, the general mathematical model of non-linear systems is proposed, as a second part, the Neural Network is proposed that will adapt to the non-linear system and the reference signal that both must follow, as a third part obtains the dynamics of the tracking error between the non-linear system and the reference, after obtaining conditions in the laws of adaptation of weights in the Neural Network and obtaining the control law that guarantees that the tracking error converges to zero, so that the non-linear system will follow the indicated reference signal, which is what was wanted to be demonstrated. Finally simulations are presented, which illustrate the theoretical results previously demonstrated. The proposed new control scheme is applied via simulations to control of a 4-DOF Biped Robot [1].

We use the scheme of **Figure 1** to indicate the procedure used in the obtaining of the laws of adaptation of weights and the laws of control that guarantee that the tracking error between the non-linear system, the neural network and the reference signal converges to zero.

2. Time-delay adaptive neural network and the reference

2.1 List of variables

W^* is the matrix weights.

$e = x_p - x_r$, error between the plant and the reference.

\hat{W} is part of the approach, given by W^* .

$\Omega u_1, \Omega u_2, u_p, u_n$ are the controls

$PI^\lambda D^\alpha = K_p e(t) + K_i a D_t^{-\lambda} e(t) + K_d a D_t^\alpha e(t)$ control law

τ is time delay

$tr\{aD_t^\alpha \tilde{W}^T \tilde{W}\} = -e^T \tilde{W} \sigma(x(t - \tau))$, learning law from the neural network weights
 $\int_{t-\tau}^t [\Phi_\sigma^T(s) \hat{W}^T \hat{W} \Phi_\sigma(s)] ds$, Lyapunov-Krasovskii Function
 $D(q(t))\ddot{q}(t) + C(q(t), \dot{q}(t))\dot{q}(t) + G(q(t)) = B\tau(t)$, dynamics of the bipedal robot
 $D(q(t))$ is the inertia matrix
 $C(q(t), \dot{q}(t))$ is the matrix of Coriolis and centripetal forces
 $G(q(t))$ represents a matrix of gravitational effects
 B defines the input matrix

There are several ways to define the fractional calculation, in this research we will use the well-known derivative of Caputo, which has the following notation:

$$aD_t^\alpha f(t) = \frac{1}{\Gamma(\alpha - n)} \int_a^t \frac{f^{(n)}(\tau)}{(t - \tau)^{\alpha - n + 1}} d\tau \quad (1)$$

For $(n - 1 < \alpha < n)$.

The nonlinear system, Eq. (2), which is forced to follow a reference signal:

$$aD_t^\alpha x_p = f_p(t, x_p(t) + x_p(t - \tau)), t \in [0, T], 0 < \alpha \leq 1, \quad (2)$$

$$x_p(t) = g(t)$$

$$x_p, f_p \in \mathbb{R}^n, u \in \mathbb{R}^m, g_p \in \mathbb{R}^{n \times n}.$$

The differential equation will be modeled by the neural network [2]:

$$aD_t^\alpha x_p = A(x) + W^* \Gamma_z(x(t - \tau) + \Omega_u.$$

The tracking error between these two systems:

$$w_{per} = x - x_p \quad (3)$$

We use the next hypotheses.

$$aD_t^\alpha w_{per} = -k w_{per} \quad (4)$$

In this research we will use $k = 1$, so that, Eq. (5), $aD_t^\alpha w_{per} = aD_t^\alpha x - aD_t^\alpha x_p$, so:

$$aD_t^\alpha x_p = aD_t^\alpha x + w_{per}$$

The nonlinear system is [3]:

$$aD_t^\alpha x_p = aD_t^\alpha x + w_{per} = A(x) + W^* \Gamma_z[x(t - \tau)] + w_{per} + \Omega_u \quad (5)$$

where the W^* is the matrix weights.

3. Tracking error problem

In this part, we will analyze the trajectory tracking problem generated by

$$aD_t^\alpha x_r = f_r(x_r, u_r), w_r, x_r \in \mathbb{R}^n \quad (6)$$

are the state space vector, input vector and f_r , is a nonlinear vectorial function.

To achieve our goal of trajectory tracking, we propose the error between the plant and the reference as: $e = x_p - x_r = (x_p - x_n) + (x_n - x_r) = (x_p - x) + (x - x_r)$.

Let $e_p = x_p - x$, and $e_n = x - x_r$, be the trajectory tracking error and $e = e_p + e_r$

$$e_n = x - x_r \quad (7)$$

The time derivative of the error is:

$$aD_t^\alpha e_n = aD_t^\alpha x - aD_t^\alpha x_r = A(x) + W^* \Gamma_z[x(t - \tau)] + w_{per} + \Omega_u - f_r(x_r, u_r) \quad (8)$$

Eq. (8), can be rewritten as follows, adding and subtracting, the next terms $\hat{W}\Gamma_z(x_r x(t - \tau))$, $\alpha_r(t, \hat{W})$, Ae and $w_{per} = x - x_p$, then,

$$\begin{aligned} aD_t^\alpha e &= A(x) + W^* \Gamma_z(x(t - \tau)) + x - x_p + \Omega_u - f_r(x_r, u_r) + \hat{W}\Gamma_z(x_r(t - \tau)) \\ &\quad - \hat{W}\Gamma_z(x_r(t - \tau)) + \Omega\alpha_r(t, \hat{W}) - \Omega\alpha_r(t, \hat{W}) + Ae - Ae \\ aD_t^\alpha e &= Ae + W^* \Gamma_z(x(t - \tau)) + \Omega_u - f_r(x_r, u_r) + \hat{W}\Gamma_z(x_r(t - \tau)) \quad (9) \\ &\quad + \Omega\alpha_r(t, \hat{W}) - \Omega\alpha_r(t, \hat{W}) - e - x_r - Ae + x + A(x) - \hat{W}\Gamma_z(x_r(t - \tau)) \end{aligned}$$

The unknown plant will follow the fractional order reference signal, if:

$$Ax_r + \hat{W}\Gamma_z(x_r(t - \tau)) + x_r - x_p + \Omega\alpha_r(t, \hat{W}) = f_r(x_r, u_r),$$

where

$$\Omega\alpha_r(t, \hat{W}) = f_r(x_r, u_r) - Ax_r - \hat{W}\Gamma_z(x_r(t - \tau)) - x_r + x_p \quad (10)$$

$$\begin{aligned} aD_t^\alpha e &= Ae + W^* \Gamma_z(x(t - \tau)) - \hat{W}\Gamma_z(x_r(t - \tau)) - Ae + (A + I)(x - x_r) \\ &\quad + \Omega(u - \alpha_r(t, \hat{W})) \quad (11) \end{aligned}$$

Now, \hat{W} is part of the approach, given by W^* . Eq. (11) can be expressed as Eq. (12), adding and subtracting the term $\hat{W}\Gamma_z(x(t - \tau))$ and if $\Gamma_z(x(t - \tau)) = \Gamma(z(x(t - \tau)) - z(x_r(t - \tau)))$

$$\begin{aligned} aD_t^\alpha e &= Ae + (W^* - \hat{W})\Gamma_z(x(t - \tau)) + \hat{W}\Gamma(z(x(t - \tau)) - z(x_r(t - \tau))) \\ &\quad + (A + I)(x - x_r) - Ae + \Omega(u - \alpha_r(t, \hat{W})) \quad (12) \end{aligned}$$

If

$$\tilde{W} = W^* - \hat{W} \text{ and } \tilde{u} = u - \alpha_r(t, \hat{W}) \quad (13)$$

And by replacing Eq. (13) in Eq. (12), we have:

$$\begin{aligned} aD_t^\alpha e &= Ae + \tilde{W}\Gamma_z(x(t - \tau)) + \hat{W}\Gamma(z(x(t - \tau)) - z(x_r(t - \tau))) \\ &\quad + (A + I)(x - x_r) - Ae + \Omega\tilde{u} \\ aD_t^\alpha e &= Ae + \tilde{W}\Gamma_z(x(t - \tau)) \\ &\quad + \hat{W}\Gamma(z(x(t - \tau)) - z(x_p(t - \tau)) + z(x_p(t - \tau)) - z(x_r(t - \tau))) \\ &\quad + (A + I)(x - x_p + x_p - x_r) - Ae + \Omega\tilde{u} \quad (14) \end{aligned}$$

And:

$$\tilde{u} = u_1 + u_2 \quad (15)$$

So, the result for Ωu_1 is

$$\Omega u_1 = -\hat{W}\Gamma(z(x(t-\tau)) - z(x_p(t-\tau))) - (A + I)(x - x_p) \quad (16)$$

and Eq. (14), is simplified:

$$\begin{aligned} aD_t^\alpha e &= Ae + \tilde{W}\Gamma_z(x(t-\tau)) + \hat{W}\Gamma(z(x_p(t-\tau)) - z(x_r(t-\tau))) \\ &+ (A + I)(x_p - x_r) - Ae + \Omega\tilde{u} \end{aligned}$$

Taking into account that $e = x_p - x_r$, shortening notation a little bit by setting $\sigma = \Gamma_z$, and defining $\hat{\sigma}(t-\tau) = \sigma(x_p(t-\tau)) - \sigma(x_r(t-\tau))$, the equation for $aD_t^\alpha e$ is

$$aD_t^\alpha e = (A + I)e + \tilde{W}\sigma(x(t-\tau)) + \hat{W}\hat{\sigma}(t-\tau) + \Omega u_2 \quad (17)$$

Now, the problem is to find the control law Ωu_2 , which it stabilizes to the system Eq. (20). The control law, we will obtain using the fractional order Lyapunov-Krasovskii methodology.

4. Study of trajectory tracking error

Our mathematical model of the dynamics in the tracking error is described in (17). In this equation we can see that an equilibrium state of this system is $(e, \hat{W}) = 0$.

Without loss of generality we can assume that the matrix A is given $A = -\lambda I$, $\lambda > 0$, where I is the identity matrix of order $n \times n$.

For the study of the stability of the tracking error we propose the following PID control law [4], widely used in science and engineering.

We will determine conditions in the parameters that guarantee that the tracking error converges to zero, and we will also use the following control law [5].

$$\Omega u_2 = K_p e + K_i aD_t^{-\alpha} e + K_v aD_t^\alpha e - \gamma \left(\frac{1}{2} + \frac{1}{2} \|\hat{W}\|^2 L_\phi^2 \right) e \quad (18)$$

We also include the following control law, $PI^\lambda D^\alpha$ [6]:

$$u(t) = K_p e(t) + K_i aD_t^{-\lambda} e(t) + K_d aD_t^\alpha e(t)$$

Substituting Eq. (18) in Eq. (17):

$$\begin{aligned} aD_t^\alpha e &= (A + I)e + \tilde{W}\sigma(x(t-\tau)) + \hat{W}\hat{\sigma}(t-\tau) \\ &+ K_p e + K_i aD_t^{-\alpha} e + K_v aD_t^\alpha e - \gamma \left(\frac{1}{2} + \frac{1}{2} \|\hat{W}\|^2 L_\phi^2 \right) e, \end{aligned}$$

then

$$\begin{aligned} (1 - K_v) aD_t^\alpha e &= (A + I)e + \tilde{W}\sigma(x(t-\tau)) + \hat{W}\hat{\sigma}(t-\tau) \\ &+ K_p e + K_i aD_t^{-\alpha} e - \gamma \left(\frac{1}{2} + \frac{1}{2} \|\hat{W}\|^2 L_\phi^2 \right) e. \end{aligned}$$

If $a = (1 - K_v)$, then

$$\begin{aligned}
 aD_t^\alpha e &= \frac{1}{a}(A + I)e + \frac{1}{a}\tilde{W}\sigma(x(t - \tau)) + \frac{1}{a}\hat{W}\mathcal{O}_\sigma(t - \tau) + \frac{1}{a}K_p e + \frac{1}{a}K_i aD_t^{-\alpha} e \\
 &\quad - \frac{\gamma}{a} \left(\frac{1}{2} + \frac{1}{2} \|\hat{W}\|^2 L_\phi^2 \right) e
 \end{aligned} \tag{19}$$

$$\begin{aligned}
 aD_t^\alpha e &= \frac{-1}{a}(\lambda - 1 + K_p)e + \frac{1}{a}\tilde{W}\sigma(x(t - \tau)) + \frac{1}{a}\hat{W}\mathcal{O}_\sigma(t - \tau) + \frac{1}{a}K_i aD_t^{-\alpha} e \\
 &\quad - \frac{\gamma}{a} \left(\frac{1}{2} + \frac{1}{2} \|\hat{W}\|^2 L_\phi^2 \right) e
 \end{aligned} \tag{20}$$

And if $w = \frac{1}{a}K_i aD_t^{-\alpha} e$, then $aD_t^\alpha w = \frac{1}{a}K_i e(t)$, [7], then Eq. (20) we rewrite as:

$$\begin{aligned}
 aD_t^\alpha e_n &= \frac{-1}{a}(\lambda - 1 + K_p)e + \frac{1}{a}\tilde{W}\sigma(x(t - \tau)) + \frac{1}{a}\hat{W}\mathcal{O}_\sigma(t - \tau) + w \\
 &\quad - \frac{\gamma}{a} \left(\frac{1}{2} + \frac{1}{2} \|\hat{W}\|^2 L_\phi^2 \right) e
 \end{aligned} \tag{21}$$

We will show, the new state $(e_n, w)^T$ is asymptotically stable, and the equilibrium point is $(e_n, w)^T = (0, 0)^T$, when $\tilde{W}\sigma(x_r(t - \tau)) = 0$, as an external disturbance.

Let V be, the next candidate Lyapunov function as [8, 9]:

$$\begin{aligned}
 V &= \frac{1}{2}(e_n^T, w^T)(e_n, w)^T + \frac{1}{2a} \text{tr} \{ \tilde{W}^T \tilde{W} \} \\
 &\quad + \frac{1}{a} \int_{t-\tau}^t \left[\mathcal{O}_\sigma^T(s) \hat{W}^T \hat{W} \mathcal{O}_\sigma(s) \right] ds
 \end{aligned} \tag{22}$$

The fractional order time derivative of (22) along the trajectories of Eq. (21) is:

$$\begin{aligned}
 aD_t^\alpha V &= e^T aD_t^\alpha e + w^T aD_t^\alpha w + \frac{1}{a} \text{tr} \{ aD_t^\alpha \tilde{W}^T \tilde{W} \} \\
 &\quad + \frac{1}{a} \left[\mathcal{O}_\sigma^T(t) \hat{W}^T \hat{W} \mathcal{O}_\sigma(t) - \mathcal{O}_\sigma^T(t - \tau) \hat{W}^T \hat{W} \mathcal{O}_\sigma(t - \tau) \right]
 \end{aligned} \tag{23}$$

$$\begin{aligned}
 aD_t^\alpha V &= e^T \left(\frac{-1}{a}(\lambda - 1 + K_p)e + \frac{1}{a}\tilde{W}\sigma(x(t - \tau)) + \frac{1}{a}\hat{W}\mathcal{O}_\sigma(t - \tau) + w \right. \\
 &\quad \left. - \frac{\gamma}{a} \left(\frac{1}{2} + \frac{1}{2} \|\hat{W}\|^2 L_\phi^2 \right) e \right) + \frac{1}{a} \tilde{W}^T K_i e + \frac{1}{a} \text{tr} \{ aD_t^\alpha \tilde{W}^T \tilde{W} \} \\
 &\quad + \frac{1}{a} \left[\mathcal{O}_\sigma^T(t) \hat{W}^T \hat{W} \mathcal{O}_\sigma(t) - \mathcal{O}_\sigma^T(t - \tau) \hat{W}^T \hat{W} \mathcal{O}_\sigma(t - \tau) \right]
 \end{aligned} \tag{24}$$

In this part, we select the next learning law from the neural network weights as in [10, 11]:

$$\text{tr} \{ aD_t^\alpha \tilde{W}^T \tilde{W} \} = -e^T \tilde{W} \sigma(x(t - \tau)) \tag{25}$$

Then Eq. (24) is reduced to

$$\begin{aligned}
 aD_t^\alpha V &= \frac{-1}{a} (\lambda - 1 + K_p) e^T e + \frac{e^T}{a} \hat{W} \varnothing_\sigma(t - \tau) \\
 &+ \left(1 + \frac{K_i}{a} \right) e^T w - \frac{\gamma}{a} \left(\frac{1}{2} + \frac{1}{2} \|\hat{W}\|^2 L_\phi^2 \right) e^T e \\
 &+ \frac{1}{a} \left[\varnothing_\sigma^T(t) \hat{W}^T \hat{W} \varnothing_\sigma(t) - \varnothing_\sigma^T(t - \tau) \hat{W}^T \hat{W} \varnothing_\sigma(t - \tau) \right]
 \end{aligned} \tag{26}$$

Next, let us consider the following inequality proved in [12]

$$X^T Y + Y^T X \leq X^T \Lambda X + Y^T \Lambda^{-1} Y \tag{27}$$

Which holds for all matrices $X, Y \in \mathbb{R}^{n \times k}$ and $\Lambda \in \mathbb{R}^{n \times n}$ with $\Lambda = \Lambda^T > 0$. Applying (27) with $\Lambda = I$ to the term $\frac{e^T}{a} \hat{W} \varnothing_\sigma(t - \tau)$ from Eq. (26), where

$$\frac{e^T}{a} \hat{W} \varnothing_\sigma(t - \tau) \leq \frac{1}{a} \left[e^T e + \varnothing_\sigma^T(t - \tau) \hat{W}^T \hat{W} \varnothing_\sigma(t - \tau) \right]$$

we get

$$\begin{aligned}
 aD_t^\alpha V &\leq \frac{-1}{a} (\lambda - 1 + K_p) e^T e + \frac{1}{a} \left(\frac{e^T e}{2} + \frac{1}{2} \|\hat{W}\|^2 L_\phi^2 \right) e^T e \\
 &+ \left(1 + \frac{K_i}{a} \right) e^T w - \frac{\gamma}{a} \left(\frac{1}{2} + \frac{1}{2} \|\hat{W}\|^2 L_\phi^2 \right) e^T e
 \end{aligned} \tag{28}$$

Here, we select $\left(1 + \frac{K_i}{a} \right) = 0$ and $K_v = K_i + 1$, with $K_v \geq 0$ then $K_i \geq -1$, with this selection of the parameters from Eq. (28) is reduced to:

$$aD_t^\alpha V \leq \frac{-1}{a} (\lambda - 1 + K_p) e^T e - \frac{(\gamma - 1)}{a} \left(\frac{1}{2} + \frac{1}{2} \|\hat{W}\|^2 L_\phi^2 \right) e^T \tag{29}$$

From the previous inequality, we need to guarantee that Eq. (29) is less than zero, for which we select,

$\lambda - 1 + K_p > 0, a > 0, (\gamma - 1) > 0$, so that: $aD_t^\alpha V \leq 0, \forall e, w, \hat{W} \neq 0, e \neq 0$, is wanted to be demonstrate.

The control law is given by Eq. (30)

$$\begin{aligned}
 u_n &= \Omega^\dagger \left[-\hat{W} \Gamma (z(x_n(t - \tau)) - z(x_p(t - \tau))) \right. \\
 &\quad \left. - (A + I)(x - x_p) + K_p e + K_i a D_t^{-\alpha} e + K_v a D_t^\alpha e \right. \\
 &\quad \left. - \Gamma \left(\frac{1}{2} + \frac{1}{2} \|\hat{W}\|^2 L_\phi^2 \right) e_n + f_r(x_r, u_r) - A x_r \right. \\
 &\quad \left. - \hat{W} \Gamma_z(x_r(t - \tau)) - x_r + x_p \right]
 \end{aligned} \tag{30}$$

Theorem: The control law Eq. (30) and the neuronal adaptation law given by Eq. (25) guarantee that the fractional tracking error converges to zero, by which the tracking of trajectories of the non-linear system is guaranteed Eq. (5).

Corollary 2: If $aD_t^\alpha V \leq \frac{-1}{a} (\lambda - 1 + K_p) (e_n^T)(e_n) - \frac{(\gamma-1)}{a} \left(\frac{1}{2} + \frac{1}{2} \|\hat{W}\|^2 L_\phi^2 \right) (e_n^T)(e_n) < 0, \forall e \neq 0, \forall \hat{W}$, where V is decreasing and bounded from below by $V(0)$, and:

$$V = \frac{1}{2}(e_n^T, w^T)(e_n, w)^T + \frac{1}{2a} \text{tr}\{\tilde{W}^T \tilde{W}\} + \frac{1}{a} \int_{t-\tau}^t [\hat{\mathcal{O}}_\sigma^T(s) \hat{W}^T \hat{W} \hat{\mathcal{O}}_\sigma(s)] ds,$$

then we conclude that $e, \tilde{W} \in L_1$; this means that the weights remain bounded.

5. Modeling of the time-delay adaptive neural network and the delayed plant

The nonlinear delayed unknown plant and the neural network are given as:

$$\begin{aligned} aD_t^\alpha x_p &= f_p(x_p(t-\tau)) + g_p(x_p(t))u_p, \\ aD_t^\alpha x_n &= A(x) + W^* \Gamma_z[x(t-\tau)] + w_{per} + \Omega_u \end{aligned}$$

where $x_p, f_p \in \mathbb{R}^n, u \in \mathbb{R}^m, g_p \in \mathbb{R}^{n \times n}$. And f_p , is unknown and $g_p = I, A = -\lambda I$, with Γ Lipschitz function, W^* are the fixed weights but unknown from the neural networks, which minimize the modeling error.

Theorem: We will show that e_p and e_n tend to zero and therefore e tends to zero, that is, the neural network follows the plant.

For this proposal, we first define the modeling error between the neural network and the plant: $e_p = x_p - x_n$, whose derivative in the time is

$$aD_t^\alpha e_p = aD_t^\alpha x_p - aD_t^\alpha x_n \quad (31)$$

Adding and subtracting, to the right hand side from (34) the terms $\hat{W} \Gamma_z(x_p, x(t-\tau)), \alpha_p(t, \hat{W})$

$$aD_t^\alpha e_p = A(e_p) - \tilde{W} \Gamma_z[x_n(t-\tau)] + \hat{W} \hat{\mathcal{O}}(e_p(t-\tau)) + \tilde{u}_p \quad (32)$$

6. Identification of the unknown non-linear system by the neural network

First, it is easy to see that $(e, \hat{W}) = 0$ is a state of equilibrium (equilibrium point). Previous, so we propose to demonstrate that this point of equilibrium is asymptotically stable; for this, be:

$$\tilde{u}_p = -\gamma \left(\frac{1}{2} + \frac{1}{2} \|\hat{W}\|_{L_\phi}^2 \right) e_p \quad (33)$$

We will show, the feedback system is asymptotically stable. Replacing (36) in (35)

$$aD_t^\alpha e_p = A(e_p) - \tilde{W} \Gamma_z[x_n(t-\tau)] + \hat{W} \hat{\mathcal{O}}(e_p(t-\tau)) - \gamma \left(\frac{1}{2} + \frac{1}{2} \|\hat{W}\|_{L_\phi}^2 \right) e_p \quad (34)$$

We will show, the new state e_p is asymptotically stable, and the equilibrium point is $e_p \rightarrow 0$, when $\hat{W} \sigma(x_n(t-\tau)) = 0$, as an external disturbance.

Let V be, the next candidate Lyapunov function as

$$V = \frac{1}{2} (e_p^T, w^T) (e_p, w)^T + \frac{1}{2a} \text{tr} \{ \tilde{W}^T \tilde{W} \} \quad (35)$$

$$+ \frac{1}{a} \int_{t-\tau}^t \left[\varnothing_\sigma^T(s) \hat{W}^T \hat{W} \varnothing_\sigma(s) \right] ds$$

Then, (35) is reduced to

$$aD_t^\alpha V \leq \frac{-1}{a} (\lambda - 1 + K_p) (e_p^T) (e_p) - \frac{(\gamma - 1)}{a} \left(\frac{1}{2} + \frac{1}{2} \|\hat{W}\|^2 L_\phi^2 \right) (e_p^T) (e_p) < 0 \quad (36)$$

The previous inequality guarantees that the identification of the non-linear system is satisfied, that is, the approach error converges to zero asymptotically

$$u_p = \Omega^\dagger \left[\hat{W} \Gamma z(x_r(t - \tau)) - \hat{W} \Gamma (z(x_n(t - \tau)) - z(x_p(t - \tau))) \right]$$

$$- (A + I)(x - x_p) + K_p e + K_i a D_t^{-\alpha} e + K_v a D_t^\alpha e \quad (37)$$

$$- \Gamma \left(\frac{1}{2} + \frac{1}{2} \|\hat{W}\|^2 L_\phi^2 \right) e_n - \Gamma \left(\frac{1}{2} + \frac{1}{2} \|\hat{W}\|^2 L_\phi^2 \right) e_p + f_r(x_r, u_r)$$

$$- f_p(x_p) + A x_p - A x_r + \hat{W} \Gamma z(x_p) - x_r + x_p]$$

7. Simulation

The mathematical model, which describes the movement dynamics of the bipedal robot, is obtained using the Euler-Lagrange equations [1, 13] (**Figure 2**).

$$D(q(t))\ddot{q}(t) + C(q(t), \dot{q}(t))\dot{q}(t) + G(q(t)) = B\tau(t)$$

where $q(t) = [q_{31}(t)q_{32}(t)q_{41}(t)q_{42}(t)]^T$, is the generalized coordinates vector. As usual, $D(q(t))$ is the inertia matrix, bounded and positive definite, and $C(q(t), \dot{q}(t))$ is the matrix of Coriolis and centripetal forces. $G(q(t))$ represents a matrix of gravitational effects and B defines the input matrix. The vector $\tau(t) = [\tau_{31}(t)\tau_{32}(t)\tau_{41}(t)\tau_{42}(t)]^T$, defines the applied joint torques of the robot.

To illustrate the theoretical results obtained, we propose an example, which, as can be seen in the simulations, trajectory tracking is guaranteed.

The neural network is described by:

$aD_t^\alpha x_p = A(x) + W^* \Gamma_z(x(t - \tau)) + \Omega_u$, with $\tau = 25$ s, $A = -20I$, $I \in \mathbb{R}^{4 \times 4}$, and, W^* is estimated using the learning law given in (28).

$\Gamma_z(x(t - \tau)) = (\tanh(x_1(t - \tau)), \tanh(x_2(t - \tau)), \dots, \tanh(x_n(t - \tau)))^T$,
 $\Omega = \begin{pmatrix} 0 & 0 & 1 & 0 \\ 0 & 0 & 0 & 1 \end{pmatrix}^T$ and the u is obtained using (33).

and the reference signal that they have to follow, both the non-linear system and the neural network is given by the Duffing equation [14].

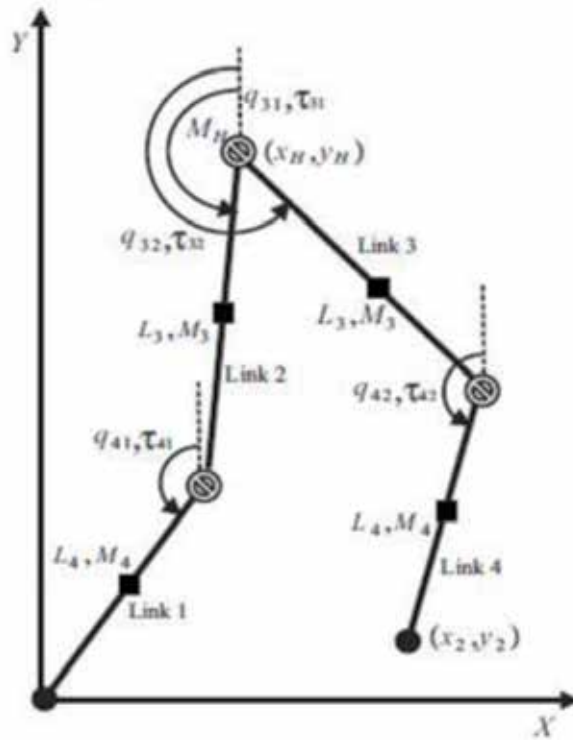


Figure 2.
Dynamic model of biped robot.

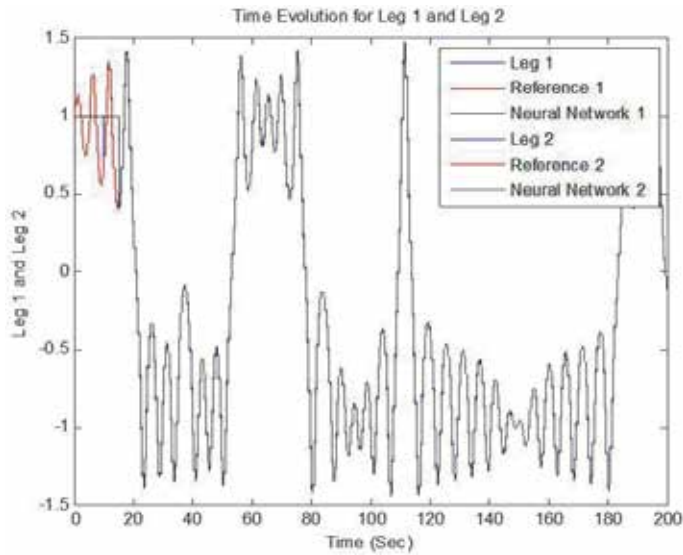


Figure 3.
Time evolution for the angular position Leg 1 and Leg 2 (rad) of link 1.

$$\ddot{x} - x + x^3 = 0.114 \cos(1.1t) : x(0) = 1, \dot{x}(0) = 0.114$$

$$\frac{x(t)}{dt} = y(t)$$

$$\frac{y(t)}{dt} = x(t) - x^3(t) - \alpha y(t) + \delta \cos(\omega t)$$

Here, the conventional derivatives are replaced by the fractional derivatives as follows:

$$aD_t^\alpha x(t) = y(t)$$

$$aD_t^\alpha x(t) = x(t) - x^3(t) - \alpha y(t) + \delta \cos(\omega t)$$

where α, ω, δ , are the parameters of the Duffing differential equation, which we will use as a reference trajectory, that the non-linear system and the neural network have to follow.

As can be seen in **Figures 3–6**, the tracking of trajectories in the states of the system are performed with satisfaction, **Figure 7** shows the phase plane of the

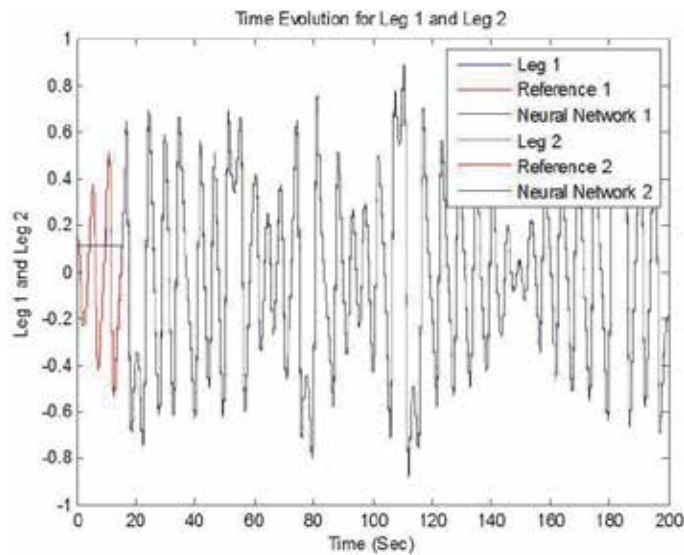


Figure 4.
 Time evolution for the angular position Leg 1 and Leg 2 (rad) of link 2.

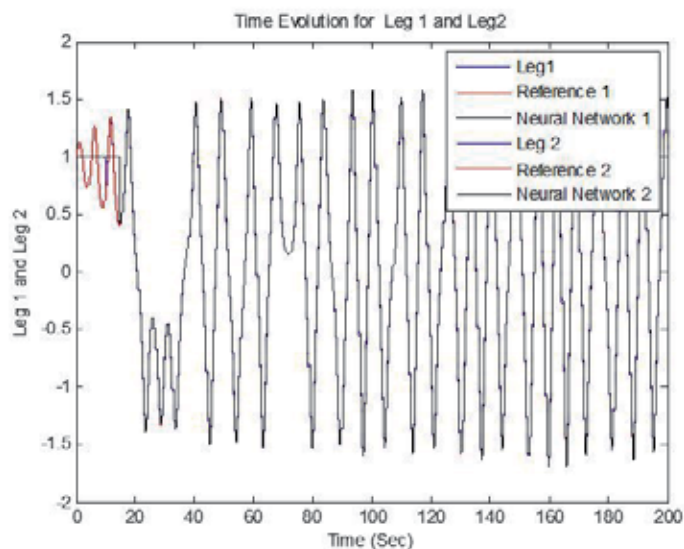


Figure 5.
 Time evolution for the angular position Leg 1 and Leg 2 (rad) of link 1.

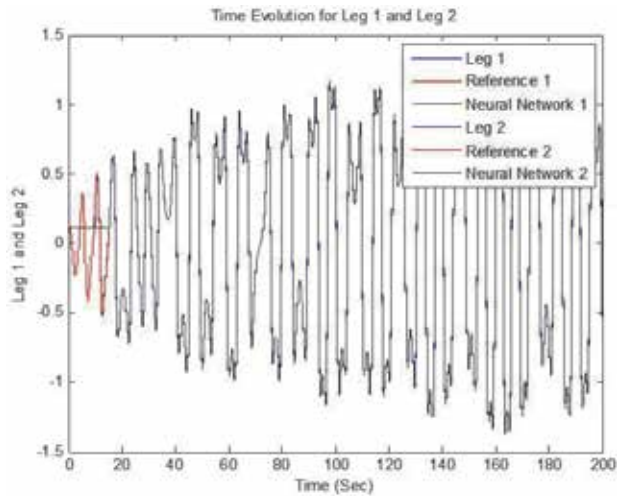


Figure 6.
Time evolution for the angular position Leg 1 and Leg 2 (rad) of link 2.

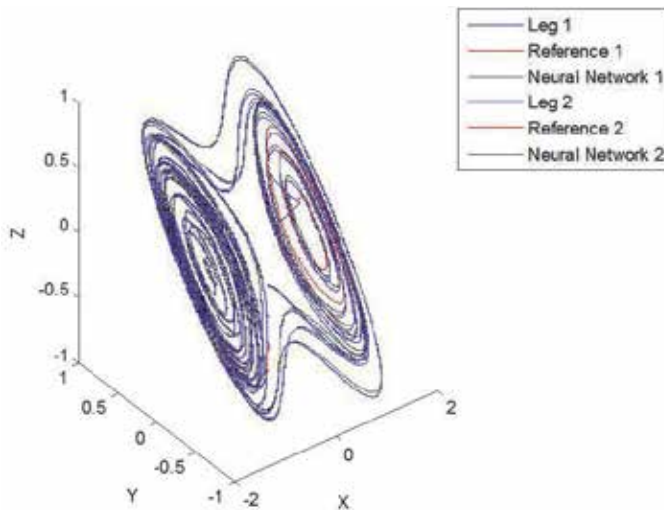


Figure 7.
A phase space trajectory of Duffing equation.

Duffing equation, while **Figure 8** shows the plane phase of the same fractional order differential equation.

Figures 9–12 show the torques applied to the ends of the bipedal robot.

Parameter values of the fractional order, alpha (0.001) and beta (0.0001) are included.

$$\alpha = 1, \quad \beta = 1$$

$$\alpha = 0.001, \quad \beta = 0.001$$

8. Conclusions

In this chapter we study the mathematical model and control of non-linear systems, which are modeled by differential equations of fractional order, where it is

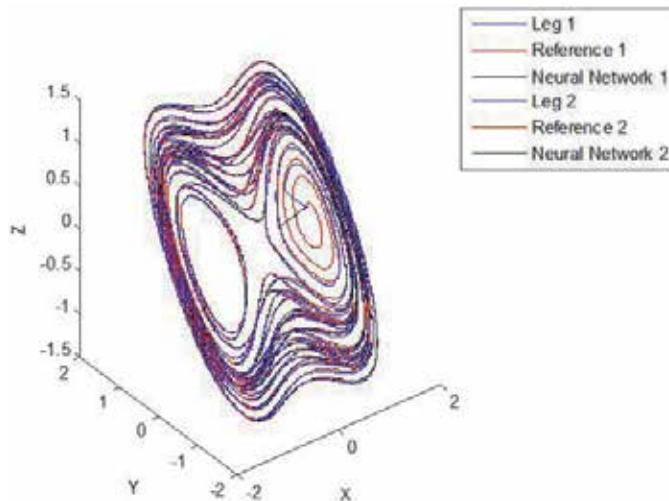


Figure 8.
A phase space trajectory of Duffing equation.

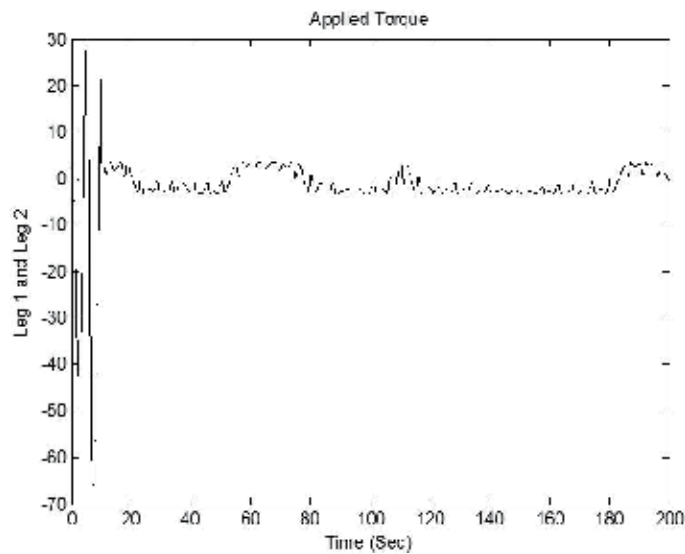


Figure 9.
Torque (Nm) applied to Leg 1 and Leg 2 of link 1.

observed that these systems have a better performance than the systems modeled by ordinary differential equations, those of fractional order they produce responses, solutions at simulation level, softer, by varying the order of the derivative.

The magnitude of the fractional order systems are smaller than the responses of the systems of ordinary differential equations, and with smaller control signals, which implies, less energy in the control process.

In this research work, conditions have been obtained in the parameters of the adaptive recurrent neural network, as well as laws of control and laws of neuronal adaptation, which, together, guarantee that the tracking error of trajectories between the non-linear system and the reference signal converges asymptotically to zero, so that trajectory tracking is develops with satisfaction.

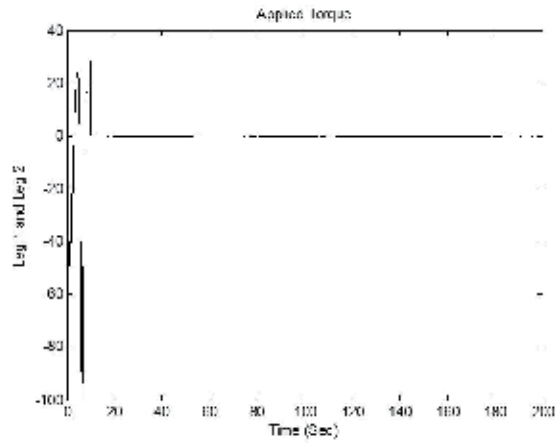


Figure 10.
Torque (Nm) applied to Leg 1 and Leg 2 of link 2.

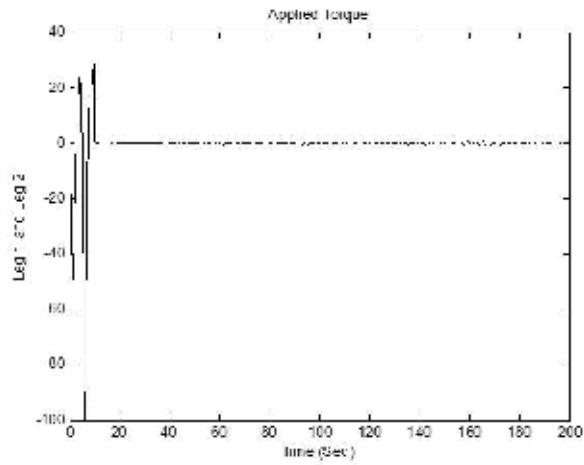


Figure 11.
Torque (Nm) applied to Leg 1 and Leg 2 of link 1.

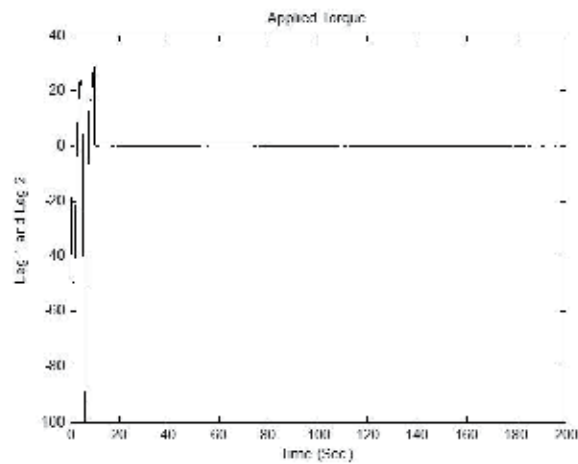


Figure 12.
Torque (Nm) applied to Leg 1 and Leg 2 of link 2.

Acknowledgements

Authors thank, Mexican National Science and Technology Council, (CONACyT), Mexico, to the Autonomous University of Nuevo Leon, Dynamical Systems Group of the Department of Physical and Mathematical Sciences, (FCFM-UANL), Centro de Investigación y Estudios de Posgrado, Facultad de Ingeniería, Dr. Manuel Nava #8, Zona Universitaria, C.P. 78290, San Luis Potosí, S.L.P., México. The research of V. Ramírez-Rivera has been supported by CONACyT-México under the project Problemas Nacionales (2015-01-786).

Conflict of interest

The first author of the reference manuscript, in his name and that of all authors, declares that there is no potential conflict of interest related to the article.

Author details

Joel Perez Padron^{1*}, Jose P. Perez¹, C.F. Mendez-Barrios² and V. Ramírez-Rivera³

¹ Department of Physical and Mathematical Sciences, Autonomous University of Nuevo Leon (FCFM, UANL), Nuevo Leon, Mexico

² Facultad de Ingeniería, Centro de Investigacion y Estudios de Posgrado, San Luis Potosí, Mexico

³ Centro de Investigación Científica de Yucatán, A.C.(CICY), Carretera Sierra Papacal-Chuburná Puerto, Mexico

*Address all correspondence to: joel.perezpd@uanl.edu.mx

IntechOpen

© 2020 The Author(s). Licensee IntechOpen. This chapter is distributed under the terms of the Creative Commons Attribution License (<http://creativecommons.org/licenses/by/3.0>), which permits unrestricted use, distribution, and reproduction in any medium, provided the original work is properly cited. 

References

- [1] Vazquez JA, Velasco-Villa M. Design and real-time control of a 4-DOF biped robot. *International Journal of Advanced Robotic Systems*. Intech; 2013
- [2] Huang X, Wang Z, Li Y. Nonlinear dynamics and chaos in fractional-order Hopfield neural networks with delay. *Advances in Mathematical Physics*. 2013;2013:657245. DOI: 10.1155/2013/657245
- [3] Zhang S, Yu Y, Wang Q. Stability analysis of fractional-order Hopfield neural networks with discontinuous activation functions. *Neurocomputing*. 2016;171:1075-1084. Available from: www.elsevier.com/locate/neucom
- [4] Joshi SD, Talange DB. Integer & fractional order PID controller for fractional order subsystems of AUV. In: 2013 IEEE Symposium on Industrial Electronics & Applications (ISIEA2013); September 22–25, 2013; Kuching, Malaysia
- [5] Kelly R, Haber RE, Haber Guerra RE, Reyes F. Lyapunov stable control of robot manipulators: A fuzzy self-tuning procedure. *Intelligent Automation & Soft Computing*. 1999;5(4):313-326
- [6] Moreno AR, Sandoval VJ. Fractional Order PD and PID Position Control of an Angular Manipulator of 3DOF. Available from: arojas@utec.edu.pe, jaravictor2000@yahoo.com
- [7] Grigoletto EC, de Oliveira EC. Fractional versions of the fundamental theorem of calculus. *Applied Mathematics*. 2013;4:23-33. DOI: 10.4236/am.2013.47A006. Available from: <http://www.scirp.org/journal/am>
- [8] Chen D, Zhang R, Liu X, Ma X. Fractional order Lyapunov stability theorem and its applications in synchronization of complex dynamical networks. *Communications in Nonlinear Science and Numerical Simulation*. 2014;19:4105-4121. Available from: www.elsevier.com/locate/cnsns
- [9] Jiang H-P, Liu Y-Q. Disturbance rejection for fractional-order time-delay systems. *Mathematical Problems in Engineering*. 2016;2016:1316046. DOI: 10.1155/2016/1316046
- [10] Rovitahkis GA, Christodoulou MA. *Adaptive Control with Recurrent High-Order Neural Networks*. New York, USA: Springer Verlag; 2000
- [11] Ioannou PA, Sun J. *Robust Adaptive Control*. Upper Saddle River, NJ: PTR Prentice-Hall. ISBN: 0-13-439100-4
- [12] Ma W, Li C, Wu Y, Wu Y. Adaptive synchronization of fractional neural networks with unknown parameters and time delays. *Entropy*. 2014;16:6286-6299. DOI: 10.3390/e16126286. ISSN: 1099-4300
- [13] Spong MW, Vidyasagar M. *Robot Dynamics and Control*. USA: John Wiley and Sons; 1989
- [14] Petras I. *Nonlinear Physical Science, Fractional-Order Nonlinear Systems, Modeling, Analysis and Simulation*. Heidelberg/Dordrecht/London/New York: Springer. ISSN: 1867-8440. ISBN: 978-3-642-18100-9

*Edited by Ahmad Hoirul Basori,
Ali Leylavi Shoushtari and Andon Venelinov Topalov*

Nowadays, our expectations of robots have been significantly increases. The robot, which was initially only doing simple jobs, is now expected to be smarter and more dynamic. People want a robot that resembles a human (humanoid) has and has emotional intelligence that can perform action-reaction interactions. This book consists of two sections. The first section focuses on emotional intelligence, while the second section discusses the control of robotics. The contents of the book reveal the outcomes of research conducted by scholars in robotics fields to accommodate needs of society and industry.

Published in London, UK

© 2020 IntechOpen
© 123dartist / iStock

IntechOpen

